

**Spatial and temporal variation in water mass characteristics and the normalized
zooplankton biomass size spectrum in the Northumberland Strait**

by

Camille Pagniello

Submitted in partial fulfilment of the requirements of the degree of Honours Bachelor of
Science in Marine Biology

at

Dalhousie University
Halifax, Nova Scotia
April 2015

© Camille Pagniello, 2015

À Maman, Daddy, Céleste et Grandmaman...même si vous ne comprenez rien ☺

Table of Contents

List of Tables.....	iii
List of Figures.....	iv
Abstract.....	xiii
List of abbreviations and symbols used	xiv
Acknowledgements	xvi
Thesis	1
1.0 Introduction	1
2.0 Methods	7
2.1 Study area	7
2.2 Sampling.....	8
2.3 BIONESS-OPC data processing	12
2.4 CTD processing.....	14
2.5 Statistical analyses	14
3.0 Results.....	17
3.1 General oceanographic conditions	17
3.1 Oceanographic zones	25
3.3 Normalized zooplankton biomass size spectra	32
3.4 Relationships amongst the NBSS parameters and environmental variables	37
3.5 Zooplankton spatial and temporal patterns	43
4.0 Discussion	48
4.1 Spatial and temporal patterns of water masses	48
4.2 Biological and physical influences on the size structure of the zooplankton community	49
4.3 Temporal patterns in the zooplankton community structure.....	51
4.4 Spatial patterns in the zooplankton community structure	52
4.5 Comparing the linear and quadratic NBSS models	53
4.6 Methodological considerations and limitations	55
4.7 Implications of the zooplankton community size structure for fishery resources in the Northumberland Strait	57
References.....	58
Appendix A: Normalized zooplankton biomass size spectra	61
Appendix B: Residuals from the linear function	65
Appendix C: Residuals from the quadratic function	69

List of Tables

Table 1. Summary of BIONESS stations occupied in the Northumberland Strait during late spring 2009 providing date and start time (ADST), location (latitude, longitude; decimal degree) and maximum tow depth.....	10
Table 2. Summary of BIONESS stations occupied in the Northumberland Strait during autumn 2009 providing date and start time (ADST), location (latitude, longitude; decimal degree) and maximum tow depth.....	11
Table 3. Summary of Seabird-25 CTD stations occupied in the Northumberland Strait during late spring 2009 providing date and start time (ADST), location (latitude, longitude; decimal degree and maximum sounding depth (m).....	12
Table 4 Range and average \pm one standard error (SError) statistics for the eight oceanographic variables from the Northumberland Strait BIONESS CTD station-specific profiles and used in the principal component analysis for late spring (n = 24) and autumn (n = 50) 2009, respectively	16
Table 5. Range, average \pm one standard error (SError) and coefficient of variation (CV) for the slope, intercept, curvature, x-coordinate of the vertex and y-coordinate of the vertex in the Northumberland Strait during late spring and autumn of 2009, respectively.	34
Table 6. P-values from the Wilcoxon rank-sum test for the slope, intercept, curvature, x- coordinate of the vertex and y-coordinate of the vertex comparisons between late spring vs. autumn, core vs. coastal water, open ocean vs. upper Strait water in autumn and open ocean vs. lower Strait in autumn. (-) indicates that the comparison was not done as a Kruskal-Wallis ANOVA revealed that there were significant differences within the clusters. Factors in bold are significant at p < 0.05.	47

List of Figures

Figure 1. Normalized biomass size spectrum (NBSS) models (a) fitted with linear regression (solid line) and (b) fitted with least-squares polynomial regression, or quadratic (solid line). The NBSS parameters (indices) derived from each spectrum are labelled. (from Krupica et al. 2012)	3
Figure 2. Example of three possible bottom-up and top-down processes altering the slope and intercept of the zooplankton NBSS at three different times: (a) a nutrient pulse, (b) a sustained nutrient supply and (c) size-selective predation by fish (from Suthers et al. 2006).	5
Figure 3. The Northumberland Strait and surrounding regions (inset) showing oceanographic zones within the Strait during July and August 2009 as west (blue square), east (red square), center (white circle), transition (yellow diamond) and spatially non-distinct (ND; black x) with colour contour similarities interpreted as areas with similar oceanographic conditions and are based on the principal component analysis by Debertin et al. (2012).	7
Figure 4. Sampling stations occupied in the Northumberland Strait during late spring (1 to 25, excluding 8; yellow symbols) and autumn (1 to 50; red symbols) of 2009.	9
Figure 5. Example vertical temperature ($^{\circ}\text{C}$; red), salinity (PSU; green) and density (σ_t ; blue) profiles at station 45 illustrating a well-mixed water mass in the Northumberland Strait during autumn of 2009.	17
Figure 6. Example vertical temperature ($^{\circ}\text{C}$; red), salinity (PSU; green) and density (σ_t ; blue) profiles at station 2 illustrating shallow but strong water mass stratification in the Northumberland Strait during late spring of 2009.	18
Figure 7. Example vertical temperature ($^{\circ}\text{C}$; red), salinity (PSU; green) and density (σ_t ; blue) profiles at station 11 illustrating deep but weak stratification in the Northumberland Strait during late spring of 2009.	18
Figure 8. Example vertical temperature ($^{\circ}\text{C}$; red), salinity (PSU; green) and density (σ_t ; blue) profiles at station 6 illustrating deep and strong water mass stratification in the Northumberland Strait during autumn of 2009.	19
Figure 9. Temperature-salinity (TS) diagram derived from CTD profiles at each sampling station (1 to 25) in the Northumberland Strait in late spring of 2009. Lines of constant density (σ_t) are noted.	20

Figure 10. Temperature ($^{\circ}\text{C}$) section across the Northumberland Strait (left to right, NB to PEI; km) at the stations 15 through 19 in late spring of 2009 illustrating colder (~ 16 $^{\circ}\text{C}$), deep water in the interior of the Strait. Open circles represent each datum used to contour the section.	21
Figure 11. Salinity (PSU) section across the Northumberland Strait (left to right, NB to PEI; km) at the stations 15 through 19 in late spring of 2009 illustrating saltier (~ 28.5 PSU) core water in the interior of the Strait. Open circles represent each datum used to contour the section.	21
Figure 12. Density (σ_t) section across the Northumberland Strait (left to right, NB to PEI; km) at the stations 15 through 19 in late spring of 2009 illustrating dense (~ 20.6 kg/m^3) core water in the interior of the Strait. Open circles represent each datum used to contour the section.	22
Figure 13. Temperature-salinity (TS) diagram derived from CTD profiles at each sampling station (1 to 50) in the Northumberland Strait in autumn of 2009. Lines of constant density (σ_t) are noted.	23
Figure 14. Temperature ($^{\circ}\text{C}$) section along the Northumberland Strait (SE to NW; km) at stations 8, 2, 9, 12, 16, 19, 27, 30, 31, 47, 46 and 44 in autumn of 2009 illustrating the warm well-mixed surface layer and a weak thermocline at depth along the interior of the Strait.	23
Figure 15. Salinity (PSU) section along the Northumberland Strait (SE to NW; km) at stations 8, 2, 9, 12, 16, 19, 27, 30, 31, 47, 46 and 44 in autumn of 2009 illustrating the alternating salty/fresh well-mixed surface layer, a weak halocline at depth and the relatively fresh water at the entrance (NW) to the Strait compared to the salty water near the exit (SE) from the Strait.	24
Figure 16. Density (σ_t) section along the Northumberland Strait (SE to NW; km) at stations 8, 2, 9, 12, 16, 19, 27, 30, 31, 47, 46 and 44 in autumn of 2009 illustrating the alternating dense/less dense well-mixed surface layer, a pycnocline at depth and the relatively less dense water at the entrance (NW) to the Strait compared to the dense water near the exit (SE) from the Strait.	24
Figure 17. Explained variance among the first three principal components of the PCA analysis of water mass structure in the Northumberland Strait in late spring and autumn of 2009 based on eight oceanographic variables (Table 4), season, and distance from the nearest coast.	26

Figure 18. Dendrogram of sampling stations grouped into oceanographic zones based on similar environmental conditions measured at stations within Northumberland Strait in both late spring and autumn of 2009.....	27
Figure 19. Distribution of late spring (yellow, n = 21) and autumn (red, n = 43) clusters within the Northumberland Strait. The single five-point star represents the late spring station erroneously clustered as autumn.	28
Figure 20. Distribution of upper Strait (cyan, n = 16) and open ocean (blue, n = 5) clusters within the Northumberland Strait in late spring of 2009.	29
Figure 21. Distribution of coastal (cyan, n = 12) and core (blue, n = 4) stations within the upper Northumberland Strait in late spring of 2009.....	29
Figure 22. Distribution of low (cyan, n = 20) and high bottom density (blue, n = 23) stations within the Northumberland Strait in autumn of 2009.	30
Figure 23. Distribution of coastal (cyan, n = 5) and core (blue, n = 14) stations within the low bottom density waters of the Northumberland Strait in autumn of 2009. A black cross marks the single non-distinct station.....	31
Figure 24. Distribution of coastal (cyan, n = 13), core (blue, n = 8) and open ocean (pink, n = 1) stations within the high bottom density waters of the lower Northumberland Strait in autumn of 2009. A black cross marks the single non-distinct station.....	31
Figure 25. Example of \log_{10} normalized biomass size spectrum (NBSS) showing the normalized biomass ($\text{mg mm}^{-3}/\Delta \text{ volume}$) as a function of size categories at station 4 in the Northumberland Strait during autumn of 2009 illustrating the simple parabolic dome shape.	33
Figure 26. Example of \log_{10} normalized biomass size spectrum (NBSS) showing the normalized biomass ($\text{mg mm}^{-3}/\Delta \text{ volume}$) as a function of size categories at station 22 in the Northumberland Strait during late spring of 2009 illustrating the deviations from dome shape at larger size classes.	33
Figure 27. Example of residuals from linear function fitted to the \log_{10} normalized biomass size spectra (NBSS) as a function of size-class at station 4 in the Northumberland Strait during autumn of 2009 illustrating the distribution of residuals over a single dome.	35

Figure 28. Example of residuals from linear function fitted to the \log_{10} normalized biomass size spectra (NBSS) as a function of size-class at station 22 in the Northumberland Strait during late spring of 2009 illustrating the a second peak at larger size classes.....	35
Figure 29. Example of residuals from quadratic function fitted to the \log_{10} normalized biomass size spectra (NBSS) (blue) and residuals from quadratic function fitted to the residuals from the linear function fitted to the \log_{10} NBSS (red) as a function of size-class at station 4 in the Northumberland Strait during autumn of 2009 illustrating the distribution of residuals over a single dome.....	36
Figure 30. Example of residuals from quadratic function fitted to the \log_{10} normalized biomass size spectra (NBSS) (blue) and residuals from quadratic function fitted to the residuals from the linear function fitted to the \log_{10} NBSS (red) as a function of size-class at station 22 in the Northumberland Strait during late spring of 2009 illustrating a second peak at larger size classes.	36
Figure 31. Scatterplot of (a) the intercept (late spring, yellow: $r = 0.692$, $n = 21$; autumn, red: $r = 0.901$, $n = 49$), (b) the x-coordinate of the vertex (late spring, yellow: $r = 0.606$, $n = 21$; autumn, red: $r = 0.799$, $n = 49$), and (c) the y-coordinate of the vertex (autumn $r = -0.248$, $n = 49$) of the normalized zooplankton size spectra (NBSS) in relation to the slope of the NBSS. All correlation coefficients (r) are significant.....	37
Figure 32. Scatterplot of (a) the curvature (autumn: $r = 0.85$, $n = 49$), (b) the x-coordinate of the vertex (late spring, yellow: $r = 0.573$, $n = 21$; autumn, red: $r = 0.831$, $n = 49$), and (c) the y-coordinate of the vertex (autumn: $r = -0.286$, $n = 49$) of the normalized zooplankton size spectra (NBSS) in relation to the intercept of the NBSS. All correlation coefficients (r) are significant.	38
Figure 33. Scatterplot of (a) the x-coordinate of the vertex (late spring, yellow: $r = -0.439$, $n = 21$; autumn, red: $r = 0.391$, $n = 49$) and (b) the y-coordinate of the vertex (late spring, yellow: $r = -0.640$, $n = 21$; autumn, red: $r = -0.758$, $n = 49$) in relation to the curvature of the normalized zooplankton size spectra (NBSS). All correlation coefficients (r) are significant.....	38
Figure 34. Scatterplot of the y-coordinate of the vertex in relation to the x-coordinate of the vertex of the normalized zooplankton size spectra during autumn ($r = -0.420$, $n = 49$). The correlation coefficient is significant.....	39

Figure 35. Scatterplot of (a) total biomass ($\text{mg}^*\text{mm}^{-3}$) (late spring, yellow: $r = 0.630$, $n = 21$; autumn, red: $r = 0.731$, $n = 49$), (b) surface temperature ($^\circ\text{C}$) (autumn: $r = 0.341$, $n = 49$), (c) surface density (σ_t , kg/m^3) (autumn: $r = -0.366$, $n = 49$), (d) bottom light attenuation (mV) (autumn: $r = 0.362$, $n = 49$), and (e) surface (late spring, circle: $r = 0.443$, $n = 21$) and average salinity (PSU) (late spring, diamond: $r = 0.442$, $n = 21$) in relation to the slope of the normalized zooplankton biomass spectra (NBSS). All correlation coefficients (r) are significant 40

Figure 36. Scatterplot of (a) total biomass ($\text{mg}^*\text{mm}^{-3}$) (late spring, yellow: $r = 0.973$, $n = 21$; autumn, red: $r = 0.876$, $n = 49$), (b) surface temperature ($^\circ\text{C}$) (autumn: $r = 0.467$, $n = 49$), (c) surface density (σ_t , kg/m^3) (autumn: $r = -0.366$, $n = 49$), and (d) average salinity (PSU) (late spring: $r = 0.475$, $n = 21$) in relation to the intercept of the normalized zooplankton biomass spectra (NBSS). All correlation coefficients (r) are significant 41

Figure 37. Scatterplot of (a) total biomass ($\text{mg}^*\text{mm}^{-3}$) (autumn: $r = 0.426$, $n = 49$), (b) bottom temperature ($^\circ\text{C}$) (autumn: $r = -0.332$, $n = 49$), (c) surface (late spring, yellow: $r = 0.479$, $n = 21$), bottom (autumn, red square: $r = 0.557$, $n = 49$) and average salinity (PSU) (autumn, red diamond: $r = 0.388$, $n = 49$), (d) bottom (square: $r = 0.513$, $n = 49$) and average density (σ_t , kg/m^3) (diamond: $r = 0.366$, $n = 49$) during autumn and (e) surface (circle: $r = -0.530$, $n = 49$), bottom (square: $r = -0.345$) and average light attenuation (mV) (diamond: $r = -0.460$, $n = 49$) during autumn in relation to the curvature of the normalized zooplankton biomass spectra (NBSS). All correlation coefficients (r) are significant 41

Figure 38. Scatterplot of (a) total biomass ($\text{mg}^*\text{mm}^{-3}$) (late spring, yellow: $r = 0.531$, $n = 21$; autumn, red: $r = 0.911$, $n = 49$), (b) surface density (σ_t , kg/m^3) (autumn: $r = -0.380$, $n = 49$), (c) surface (circle: $r = 0.542$, $n = 49$) and average temperature ($^\circ\text{C}$) (diamond: $r = 0.377$, $n = 49$) during autumn, and (d) bottom (late spring, yellow square: $r = 0.523$, $n = 21$; autumn, red: $r = 0.317$, $n = 49$) and average light attenuation (mV) (late spring, yellow diamond: $r = 0.538$, $n = 21$) in relation to the x-coordinate of the vertex of the normalized zooplankton biomass spectra (NBSS). All correlation coefficients (r) are significant 42

Figure 39. Scatterplot of (a) bottom (square: $r = -0.320$, $n = 49$) and average salinity (PSU) (diamond: $r = -0.335$, $n = 49$) during autumn, (b) bottom density (σ_t , kg/m^3) (autumn: $r = 0.270$, $n = 49$), and (c) surface (autumn, red circle: $r = 0.355$, $n = 49$), bottom (late spring, yellow: $r = 0.579$, $n = 21$) and average light attenuation (mV) (autumn, red diamond: $r = 0.270$, $n = 49$) in relation to the y-coordinate of the vertex of the normalized zooplankton biomass spectra (NBSS). The correlation coefficient (r) is significant.....	42
Figure 40. Distribution of the slope of normalized biomass size spectra (NBSS) within the Northumberland Strait in late spring (yellow, $n = 21$) and autumn of 2009 (red, $n = 49$).....	44
Figure 41. Distribution of the intercept of normalized biomass size spectra (NBSS) within the Northumberland Strait in late spring (yellow, $n = 21$) and autumn of 2009 (red, $n = 49$).....	45
Figure 42. Distribution of the curvature of the normalized biomass size spectra (NBSS) within the Northumberland Strait in late spring (yellow, $n = 21$) and autumn of 2009 (red, $n = 49$).....	45
Figure 43. Distribution of the x-coordinate of the vertex of normalized biomass size spectra (NBSS) within the Northumberland Strait in late spring (yellow, $n = 21$) and autumn of 2009 (red, $n = 49$).....	46
Figure 44. Distribution of the y-coordinate of the vertex of normalized biomass size spectra (NBSS) within the Northumberland Strait in late spring (yellow, $n = 21$) and autumn of 2009 (red, $n = 49$).....	46
Figure A1. Log ₁₀ normalized biomass size spectra (NBSS) showing the normalized biomass ($\text{mg mm}^{-3}/\Delta \text{volume}$) as a function of size-classes from all stations in the Northumberland Strait during late spring of 2009. The linear slope (s), linear intercept (i), curvature of the quadratic function (c), x-coordinate of the vertex of the quadratic function (x) and y-coordinate of the vertex of the quadratic function (y) are provided for each station. Panels progress among stations in an along-Strait, NW→SE (top to bottom) and across-Strait, SW→NE (left to right).	61

Figure A2. Log₁₀ normalized biomass size spectra (NBSS) showing the normalized biomass (mg mm⁻³/Δ volume) as a function of size categories from stations 37 to 50 in the Northumberland Strait during autumn of 2009 upstream of Confederation Bridge. The linear slope (s), linear intercept (i), curvature of the quadratic function (c), x-coordinate of the vertex of the quadratic function (x) and y-coordinate of the vertex of the quadratic function (y) are given for each station. Panels progress among stations in an along-Strait, NW→SE (top to bottom) and across-Strait, SW→NE (left to right). 62

Figure A3. Log₁₀ normalized biomass size spectra (NBSS) showing the normalized biomass (mg mm⁻³/Δ volume) as a function of size categories from stations 19 to 36 in the Northumberland Strait during autumn of 2009 located downstream of Confederation Bridge, but upstream of Tatamagouche, New Brunswick. The linear slope (s), linear intercept (i), curvature of the quadratic function (c), x-coordinate of the vertex of the quadratic function (x) and y-coordinate of the vertex of the quadratic function (y) are given for each station. Panels progress among stations in an along-Strait, NW→SE (top to bottom) and across-Strait, SW→NE (left to right). 63

Figure A4. Log₁₀ normalized biomass size spectra (NBSS) showing the normalized biomass (mg mm⁻³/Δ volume) as a function of size categories from stations 1 to 18 in the Northumberland Strait during autumn of 2009 located downstream of Tatamagouche, New Brunswick. The linear slope (s), linear intercept (i), curvature of the quadratic function (c), x-coordinate of the vertex of the quadratic function (x) and y-coordinate of the vertex of the quadratic function (y) are given for each station. Panels progress among stations in an along-Strait, NW→SE (top to bottom) and across-Strait, SW→NE (left to right). 64

Figure B1. Residuals from linear function fitted to the log₁₀ normalized biomass size spectra (NBSS) as a function of size-class from all stations in the Northumberland Strait during late spring of 2009. The curvature value of the quadratic function (c) fitted to the linear residuals is given for each station. Panels progress among stations in an along-Strait, NW→SE (top to bottom) and across-Strait, SW→NE (left to right). 65

Figure B2. Residuals from linear function fitted to the log₁₀ normalized biomass size spectra (NBSS) as a function of size-class from stations 37 to 50 in the Northumberland Strait during autumn 2009 located upstream of Confederation Bridge. The curvature value of the quadratic function (c) fitted to the linear residuals (c) is given for each station. Panels progress among stations in an along-Strait, NW→SE (top to bottom) and across-Strait, SW→NE (left to right). 66

Figure B3. Residuals from linear function fitted to the \log_{10} normalized biomass size spectra (NBSS) as a function of size-class from stations 19 to 36 in the Northumberland Strait during autumn of 2009 located downstream of Confederation Bridge, but upstream of Tatamagouche, New Brunswick. The curvature value of the quadratic function (c) fitted to the linear residuals is given for each station. Panels progress among stations in an along-Strait, NW→SE (top to bottom) and across-Strait, SW→NE (left to right).....	67
Figure B4. Residuals from linear function fitted to the \log_{10} normalized biomass size spectra (NBSS) as a function of size-class from stations 1 to 18 in the Northumberland Strait during autumn 2009 located downstream of Tatamagouche, New Brunswick. The curvature value of the quadratic function (c) fitted to the linear residuals is given for each station. Panels progress among stations in an along-Strait, NW→SE (top to bottom) and across-Strait, SW→NE (left to right).	68
Figure C1. Residuals from quadratic function fitted to the \log_{10} normalized biomass size spectra (NBSS) (blue) and residuals from quadratic function fitted to the residuals from the linear function fitted to the \log_{10} NBSS (red) as a function of size-class from all stations in the Northumberland Strait during late spring of 2009. Panels progress among stations in an along-Strait, NW→SE (top to bottom) and across-Strait, SW→NE (left to right).	69
Figure C2. Residuals from quadratic function fitted to the \log_{10} normalized biomass size spectra (NBSS) (blue) and residuals from quadratic function fitted to the residuals from the linear function fitted to the \log_{10} NBSS (red) as a function of size-class from stations 37 to 50 in the Northumberland Strait during autumn 2009 located upstream of Confederation Bridge. Panels progress among stations in an along-Strait, NW→SE (top to bottom) and across-Strait, SW→NE (left to right).	70
Figure C3. Residuals from quadratic function fitted to the \log_{10} normalized biomass size spectra (NBSS) (blue) and residuals from quadratic function fitted to the residuals from the linear function fitted to the \log_{10} NBSS (red) as a function of size-class from stations 19 to 36 in the Northumberland Strait during autumn of 2009 located downstream of Confederation Bridge, but upstream of Tatamagouche, New Brunswick. Panels progress among stations in an along-Strait, NW→SE (top to bottom) and across-Strait, SW→NE (left to right).....	71

Figure C4. Residuals from quadratic function fitted to the \log_{10} normalized biomass size spectra (NBSS) (blue) and residuals from quadratic function fitted to the residuals from the linear function fitted to the \log_{10} NBSS (red) as a function of size-class from stations 1 to 18 in the Northumberland Strait during autumn 2009 located downstream of Tatamagouche, New Brunswick. Panels progress among stations in an along-Strait, NW→SE (top to bottom) and across-Strait, SW→NE (left to right).72

Abstract

Quantifying the size-structured biomass of marine communities and their governing processes is directly relevant to ecosystem-based management of exploited resources, yet shallow, fluctuating, coastal ecosystems, such as the Northumberland Strait, receive little research effort despite the presence of valuable fisheries. Here, I investigate whether spatial and temporal variation in the size-structured biomass of the zooplankton community is related to variation in water mass structure based on oceanographic and plankton abundance-at-size data collected in the Northumberland Strait. Principal component analysis and hierarchical agglomerative clustering of physical variables were used to define distinct oceanographic zones within the Strait. Linear and quadratic normalized biomass size spectra (NBSS) were used to quantify the size-structured biomass of the associated zooplankton community. Correlations amongst the NBSS parameters showed that biological processes governed most of the size structure variation in the zooplankton community. In spring, the NBSS was primarily influenced by biological processes while in autumn physical factors had more influence on the size structure. Top-down processes, such as predation on larger zooplankton, appeared to explain the steeper NBSS slopes relative to the hypothetical steady-state slope of -1.00. Differences in all of the NBSS parameters, except slope, between seasons, were likely due to bottom-up processes such as increased nutrient input. Similarly, bottom-up processes may have resulted in the steeper slopes in coastal waters relative to core waters in late spring. The NBSS also varied between the open ocean and each of the upper and lower Strait. The interpretation of pattern requires caution due to the effects of aliased sampling. Limitations of the quadratic NBSS, when the shape of the spectrum deviates from the parabola, indicate that the linear NBSS better describes processes governing NBSS variation. Overall, the results of this thesis have created the first quantitative zooplankton community baseline for detecting ecosystem change in the Strait.

List of abbreviations and symbols used

Abbreviation	Definition	Units
®	registered trademark	
a''_n	abundance of the n th size class	
ADST	Atlantic Daylight Saving Time	
ANOVA	Analysis of Variance	
BIONESS	Bedford Institute of Oceanography Net and Environment Sensing System	
BSS	Biomass Size Spectrum	
C_q	curvature of the quadratic function	
CCGS	Canadian Coast Guard Ship	
CTD	Conductivity, Temperature, Depth instrument	
CV	coefficient of variation	
DS	Digital Size class	
ESD	Equivalent Spherical Diameter	µm
G.O.	General Oceanics	
GPS	Global Positioning System	
i_l	intercept of the linear function	
KW	Kruskal-Wallis	
m_n	biomass of the n th size class	mg mm ⁻³
M_n	normalized biomass of the n th size class	mg mm ³ mm ⁻³
NB	New Brunswick	
NBSS	Normalized Biomass Size Spectrum	
NS	Nova Scotia	
NSERI	Northumberland Strait Ecosystem Research Initiative	
NW	Northwest	
OPC	Optical Particle Counter	
p	p-value statistic	
PC	Principal Component	
PCA	Principal Component Analysis	
PEI	Prince Edward Island	
r	Spearman's rank correlation coefficient	
r^2	coefficient of determination	
S	reduced digital Size class	
s_l	slope of the linear function	
SE	Southeast	
SError	Standard Error	
t	time of day	
TS	Temperature-Salinity	
$V_{n,ESD}$	volume of the n th size class using its geometric mean ESD	mg

Abbreviation	Definition	Units
V_{filtered}	filtered volume	mm^3
WRS	Wilcoxon Rank-Sum	
w_n	weight of the n th size class	mg
X_q	x-coordinate of the vertex of the quadratic function	
x	latitude	
Y_q	y-coordinate of the vertex of the quadratic function	
y	longitude	
z	depth	
$\Delta v_{n,k,\text{ESD}}$	size-interval; distance between the midpoints on either size of the n th and k th size-class	mm^3
σ_t	water mass density - 1000	kg m^{-3}

Acknowledgements

Many thanks to my advisor and mentor, Dr. CT Taggart, for giving me a Batcave to call home. Under your tutelage, I now know what it takes to become a scientist and your guidance led me one step closer to my dream. Thanks also to Drs. M Hanson, KT Frank and I Suthers for their ongoing help and support, all those who provided me with samples of code and thus, saving countless hours with Matlab®, and the members of the Fisheries Oceanography Lab for help, advice and counsel.

Merci à ma famille, Maman, Daddy, Céleste et Grandmaman, pour tout l'amour et soutien au cours de ces 22 années. Sans vous, ma liste d'expériences, de réussites et joies serait beaucoup plus courte. Je dédie cette thèse à vous, même si vous n'aurez probablement aucune idée de quoi il s'agit.

This document reflects three years of work and 6.5 MB of Matlab® code written to process an enormous amount of data, the seemingly endless figures illustrating every physical and biological aspect of the Strait and the blood spilled while organizing data that had previously been altered in the raw files. You won't believe after reading this that there is much more to do.

Funding was provided by a Natural Sciences and Engineering Research Council of Canada (NSERC) for an Undergraduate Student Research Award to me, an NSERC Discovery Grant to CT Taggart, the Fisheries and Oceans, Canada, Northumberland Strait Ecosystem Research Initiative (NSERI) and Dr. KT Frank, Fisheries and Oceans, Canada.

Thesis

1.0 Introduction

The aquatic biomass size spectrum (BSS) is a statistical, size-based, classification of organism biomass that has a strong theoretical basis in predator-prey dynamics (Sheldon et al. 1972; Kerr and Dickie 2001). It is frequently used to quantify the structure and function of planktonic communities because it can reveal processes not readily apparent using the conventional taxonomic approach (Kerr and Dickie 2001; Suthers et al. 2006; Krupica et al. 2012). The advantages of using a sized-based classification include enabling the use of automated counting and sizing instruments for measuring plankton *in situ* and the use of advanced mathematics to infer trophic processes (Silvert and Platt 1978; Zhou and Huntley 1997; Herman et al. 2004; Zhou 2006; Krupica et al. 2012). Thus, the BSS allows the quantification of community structure and function to be analytically simplified.

Sheldon et al. (1972) first introduced the BSS concept, and they demonstrated that the concentration of biological particulate material in the ocean is (relatively) equally distributed across all size categories, from bacteria to whales. While they expressed their data in logarithmic units of average particle concentration, subsequent studies used a logarithmic measure of total biomass that is independent of body size; typically some length or mass dimension (e.g., Platt and Denman 1977; Rodriguez and Mullin 1986; Sprules and Goyke 1994; Suthers et al. 2006; Krupica et al. 2012). This “normalized” biomass size spectrum (NBSS) provides a quantitative and statistical description of the energy flow through a system that can reveal properties associated

with predator-prey interactions (Kerr and Dickie 2001).

The NBSS can be described by either a linear (Platt and Denman 1977) or a quadratic (Thiebaux and Dickie 1992) function (Fig. 1). Much effort has been made to interpret the biological meaning of the indices that arise from each of the linear (i.e., slope and intercept) and the quadratic (i.e., curvature and position of the maximum or apex) model parameters of the NBSS (Silvert and Platt 1978; Thiebaux and Dickie 1992; Thiebaux and Dickie 1993; Sprules and Goyke 1994; Heath 1995; Zhou and Huntley 1997; Zhou 2006; Krupica et al. 2012). Both the slope of the linear and the curvature of the quadratic parameterisations relate to biomass production rates, energy transfer efficiency and predator-prey interactions, whereas the intercept in the linear model and the position of the maximum in the quadratic model are typically assumed to reflect measures of organism abundance.

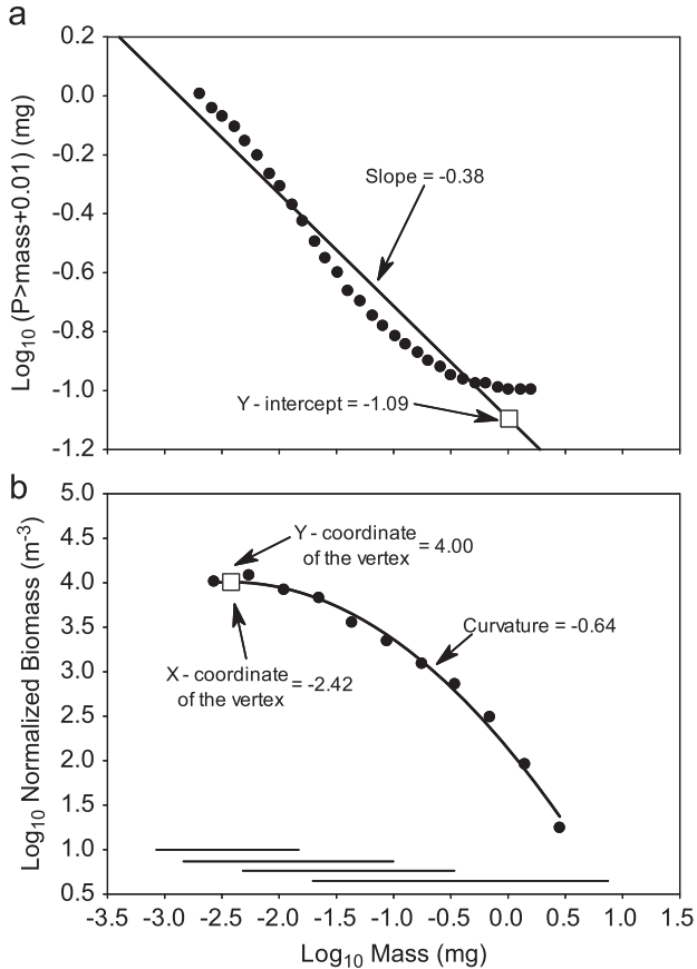


Figure 1. Normalized biomass size spectrum (NBSS) models (a) fitted with linear regression (solid line) and (b) fitted with least-squares polynomial regression, or quadratic (solid line). The NBSS parameters (indices) derived from each spectrum are labelled. (from Krupica et al. 2012)

Observations of singular (size-limited) major trophic groups (e.g., phytoplankton, zooplankton, fish, etc.) reveal distinctive parabolic biomass domes that are characterized by the quadratic function (Thiebaux and Dickie 1992; Sprules and Goyke 1994). The overall linearity arises when multiple trophic levels are considered (Sprules and Goyke 1994; Kerr and Dickie 2001; Krupica et al. 2012). Nevertheless, spectral patterns are most frequently described using the linear function.

The slope of the linear NBSS model has a theoretical steady state with a value of approximately -1.00, inferring, that in a steady-state system, the biomass is evenly

distributed across all size classes (Platt and Denman 1977; Zhou 2006; Zhou et al. 2014). A slope steeper than the -1.00 theoretical steady state implies that more biomass is concentrated in the smaller size-classes and vice versa (MacPherson and Gordoa 1996). The slope and the intercept of the linear model can vary among seasons and time (t), and in three dimensional (x, y, z ; latitude, longitude, depth) space (Rodriguez and Mullin 1986; Suthers et al. 2006), yet their relation to variation in environmental conditions, i.e., properties of the water column associated with the biomass estimates at x, y, z and t , remain unclear.

It has been postulated, in a manner consistent with ecological theory, that in marine systems, top-down and bottom-up control mechanisms can alter the local biomass size-structure with emergent properties expressed as deviations or anomalies relative to the log-linear expectation (Quintana et al. 2002; Moore and Suthers 2006; Suthers et al. 2006; Marcolin et al. 2013). These deviations are often distributed over a parabola and are sometimes referred to as “Dickie” domes (Dickie et al. 1987). Note, “Dickie” domes are different than the parabolic domes described by Thiebaux and Dickie (1992), but have also been shown to coincide with single functional groups (Quintana et al. 2002). Examples of bottom-up processes include the presence of a thermocline and nutrient input (e.g., estuaries) expressed as positive anomalies and examples of top-down processes include size-selective predation expressed as negative anomalies (Moore and Suthers 2006; Suthers et al. 2006; Marcolin et al. 2013) (Fig. 2). Such irregularities provide a more dynamic interpretation of the changes in the NBSS that relate to the trophic state of the aquatic community.

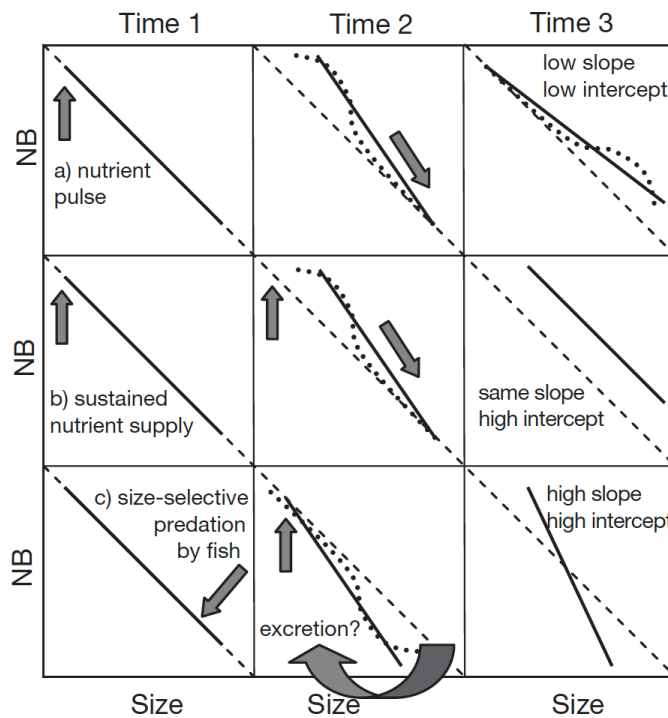


Figure 2. Example of three possible bottom-up and top-down processes altering the slope and intercept of the zooplankton NBSS at three different times: (a) a nutrient pulse, (b) a sustained nutrient supply and (c) size-selective predation by fish (from Suthers et al. 2006).

Previous studies have primarily focused on the application of the NBSS to pelagic, steady-state, marine and freshwater ecosystems (e.g., Platt and Denman 1977; Rodriguez and Mullin 1986; Sprules and Munawar 1986; Sprules and Goyke 1994; Suthers et al. 2006; Krupica et al. 2012). As highlighted by Moore and Suthers (2006), *in situ* studies in shallow, turbid, fluctuating ecosystems are difficult because the detection limit of automated counting and sizing instruments is hampered by the high concentration of under-resolved particles (< 250 µm). In such environments, slopes of the NBSS are expected to be steeper due to large nutrient input. Furthermore, studies relating the structure of the zooplankton community and environmental states are also rare (e.g., Manríquez et al. 2009; Manríquez et al. 2012; Schultes et al. 2013; García-Comas et al. 2014; Zhou et al. 2014). Most of such studies focus on the variation in the

NBSS parameters among qualitative measures of the environment and not on quantifying variation in the NBSS as a function of changes in water mass properties in x , y , z , and t .

Although recognized as an important economic (fisheries) region for generations, the Northumberland Strait is characterized as data deficient (AMEC Earth and Environmental LTD 2007); particularly regarding the role that zooplankton play on the functioning of the regional ecosystem. Additionally, clear links between the oceanographic structure of the Strait and the structure of the associated marine communities have yet to be identified. The focus of my research is on examining the spatial and temporal variation in the zooplankton NBSS in relation to water mass characteristics in an attempt to determine how water mass structure might help explain the ecological functioning of the Northumberland Strait ecosystem, where the emphasis is on bottom-up and top-down processes. Seasonal production dynamics infer that the biomass of small zooplankton in the Strait will be greater in late spring than in autumn. Additionally, if the Strait waters are well-mixed, the biomass structure is expected to be the same throughout the Strait. I also compared the size-based indices of the linear and quadratic functions describing the NBSS to assess their respective ability to characterize the zooplankton community in the Strait.

The research presented here is part of the multi-institutional Northumberland Strait Ecosystem Research Initiative (NSERI), which was designed to provide quantitative references points for the contemporary structure and ecological functioning of the Strait ecosystem.

2.0 Methods

2.1 Study area

The Northumberland Strait is a shallow (< 40 m), and typically well-mixed water body separating Prince Edward Island (PEI) from eastern New Brunswick (NB) and Nova Scotia (NS) (Fig. 3). Approximately 20 to 30 km wide and ~ 200 km long, residual flow through the Strait is normally from the northwest (NW) (entrance) to the southeast (SE) (exit) along the Strait (Lauzier 1965; Chassé and Miller 2010). The Strait is heavily influenced by nutrient-rich estuarine input and strong tidal currents (Dutil et al. 2012). Four distinct oceanographic zones have been identified within the Strait during July and August (Debertin et al. 2012) as the West, East, Center and Transition zones (Fig. 3).

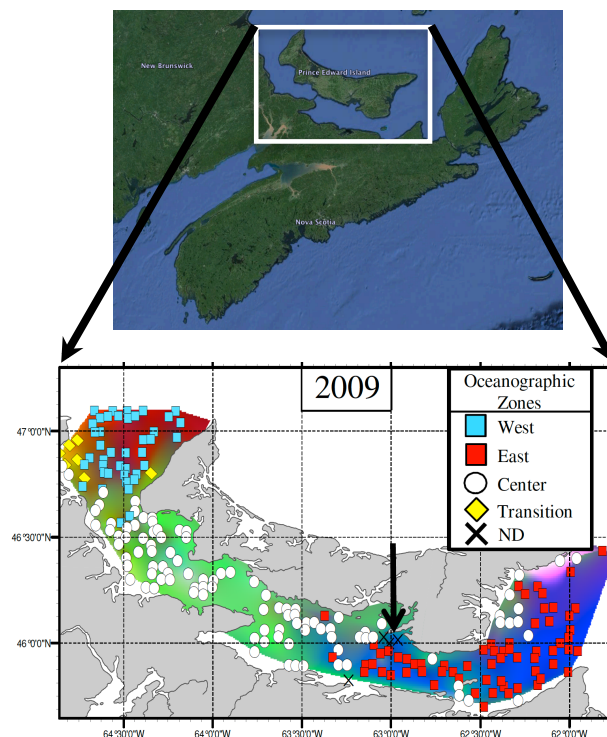


Figure 3. The Northumberland Strait and surrounding regions (inset) showing oceanographic zones within the Strait during July and August 2009 as west (blue square), east (red square), center (white circle), transition (yellow diamond) and spatially non-distinct (ND; black x) with colour contour similarities interpreted as areas with similar oceanographic conditions and are based on the principal component analysis by Debertin et al. (2012).

2.2 Sampling

Two oceanographic surveys aboard the CCGS *Opilio* were conducted in the Northumberland Strait from 25 June through 2 July 2009 (hereafter late spring), and from 2 through 15 September 2009 (hereafter autumn). Samples were collected at 24 stations (numbered 1 to 25, excluding 8), located to the NW in the upper half of the Strait in late spring, and at 50 stations (numbered 1 to 50) located throughout the Strait in autumn (Fig. 4, Table 1 & 2). At each station a Bedford Institute of Oceanography Net and Environment Sensing System (BIONESS; Sameoto et al. 1980) was towed obliquely through the water column at a nominal 1 m s^{-1} and equipped with 2 or 3 nets (note: net data was not used here). The BIONESS was fitted with an Seabird-19 (Sea-Bird Electronics) CTD (conductivity, temperature, depth sensor) used to identify water mass characteristics, and an optical particle counter (OPC) used to record plankton abundance-at-size and light attenuation data at 2 Hz (OPC-1T; Focal Technologies; Herman 1988; Herman 1992). G.O. (General Oceanics) electronic flowmeters were used to estimate volume through the OPC. Vessel GPS data were recorded at ~ 0.02 Hz in the late spring and at 1 Hz in the autumn to track location at time. A profiling Seabird-25 CTD was also deployed immediately before each BIONESS tow in late spring only (Table 3).

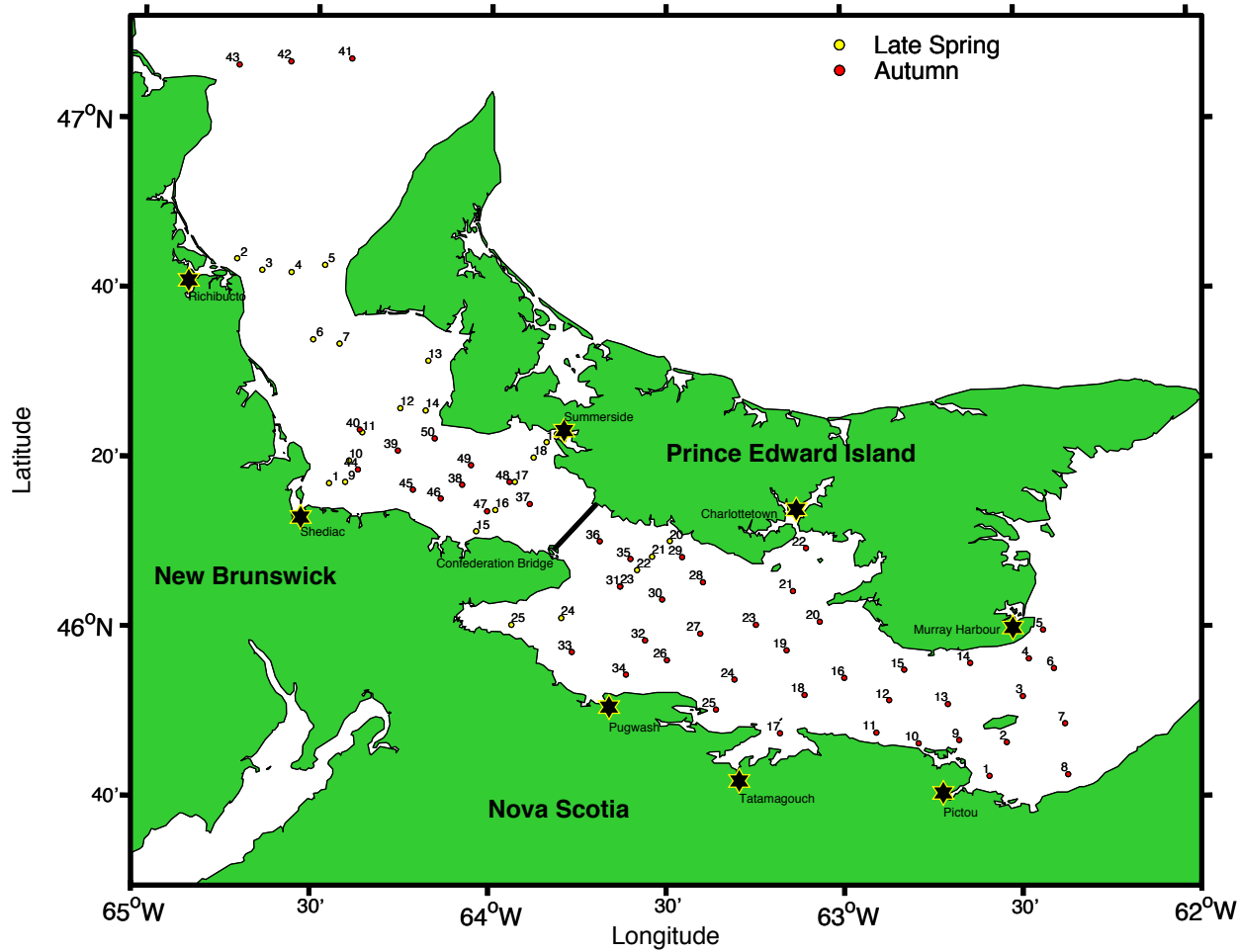


Figure 4. Sampling stations occupied in the Northumberland Strait during late spring (1 to 25, excluding 8; yellow symbols) and autumn (1 to 50; red symbols) of 2009.

Table 1. Summary of BIONESS stations occupied in the Northumberland Strait during late spring 2009 providing date and start time (ADST), location (latitude, longitude; decimal degree) and maximum tow depth.

Station Number	Date day-mon-yr	Start Time (hr:min:sec)	°N Latitude	°W Longitude	Maximum Tow Depth (m)
1	25-Jun-09	17:50:00	46.2861	64.4571	8.50
2	26-Jun-09	10:36:39	46.7254	64.7279	6.50
3	26-Jun-09	11:39:22	46.7033	64.6558	16.7
4	26-Jun-09	14:07:31	46.7000	64.5719	14.4
5	26-Jun-09	15:50:53	46.7148	64.4761	20.0
6	26-Jun-09	17:53:40	46.5681	64.5076	19.0
7a	27-Jun-09	09:49:50	46.5602	64.4321	23.7
9	28-Jun-09	08:22:08	46.2889	64.4119	10.0
10	28-Jun-09	09:23:51	46.3307	64.4014	14.6
11	28-Jun-09	10:29:45	46.3865	64.3644	14.2
12	28-Jun-09	11:56:27	46.4346	64.2567	15.5
13	28-Jun-09	13:50:25	46.5287	64.1782	9.70
14	28-Jun-09	15:00:51	46.4305	64.1845	12.0
15	1-Jul-09	09:43:33	46.1942	64.0383	8.30
16	1-Jul-09	10:49:03	46.2358	63.9844	15.3
17	1-Jul-09	12:04:04	46.2915	63.9298	16.3
18	1-Jul-09	13:44:02	46.3393	63.8766	6.20
19	1-Jul-09	14:34:12	46.3700	63.8397	4.70
20	2-Jul-09	09:44:53	46.1758	63.4892	6.20
21	2-Jul-09	10:33:04	46.1452	63.5399	11.9
22	2-Jul-09	11:26:19	46.1187	63.5823	19.2
23	2-Jul-09	13:17:18	46.0867	63.6294	16.5
24	2-Jul-09	14:44:03	46.0241	63.7966	8.00
25	2-Jul-09	15:57:08	46.0103	63.9371	5.70

Table 2. Summary of BIONESS stations occupied in the Northumberland Strait during autumn 2009 providing date and start time (ADST), location (latitude, longitude; decimal degree) and maximum tow depth.

Station Number	Date day-mon-yr	Start Time (hr:min:sec)	°N Latitude	°W Longitude	Maximum Tow Depth (m)
1	2-Sep-09	07:24:25	45.7110	62.5911	9.20
2	2-Sep-09	08:12:29	45.7768	62.5414	10.2
3	2-Sep-09	09:10:44	45.8668	62.4940	21.1
4	2-Sep-09	10:00:29	45.9408	62.4762	35.3
5	2-Sep-09	11:00:02	45.9969	62.4349	18.9
6	2-Sep-09	12:55:40	45.9210	62.4056	39.6
7	2-Sep-09	14:04:13	45.8124	62.3766	19.9
8	2-Sep-09	15:04:26	45.7123	62.3695	16.7
9	4-Sep-09	07:32:43	45.7817	62.6750	15.2
10	4-Sep-09	08:21:06	45.7760	62.7892	13.7
11	4-Sep-09	09:14:18	45.7979	62.9079	17.5
12	4-Sep-09	09:56:57	45.8615	62.8712	32.6
13	4-Sep-09	11:12:29	45.8528	62.7058	22.2
14	4-Sep-09	12:51:26	45.9331	62.6417	32.8
15	4-Sep-09	14:13:43	45.9213	62.8281	17.2
16	4-Sep-09	15:23:11	45.9058	62.9974	30.9
17	4-Sep-09	16:49:45	45.7976	63.1795	7.90
18	4-Sep-09	17:56:59	45.8728	63.1097	17.5
19	4-Sep-09	19:02:20	45.9605	63.1599	22.0
20	4-Sep-09	19:51:14	46.0165	63.0659	10.6
21	4-Sep-09	20:32:12	46.0772	63.1412	10.7
22	4-Sep-09	21:18:21	46.1613	63.1034	12.7
23	5-Sep-09	12:42:38	46.011	63.2463	17.4
24	5-Sep-09	13:39:10	45.9038	63.3073	16.2
25	5-Sep-09	14:19:26	45.8447	63.3597	10.4
26	5-Sep-09	15:27:30	45.9417	63.4977	15.0
27	5-Sep-09	16:14:21	45.9939	63.4032	18.8
28	5-Sep-09	17:08:36	46.0949	63.3957	14.3
29	10-Sep-09	09:20:17	46.1442	63.4544	9.40
30	10-Sep-09	10:11:07	46.0611	63.5111	15.2
31	10-Sep-09	11:27:16	46.0863	63.6305	13.2
32	10-Sep-09	13:36:09	45.9806	63.5591	14.1
33	10-Sep-09	14:50:12	45.9577	63.7664	10.2
34	12-Sep-09	07:20:25	45.9134	63.6132	8.10
35	12-Sep-09	09:05:04	46.1408	63.6009	13.9
36	12-Sep-09	09:53:13	46.1754	63.6878	14.0
37	12-Sep-09	11:23:50	46.2479	63.8872	19.6
38	12-Sep-09	13:11:31	46.2853	64.0795	9.80
39	12-Sep-09	14:30:07	46.3513	64.2629	20.2
40	12-Sep-09	15:20:22	46.3916	64.3717	14.0
41	13-Sep-09	12:46:22	47.1209	64.4051	33.9
42	13-Sep-09	14:36:41	47.1139	64.5807	22.7
43	13-Sep-09	15:50:26	47.1063	64.7296	14.3
44	15-Sep-09	07:18:53	46.3131	64.3756	9.70
45	15-Sep-09	08:52:45	46.2748	64.2188	14.0
46	15-Sep-09	09:30:48	46.2578	64.1399	12.5
47	15-Sep-09	10:26:42	46.2335	64.0079	10.1
48	15-Sep-09	11:13:05	46.2913	63.9448	14.0
49	15-Sep-09	12:57:16	46.3237	64.0543	10.2
50	15-Sep-09	13:55:16	46.3756	64.1581	8.80

Table 3. Summary of Seabird-25 CTD stations occupied in the Northumberland Strait during late spring 2009 providing date and start time (ADST), location (latitude, longitude; decimal degree and maximum sounding depth (m).

Station Number	Date day-mon-yr	Start Time (hr:min:sec)	°N Latitude	°W Longitude	Maximum Sounding Depth (m)
1	25-Jun-09	16:29	46.2792	64.4596	10.2
2	26-Jun-09	10:15	46.7240	64.7291	12.8
3	26-Jun-09	11:15	46.7034	64.6533	17.8
4	26-Jun-09	11:23	46.7000	64.5719	25.3
5	26-Jun-09	15:15	46.7088	64.4904	13.4
6	26-Jun-09	17:27	46.5788	64.5160	27.7
7a	27-Jun-09	9:12	46.5611	64.4257	25.2
8	27-Jun-09	10:43	46.5360	64.3213	21.4
9	28-Jun-09	07:59	46.2831	64.4147	12.7
10	28-Jun-09	09:02	46.3485	64.2996	15.6
11	28-Jun-09	10:06	46.3814	64.3626	17.0
12	28-Jun-09	11:29	46.4415	64.2708	19.3
13	28-Jun-09	13:17	46.5120	64.1796	14.0
14	28-Jun-09	14:41	46.4285	64.1729	14.2
15	1-Jul-09	09:10	46.1971	64.0440	11.5
16	1-Jul-09	10:28	46.2372	63.9871	19.0
17	1-Jul-09	11:45	46.2920	63.9303	22.5
18	1-Jul-09	13:26	46.3350	63.8759	9.00
19	1-Jul-09	14:13	46.3708	63.8342	7.10
20	2-Jul-09	09:22	46.1769	63.4885	8.40
21	2-Jul-09	10:16	46.1175	63.5434	14.8
22	2-Jul-09	11:09	46.1175	63.5819	21.7
23	2-Jul-09	12:57	46.0870	63.6311	18.4
24	2-Jul-09	14:28	46.0233	63.7915	10.6
25	2-Jul-09	15:35	46.0109	63.9337	7.80

2.3 BIONESS-OPC data processing

The majority of OPC data analyses follow Suthers et al. (2006). In summary, the plankton particles were classified by the OPC in 4096 digital size-classes (DS), each proportional to their equivalent spherical diameter (ESD, μm). The particle ESDs were then calculated from DS using the following empirical equation (Taggart et al. 1996):

$$(1) \quad \text{ESD} = 10^{0.575\log(\text{DS}) + 1.8770}.$$

To simplify the analysis, the number of digital size-classes was reduced to 64 size-classes (S) by using the integer value of the square root of DS. The number of particles in each S was then aligned with both the BIONESS-CTD and vessel GPS data. All data were then recalculated at 0.5 Hz and interpolated where needed. Filtered volume (m^3),

OPC light attenuation (mV; index related to material < 250 µm ESD) and associated data were subsequently low-pass smoothed using a centered, uniformly weighted, moving average with a window extent of 7.

The biomass (m_n) (mg/mm³) of each size-class was defined as:

$$(2) \quad m_n = a''_n \left(\frac{v_{n,ESD}}{v_{\text{filtered}}} \right),$$

where a''_n is the abundance, v_{filtered} is the filtered volume (mm³) and $v_{n,ESD}$ (mg) is the volume of the n th size-class using its geometric mean ESD. This calculation assumes that particle area, as sensed by the OPC and expressed as ESD, can be used to estimate the spherical volume of the particle and that the volume has a specific gravity of 1. The biomass estimates were then normalized (M_n) (mg/mm³/mm³) as follows:

$$(3) \quad M_n = m_n / \Delta v_{n,k,ESD},$$

where $\Delta v_{n,k,ESD}$ (mm³) is the size-interval defined as the distance between the midpoints on either side of the n th and k th size-class.

The distribution of normalized biomass by size was then analysed using the normalized biomass size spectrum (NBSS) where the slope and intercept of the NBSS were determined using linear regression:

$$(4) \quad \log M_n = s_l * \log w_n + i_l,$$

where s_l is the slope, w_n (mg) is the weight of the n th size class and i_l is the intercept.

Similarly to Krupica et al. (2012), the following least-squares polynomial (quadratic) regression was also fitted to the NBSS:

$$(5) \quad \log M_n = X_q - \left(\frac{C_q}{2} \right) * (\log w_n - Y_q)^2,$$

where X_q and Y_q are the x- and y- coordinates of the vertex and C_q is the curvature of the quadratic function. Due to the restricted sampling resolution of the OPC, only size classes between 420 and 4568 μm with non-zero counts were included. Size-classes greater than the first size-class with a zero count were also excluded, as they are under resolved for the volumes sampled.

2.4 CTD processing

All data were processed and analysed using Matlab®. Downcast CTD temperature ($^{\circ}\text{C}$), salinity (PSU) and density (kg m^{-3} ; expressed as $\sigma_t = \text{density} - 1000$) data from both the profiling CTD and BIONESS-CTD were averaged into 1 m depth bins and then, were used to create water mass profiles and sections. Bins in which large anomalies (data spikes) occurred were removed and linearly interpolated.

2.5 Statistical analyses

A principal component analysis (PCA) of eight oceanographic measurements derived from the BIONESS-CTD (Table 4), in addition to season and distance from the nearest coast, was performed to interpret overall regional patterns in the oceanographic characteristics throughout the Strait. Principal component scores were then used as input variables for a hierarchical agglomerative clustering to identify distinct oceanographic zones. Euclidean distance matrices, calculated from the principal component scores, were used to cluster stations based on the average distance between the stations using a cut-off threshold of 1.1, a value slightly less than the maximum inconsistency coefficient. The inconsistency coefficient compares the height of a cluster link in a cluster hierarchy with the average height of the links below it. A

dendrogram that identifies spatially distinct areas with common oceanographic characteristics was then created.

To determine if the spatial and temporal patterns of the zooplankton communities in the Northumberland Strait were related to water masses, a Kruskal-Wallis (KW) non-parametric one-way analysis of variance (ANOVA) was used to determine if NBSS parameters within oceanographic zones, defined by clustering with similar environmental features, were related. If a significant effect was not found, the Wilcoxon rank-sum (WRS) test (also known as Mann-Whitney U test) was used to determine if there was a significant difference among the NBSS parameters and different oceanographic zones.

To determine the influences of biological and physical oceanographic variables on the NBSS parameters, correlations amongst the NBSS parameters, in addition to correlations between the NBSS parameters and various environmental variables, were quantified using Spearman's rank correlation coefficient. Environmental variables used include those defined in Table 4 in addition to total biomass (mg/mm^3), average temperature ($^\circ\text{C}$), average salinity (PSU), average density (σ_t , kg/m^3) and average light attenuation (mV).

Table 4 Range and average \pm one standard error (SError) statistics for the eight oceanographic variables from the Northumberland Strait BIONESS CTD station-specific profiles and used in the principal component analysis for late spring ($n = 24$) and autumn ($n = 50$) 2009, respectively.

Oceanographic Variable	late spring ($n = 24$) range average \pm 1 SError	autumn ($n = 50$) range average \pm 1 SError
surface temperature ($^{\circ}$ C)	12.4 to 18.6 15.8 ± 0.3	15.9 to 19.5 17.8 ± 0.1
bottom temperature ($^{\circ}$ C)	11.6 to 18.1 15.2 ± 0.4	6.8 to 18.5 16.4 ± 0.3
surface salinity (PSU)	24.2 to 29.0 28.1 ± 0.2	27.6 to 29.0 28.4 ± 0.1
bottom salinity (PSU)	27.7 to 29.1 28.3 ± 0.1	27.7 to 30.2 28.6 ± 0.1
surface density (σ_t , kg/m ³)	17.4 to 21.2 20.4 ± 0.2	19.2 to 20.8 20.2 ± 0.04
bottom density (σ_t , kg/m ³)	19.8 to 21.4 20.7 ± 0.1	19.6 to 23.4 20.6 ± 0.1
surface light attenuation (mV)	1805.6 to 2861.8 1997.7 ± 42.3	1784.9 to 2476.7 2099.4 ± 23.8
bottom light attenuation (mV)	1826.7 to 2667.8 2003.0 ± 34.3	1699.7 to 2580.9 2086.2 ± 24.7

3.0 Results

3.1 General oceanographic conditions

In late spring and autumn, stations located near the coasts of PEI and NB were well-mixed (Fig. 5). However, stations located near freshwater input had some vertical stratification (Fig. 6). Stations located in the middle of the Strait showed weak continuous stratification with no sharp cline structure (Fig. 7). Deeper stations (>20 m) had distinct cline structure at depth (Fig. 8).

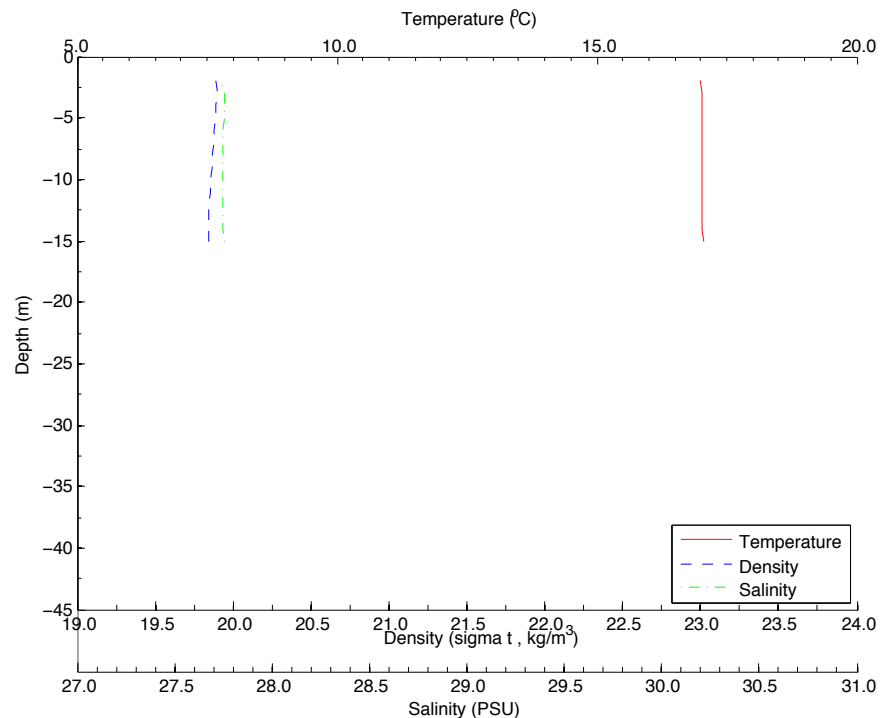


Figure 5. Example vertical temperature (°C; red), salinity (PSU; green) and density (σ_t ; blue) profiles at station 45 illustrating a well-mixed water mass in the Northumberland Strait during autumn of 2009.

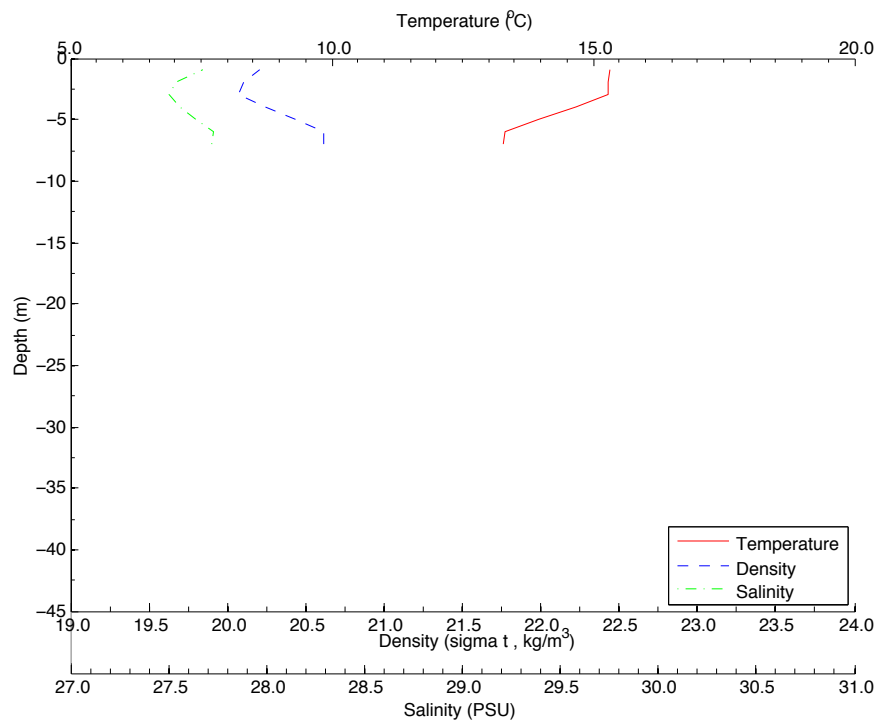


Figure 6. Example vertical temperature ($^{\circ}\text{C}$; red), salinity (PSU; green) and density (σ_t ; blue) profiles at station 2 illustrating shallow but strong water mass stratification in the Northumberland Strait during late spring of 2009.

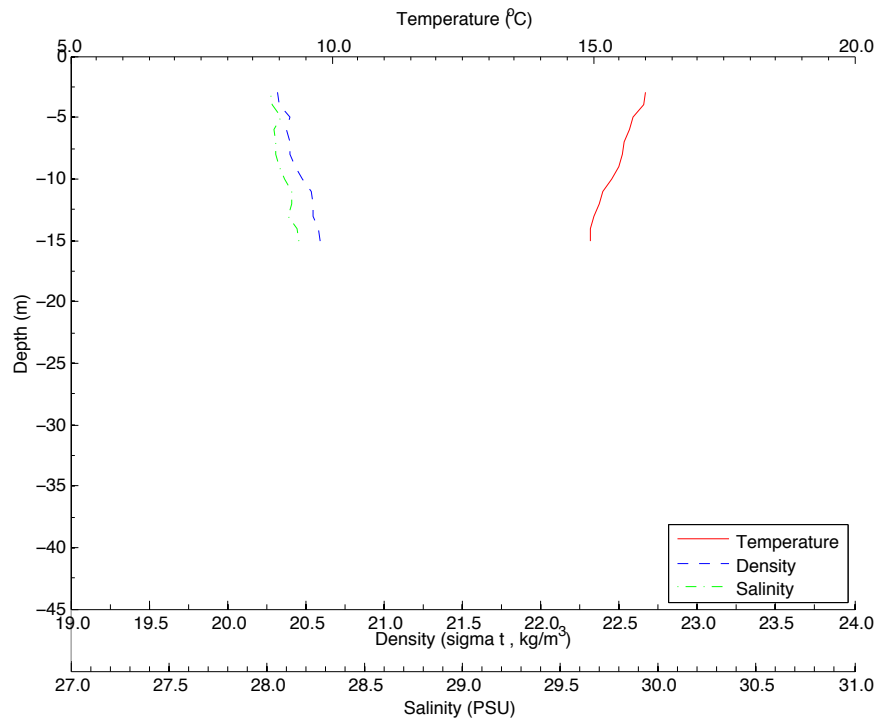


Figure 7. Example vertical temperature ($^{\circ}\text{C}$; red), salinity (PSU; green) and density (σ_t ; blue) profiles at station 11 illustrating deep but weak stratification in the Northumberland Strait during late spring of 2009.

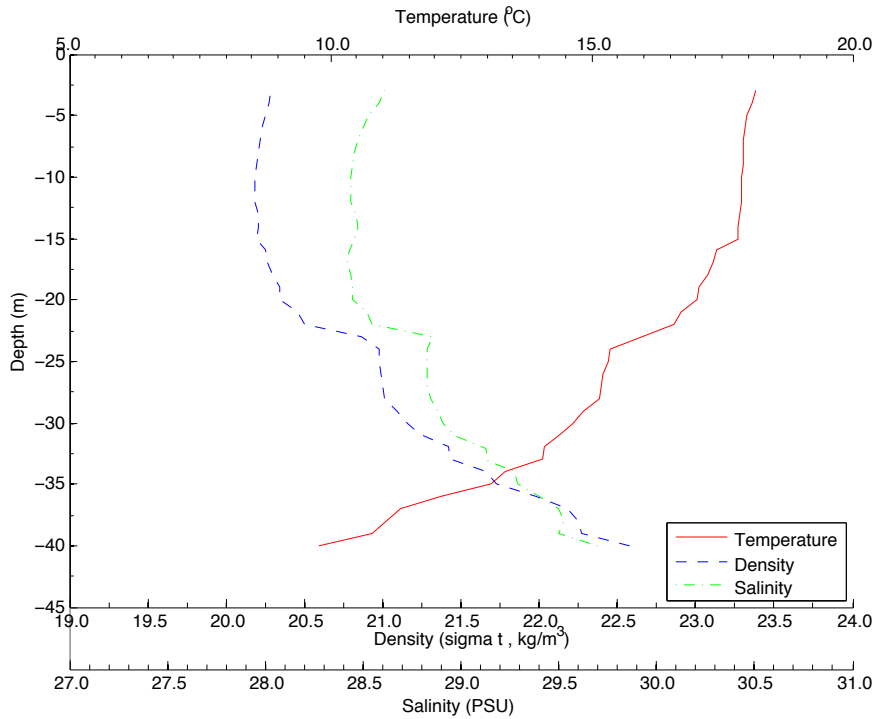


Figure 8. Example vertical temperature ($^{\circ}\text{C}$; red), salinity (PSU; green) and density (σ_t ; blue) profiles at station 6 illustrating deep and strong water mass stratification in the Northumberland Strait during autumn of 2009.

In late spring, most stations showed vertical temperature stratification with fairly constant salinity and density (Fig. 9). Trends also showed that water temperature notably increased at each station eastward along the Strait. Although salinity also increased along the Strait, changes were negligible compared to changes in water temperature. Water to the NW, near the entrance to the Strait (near Richibucto, NB) and downstream from the Confederation Bridge, was of higher density than water in-between. Hence, the mixing of at least three end-member water masses occurred near the entrance and at the exit of the sampled area within the Strait. Water upstream of the Confederation Bridge was completely mixed.

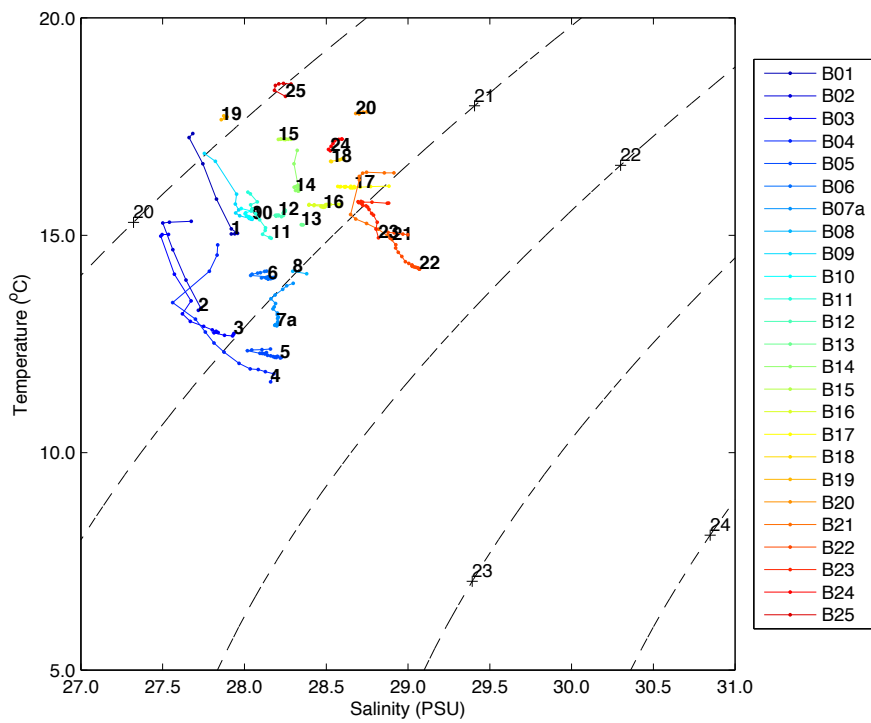


Figure 9. Temperature-salinity (TS) diagram derived from CTD profiles at each sampling station (1 to 25) in the Northumberland Strait in late spring of 2009. Lines of constant density (σ_t) are noted.

Upstream of Shédiac, NB, water temperature increased while both salinity and density decreased across the Strait from NB to PEI. Between Shédiac, NB and Summerside, PEI, a high-density core of cold, salty water was formed in the interior of the Strait (Fig. 10-12). This water mass was also present downstream of the Confederation Bridge. Accordingly, water near the coast had a higher temperature, lower salinity and lower density compared to water in the interior of the Strait.

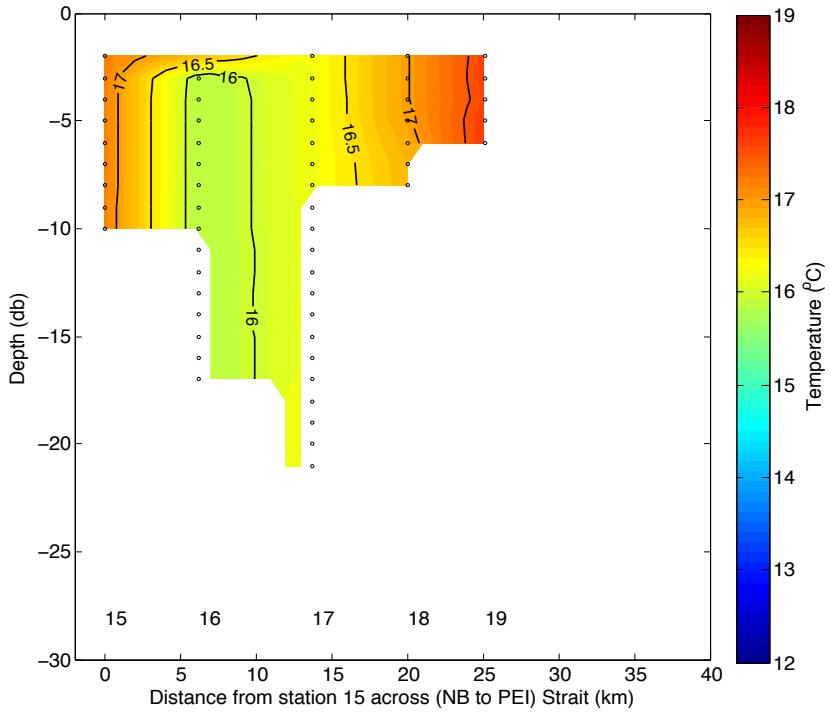


Figure 10. Temperature ($^{\circ}\text{C}$) section across the Northumberland Strait (left to right, NB to PEI; km) at the stations 15 through 19 in late spring of 2009 illustrating colder ($\sim 16\text{ }^{\circ}\text{C}$), deep water in the interior of the Strait. Open circles represent each datum used to contour the section.

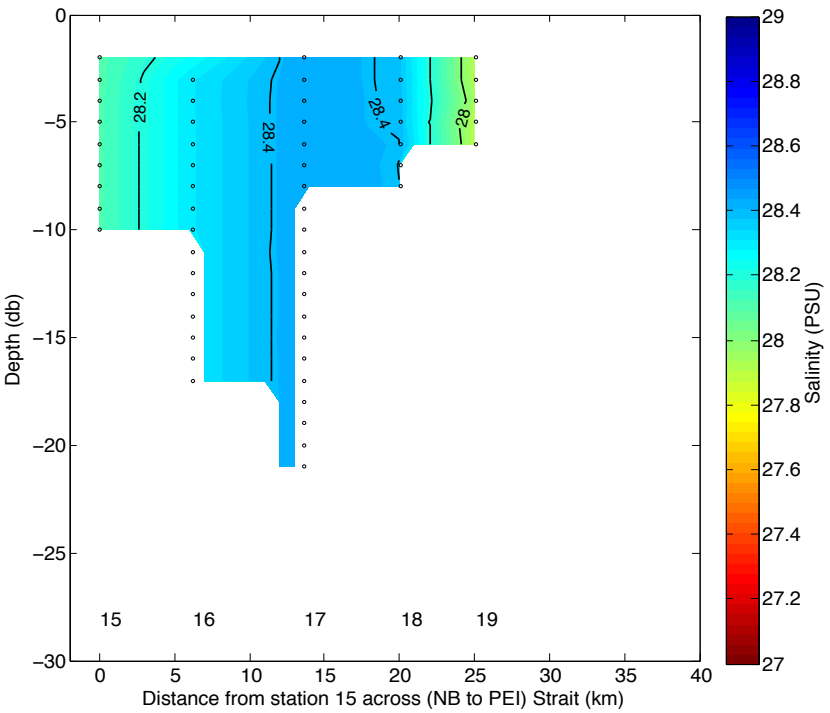


Figure 11. Salinity (PSU) section across the Northumberland Strait (left to right, NB to PEI; km) at the stations 15 through 19 in late spring of 2009 illustrating saltier (~ 28.5 PSU) core water in the interior of the Strait. Open circles represent each datum used to contour the section.

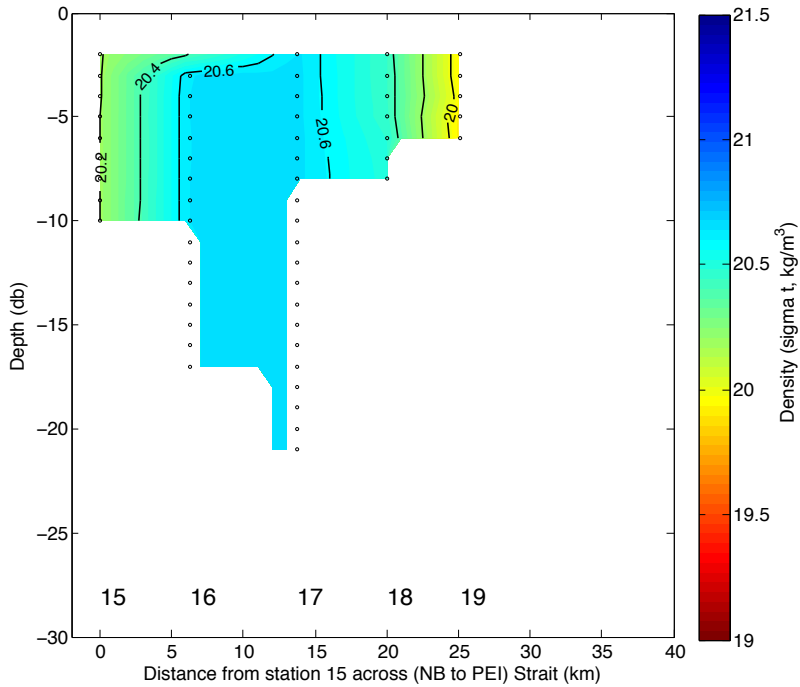


Figure 12. Density (σ_t) section across the Northumberland Strait (left to right, NB to PEI; km) at the stations 15 through 19 in late spring of 2009 illustrating dense ($\sim 20.6 \text{ kg/m}^3$) core water in the interior of the Strait. Open circles represent each datum used to contour the section.

In autumn, at least three end-member water masses were present (Fig. 13).

Inflow from the Gulf of St. Lawrence (near stations 41-43) was evident at the entrance to the Strait (near Richibucto, NB). Near-surface water temperature was relatively constant along the Strait with both salinity and density increasing downstream of the entrance to the Strait until near Charlottetown, PEI. Here, a zone of warm, fresh and light water was present and alternated with zones of cold, salty and dense water toward the outflow of the Strait (Fig. 14-16).

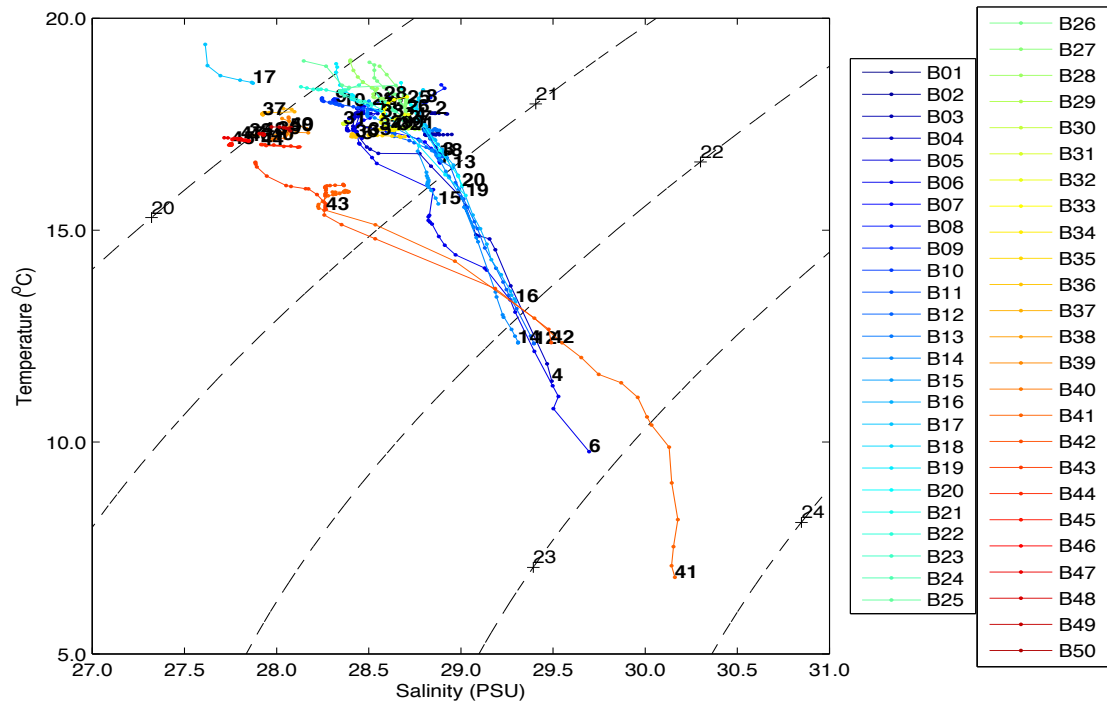


Figure 13. Temperature-salinity (TS) diagram derived from CTD profiles at each sampling station (1 to 50) in the Northumberland Strait in autumn of 2009. Lines of constant density (σ_t) are noted.

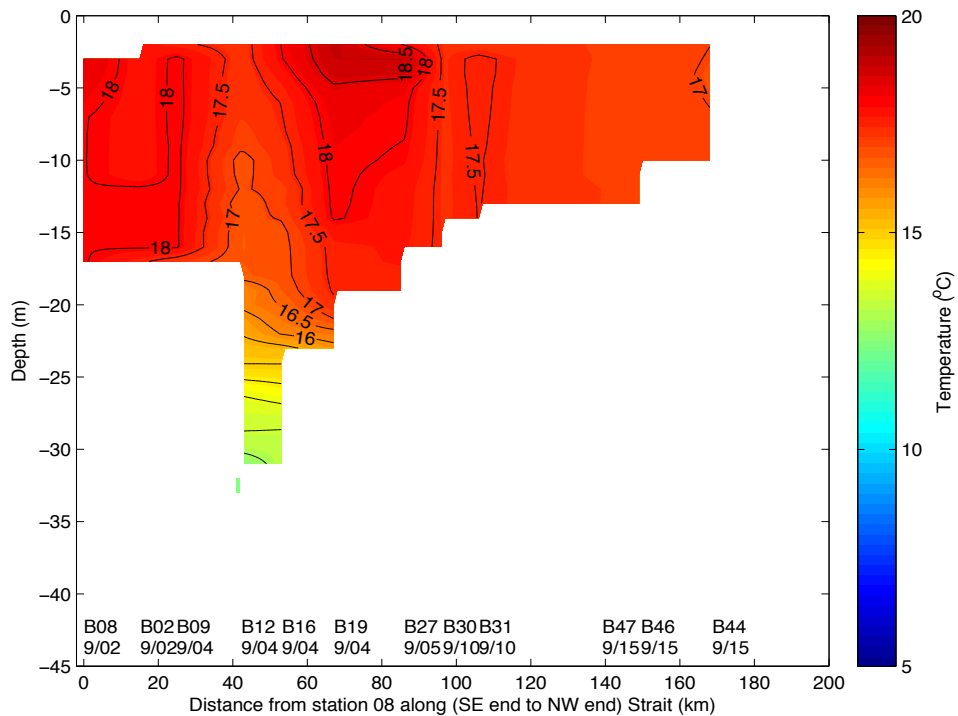


Figure 14. Temperature (°C) section along the Northumberland Strait (SE to NW; km) at stations 8, 2, 9, 12, 16, 19, 27, 30, 31, 47, 46 and 44 in autumn of 2009 illustrating the warm well-mixed surface layer and a weak thermocline at depth along the interior of the Strait.

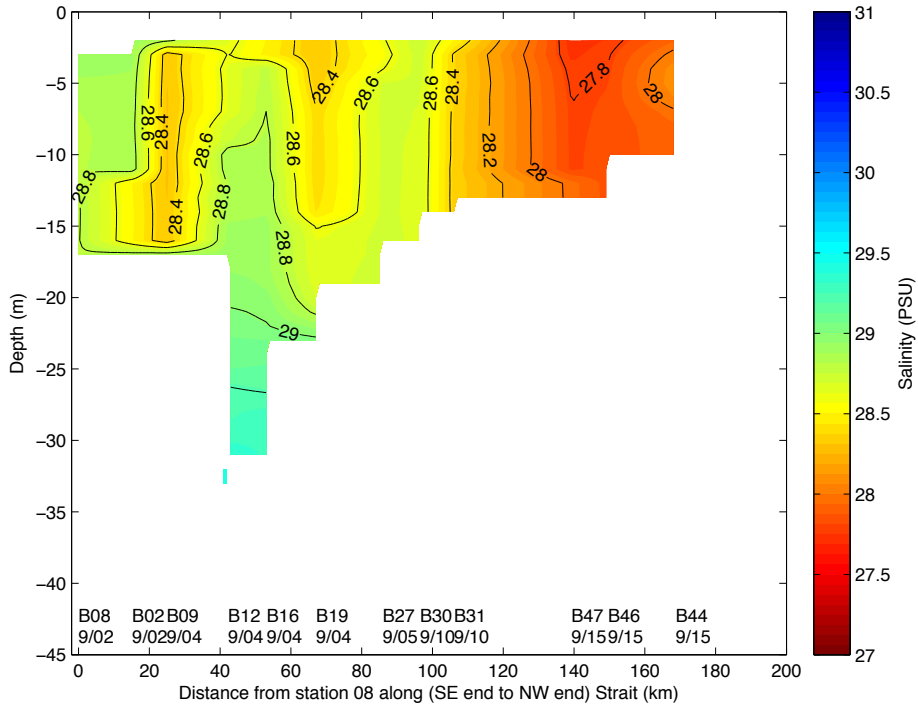


Figure 15. Salinity (PSU) section along the Northumberland Strait (SE to NW; km) at stations 8, 2, 9, 12, 16, 19, 27, 30, 31, 47, 46 and 44 in autumn of 2009 illustrating the alternating salty/fresh well-mixed surface layer, a weak halocline at depth and the relatively fresh water at the entrance (NW) to the Strait compared to the salty water near the exit (SE) from the Strait.

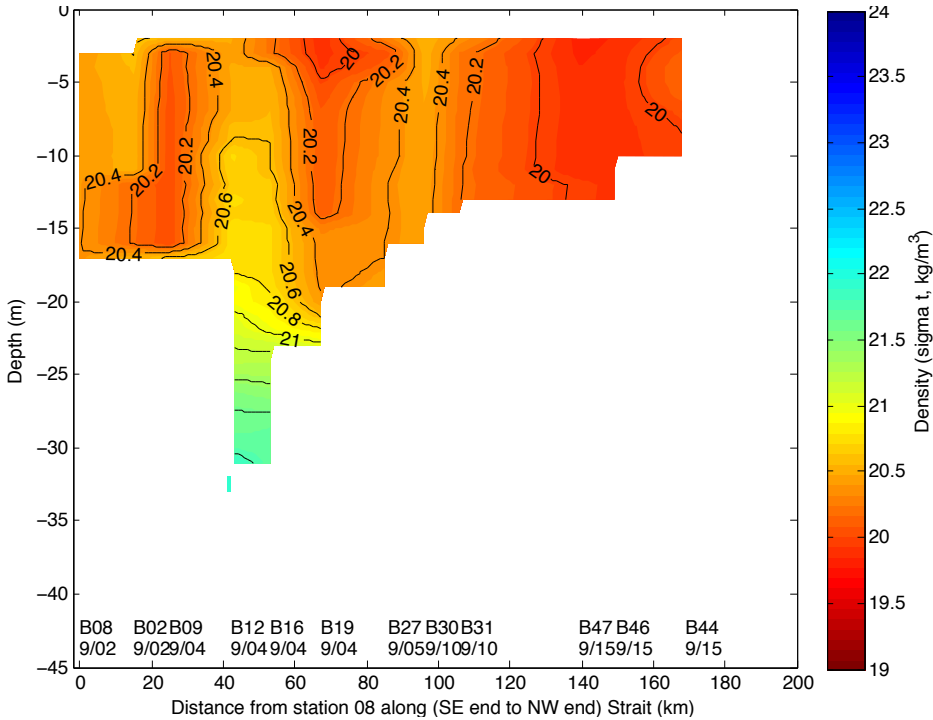


Figure 16. Density (σ_t) section along the Northumberland Strait (SE to NW; km) at stations 8, 2, 9, 12, 16, 19, 27, 30, 31, 47, 46 and 44 in autumn of 2009 illustrating the alternating dense/less dense well-mixed surface layer, a pycnocline at depth and the relatively less dense water at the entrance (NW) to the Strait compared to the dense water near the exit (SE) from the Strait.

Water upstream of the Confederation Bridge showed little variation across the Strait from NB to PEI. However, downstream of the Bridge, and upstream of Pugwash, NS, a high-density core of cold, salty water was present in the interior of the Strait; similar to oceanographic pattern observed in late spring. As the Strait widened, however, the warm, fresh water along the NB coast disappeared. At its widest extent, there was little variation in oceanographic characteristics across the Strait. As the Strait narrowed, temperature decreased while salinity and density increased. Near the outflow of the Strait, water temperature was constant, however both salinity and density increased across the Strait.

3.1 Oceanographic zones

The first three principal components of the PCA analysis explained 39.2%, 21.6% and 15.6% (total 76.4%) of water mass variation in the Strait (Fig. 17). The most influential (loading) variables were bottom density (1st PC), late spring vs. autumn season (2nd PC), and surface density (3rd PC).

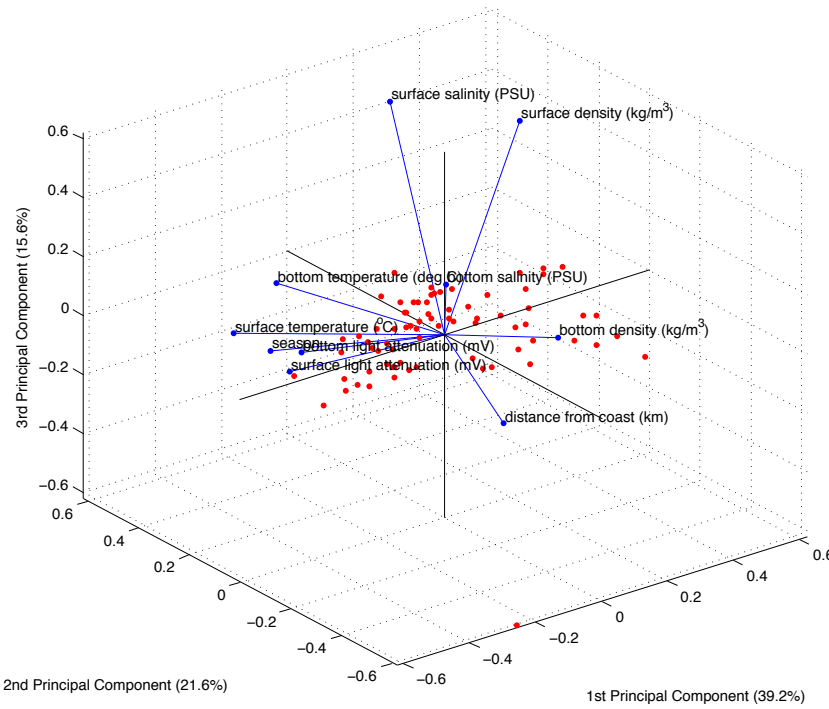


Figure 17. Explained variance among the first three principal components of the PCA analysis of water mass structure in the Northumberland Strait in late spring and autumn of 2009 based on eight oceanographic variables (Table 4), season, and distance from the nearest coast.

Cluster analysis of the principal components revealed distinct oceanographic zones that were distinguished based on season, location along and across the Strait, and depth (Fig. 18). Most stations were first separated by season, with late spring and autumn stations grouped together, respectively (Fig. 19). Only one station was erroneously clustered as an autumn station when in fact it was a late spring station. Two late spring stations and seven autumn stations were not included within the stations separated by season. Autumn stations were grouped based on maximum depth and location along the Strait. The reason for the exclusion of the two late spring stations could not be determined.

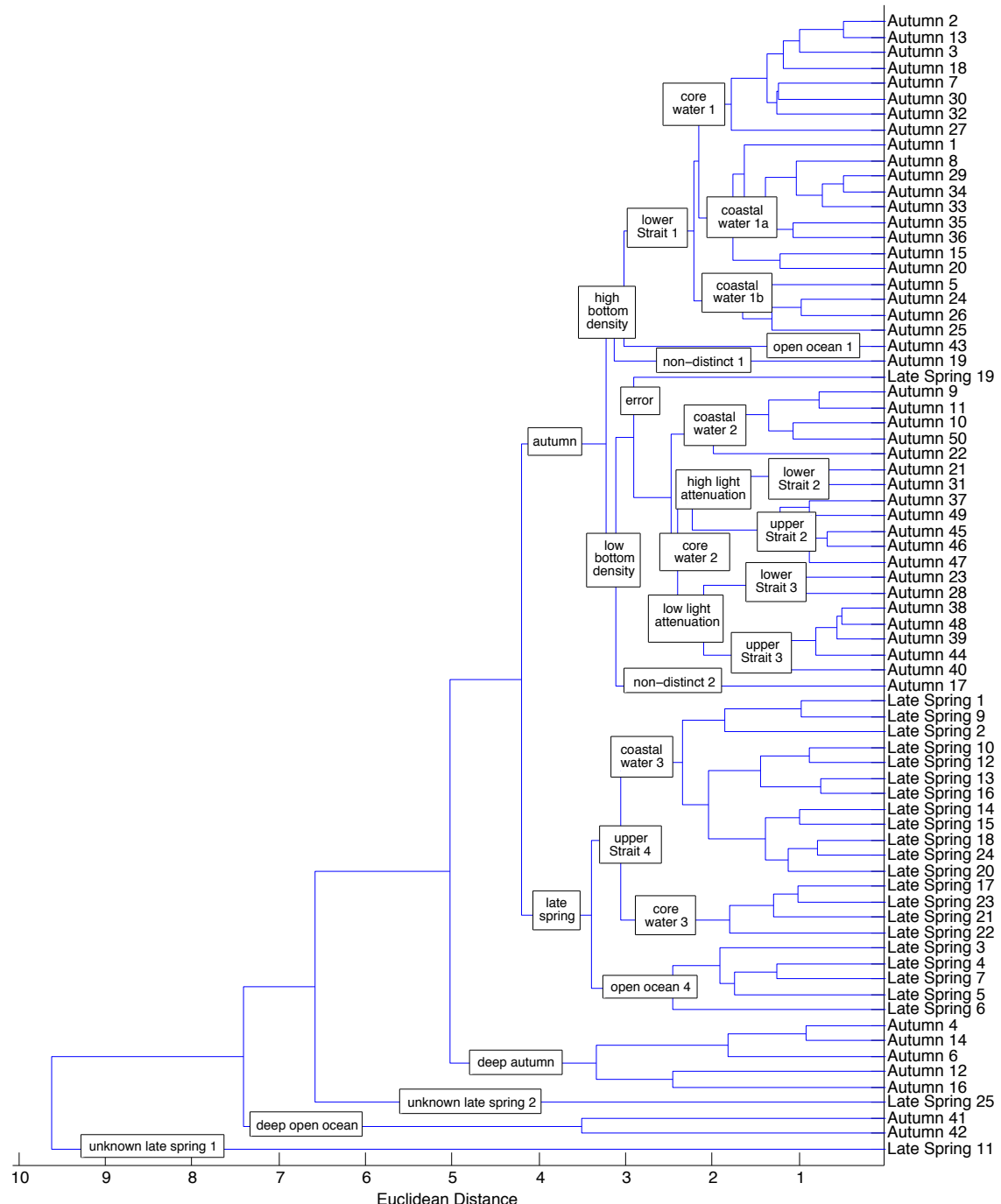


Figure 18. Dendrogram of sampling stations grouped into oceanographic zones based on similar environmental conditions measured at stations within Northumberland Strait in both late spring and autumn of 2009.

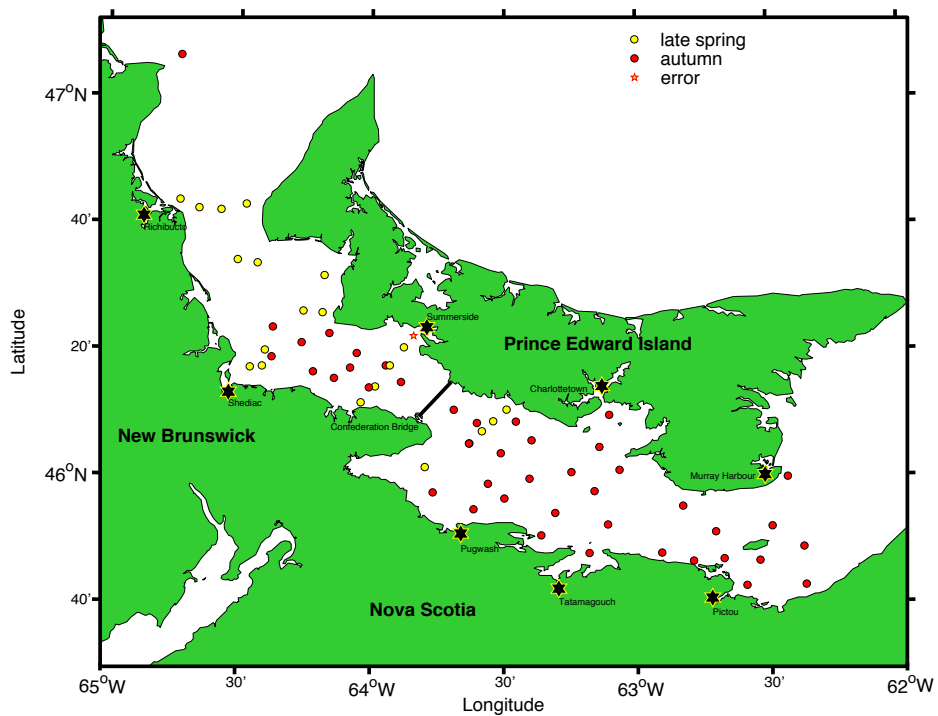


Figure 19. Distribution of late spring (yellow, $n = 21$) and autumn (red, $n = 43$) clusters within the Northumberland Strait. The single five-point star represents the late spring station erroneously clustered as autumn.

Within the late spring group, stations were further separated into groups based on location along the Strait: open ocean (i.e., stations upstream of Richibucto, NB) and upper Strait (i.e., stations downstream of Richibucto, NB, but upstream of the Confederation Bridge; Fig. 20). The upper Strait group was also separated into the core and coastal water stations (Fig. 21).

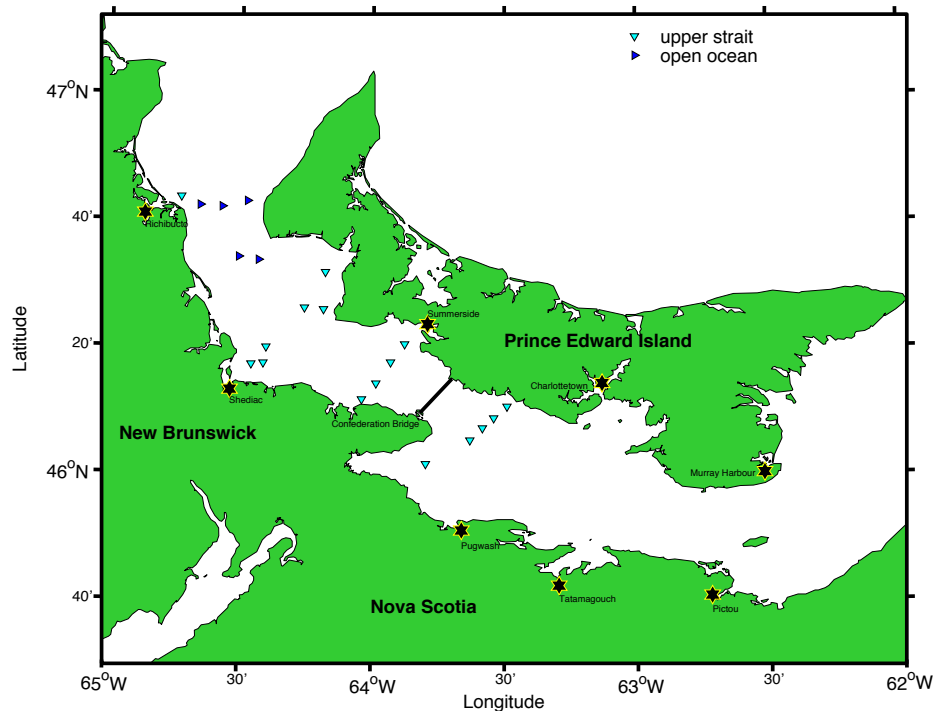


Figure 20. Distribution of upper Strait (cyan, n = 16) and open ocean (blue, n = 5) clusters within the Northumberland Strait in late spring of 2009.

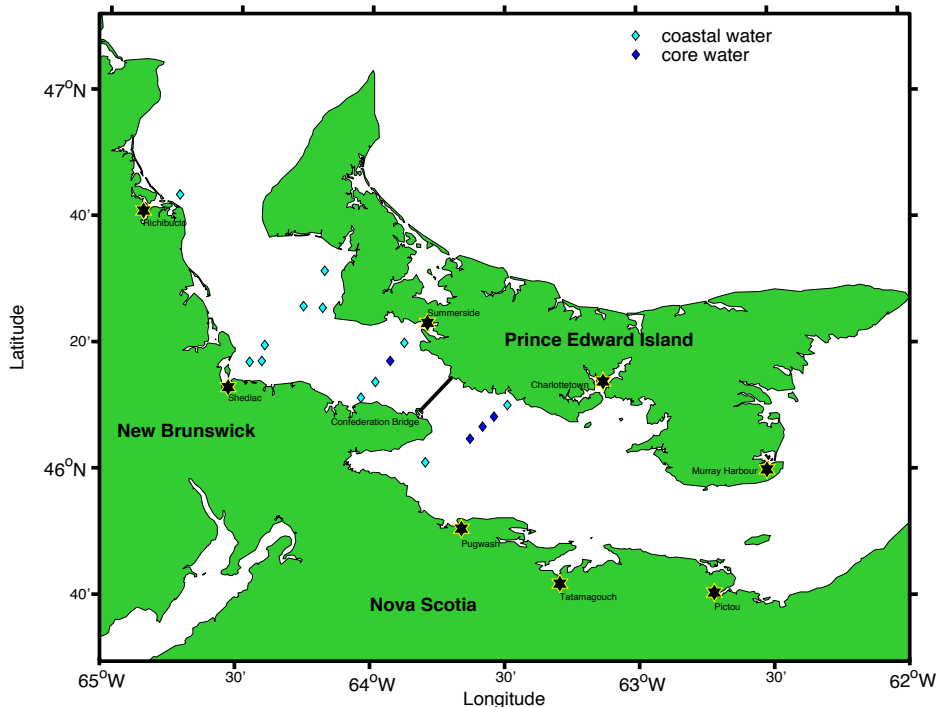


Figure 21. Distribution of coastal (cyan, n = 12) and core (blue, n = 4) stations within the upper Northumberland Strait in late spring of 2009.

Within the autumn group, stations were initially separated on the basis of bottom-water density (Fig. 22). Each of these groups was further separated based on location across the Strait (i.e., core vs. coastal water; Fig. 23 & 24). Stations with low bottom density were also separated based on location along the Strait: upper and lower Strait (i.e., stations downstream of the Confederation Bridge).

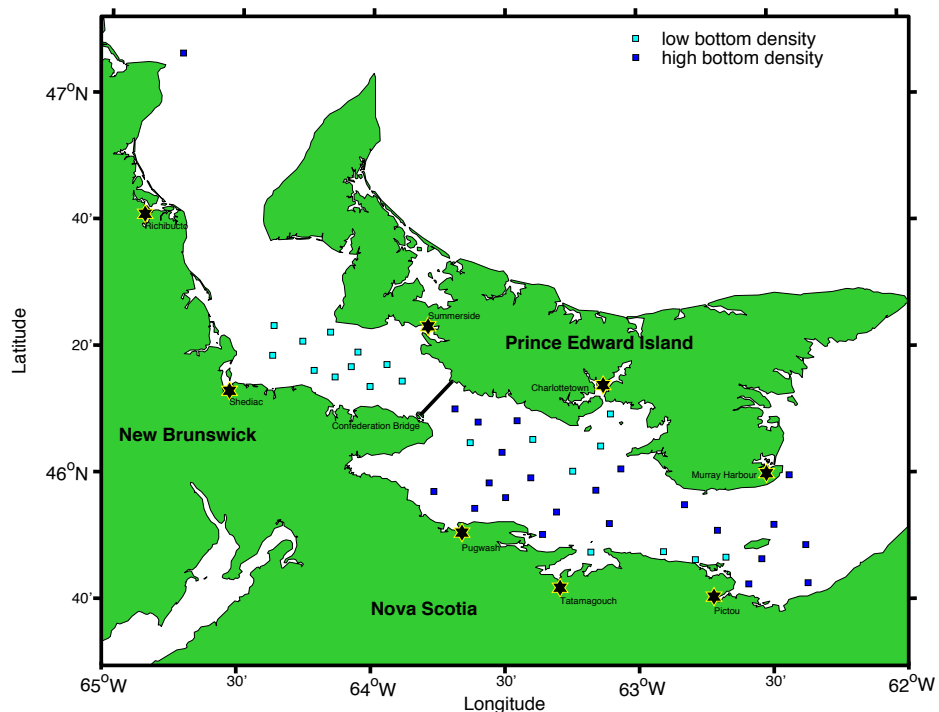


Figure 22. Distribution of low (cyan, n = 20) and high bottom density (blue, n = 23) stations within the Northumberland Strait in autumn of 2009.

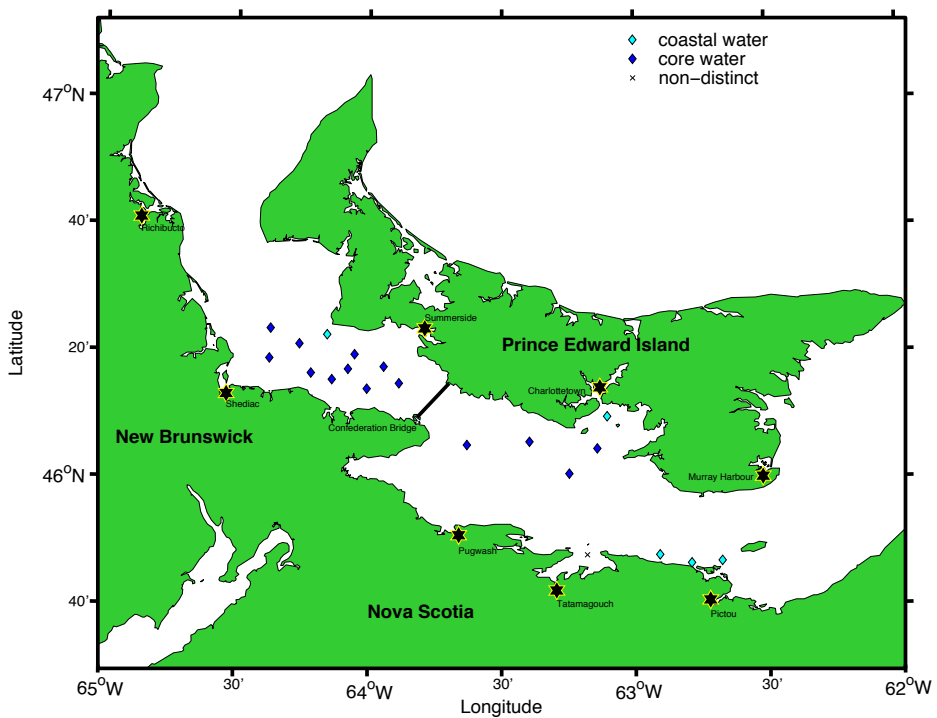


Figure 23. Distribution of coastal (cyan, $n = 5$) and core (blue, $n = 14$) stations within the low bottom density waters of the Northumberland Strait in autumn of 2009. A black cross marks the single non-distinct station.

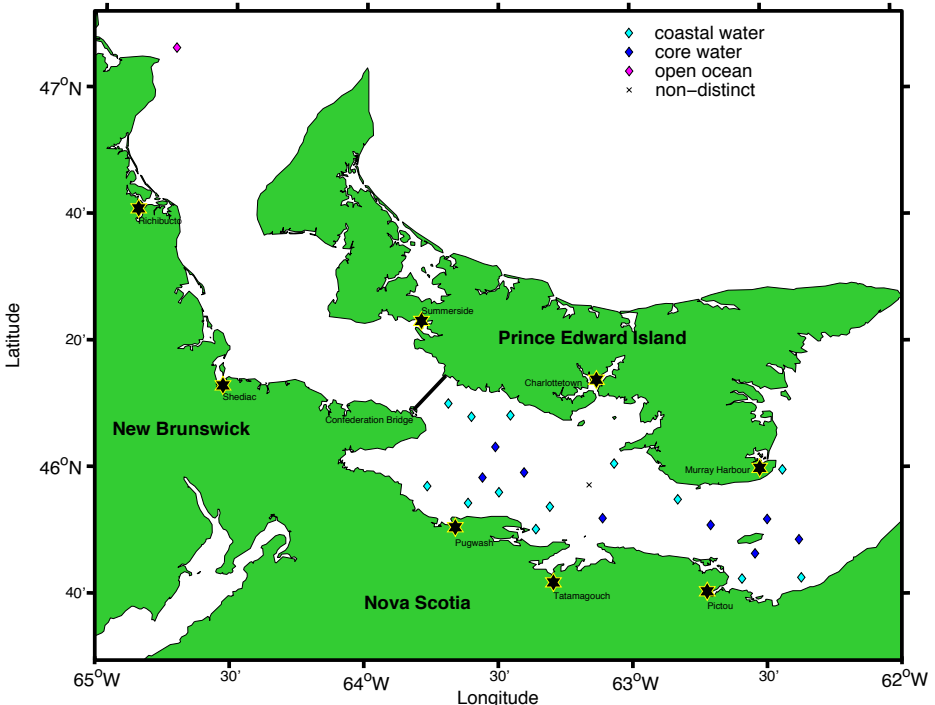


Figure 24. Distribution of coastal (cyan, $n = 13$), core (blue, $n = 8$) and open ocean (pink, $n = 1$) stations within the high bottom density waters of the lower Northumberland Strait in autumn of 2009. A black cross marks the single non-distinct station.

3.3 Normalized zooplankton biomass size spectra

All intercept and slope values of the NBSS linear regressions were significant ($P < 0.05$). In late spring, the x- and y-coordinates of the vertex, in addition to the curvature of the quadratic function were not significant at stations 16 and 21. At station 22, only the x-coordinate was not significant. At all other stations in late spring, all of the quadratic NBSS parameters were significant. All of the quadratic NBSS parameters were significant ($P < 0.05$) in autumn except the y-coordinate and curvature at station 12. NBSS parameters that were not significant were excluded from the following analyses.

Most of the NBSS had a simple parabolic dome shape (Fig. 25). However, some spectra had large deviations from this parabolic shape at larger size classes (Fig. 26). All NBSS are shown in Appendix A. In late spring, the average NBSS, using the linear function was:

$$\log M_i = -1.310 \times \log w_i - 4.363, \text{ (mean } r^2 \pm \text{SError} = 0.712 \pm 0.033; n = 24\text{).}$$

Using the quadratic function, the average NBSS was:

$$\log M_i = -3.055 + 2.399/2 \times (\log w_i + 0.879)^2, \text{ (mean } r^2 \pm \text{SError} = 0.939 \pm 0.012; n = 21\text{).}$$

In autumn, the average NBSS using the linear function was:

$$\log M_i = -1.156 \times \log w_i - 4.048, \text{ (mean } r^2 \pm \text{SError} = 0.566 \pm 0.021; n = 50\text{),}$$

and using the quadratic function, the average NBSS was:

$$\log M_i = -2.842 + 3.026/2 \times (\log w_i + 0.641)^2, \text{ (mean } r^2 \pm \text{SError} = 0.932 \pm 0.006; n = 49\text{).}$$

In every case, the fit of the quadratic model was superior to that of the linear model.

Summary statistics for all the NBSS parameters from are provided in Table 5.

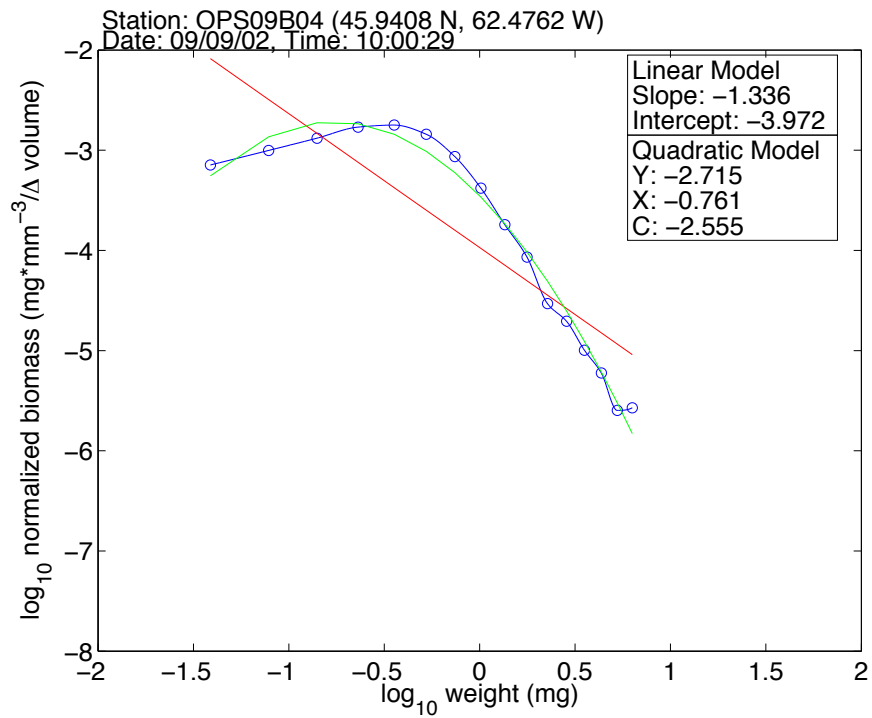


Figure 25. Example of \log_{10} normalized biomass size spectrum (NBSS) showing the normalized biomass ($\text{mg mm}^{-3}/\Delta \text{volume}$) as a function of size categories at station 4 in the Northumberland Strait during autumn of 2009 illustrating the simple parabolic dome shape.

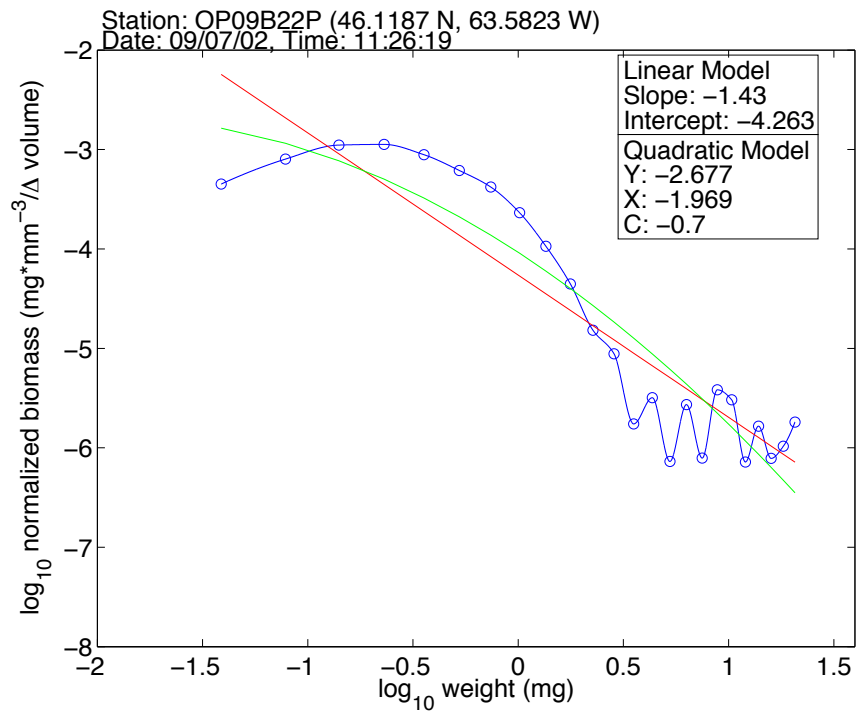


Figure 26. Example of \log_{10} normalized biomass size spectrum (NBSS) showing the normalized biomass ($\text{mg mm}^{-3}/\Delta \text{volume}$) as a function of size categories at station 22 in the Northumberland Strait during late spring of 2009 illustrating the deviations from dome shape at larger size classes.

Table 5. Range, average \pm one standard error (SError) and coefficient of variation (CV) for the slope, intercept, curvature, x-coordinate of the vertex and y-coordinate of the vertex in the Northumberland Strait during late spring and autumn of 2009, respectively.

NBSS parameter		late spring	n	autumn	n
slope	range	-1.796 to -0.445		-1.629 to -0.449	
	average \pm 1 SError	-1.310 \pm 0.064	24	-1.156 \pm 0.038	50
	CV	-0.238		-0.235	
intercept	range	-4.913 to -3.693		-4.460 to -3.688	
	average \pm 1 SError	-4.363 \pm 0.067	24	-4.048 \pm 0.030	50
	CV	-0.075		-0.053	
curvature	range	-4.706 to -0.700		-4.588 to -1.169	
	average \pm 1 SError	-2.399 \pm 0.244	22	-3.026 \pm 0.125	49
	CV	-0.477		-0.290	
x-coordinate of vertex	range	-1.529 to -0.289		-1.315 to -0.271	
	average \pm 1 SError	-0.879 \pm 0.630	21	-0.641 \pm 0.027	49
	CV	-0.330		-0.291	
y-coordinate of vertex	range	-3.723 to -2.677		-3.143 to -2.649	
	average \pm 1 SError	-3.055 \pm 0.052	22	-2.842 \pm 0.018	50
	CV	-0.081		-0.045	

Inspection of the residuals from each of the linear and quadratic NBSS models revealed non-linear trends. Residuals from the linear function appeared to be distributed over a ‘dome’ and therefore the quadratic function was fitted to these residuals (Fig. 27). In some cases, a second smaller peak occurred at larger size classes (Fig. 28). Nevertheless, the curvature of the resulting quadratic function was essentially perfectly equal to the curvature of the quadratic function fitted to the original NBSS for all stations (late spring: $r^2 = 0.999$; autumn: $r^2 = 1.000$). All residuals from the linear function are shown in Appendix B. Residuals from the quadratic function showed similar trends to the residuals from the linear function. Most of the residuals were distributed over a single dome in smaller size classes, however some had a second peak of similar value at larger size classes (Fig. 29 & 30). Further, the residuals from the resulting quadratic function were equal to the residuals from the quadratic function fitted to the original NBSS, with few exceptions. All residuals from the quadratic function are shown in Appendix C.

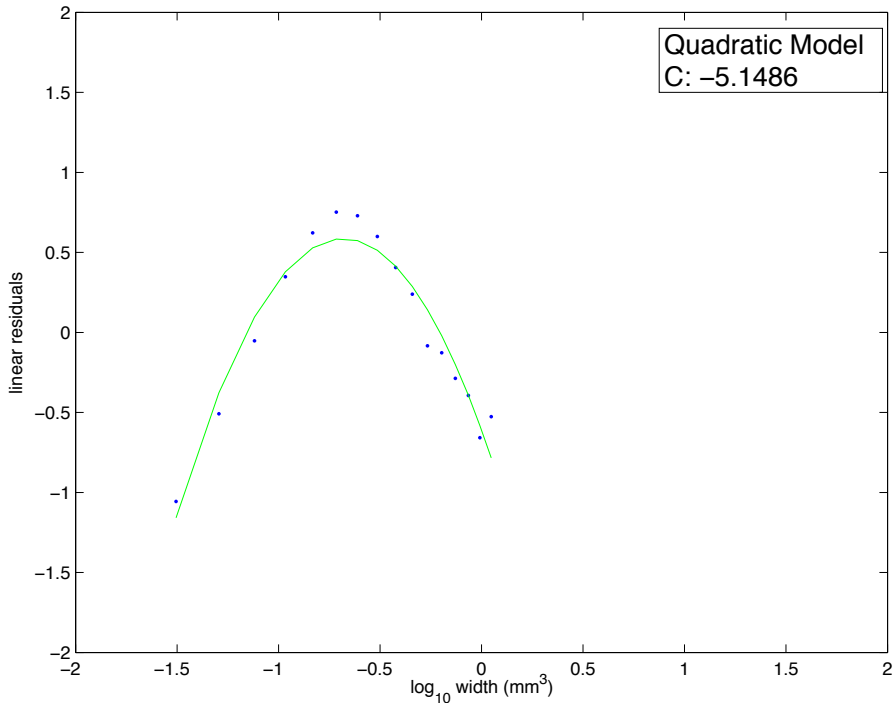


Figure 27. Example of residuals from linear function fitted to the \log_{10} normalized biomass size spectra (NBSS) as a function of size-class at station 4 in the Northumberland Strait during autumn of 2009 illustrating the distribution of residuals over a single dome.

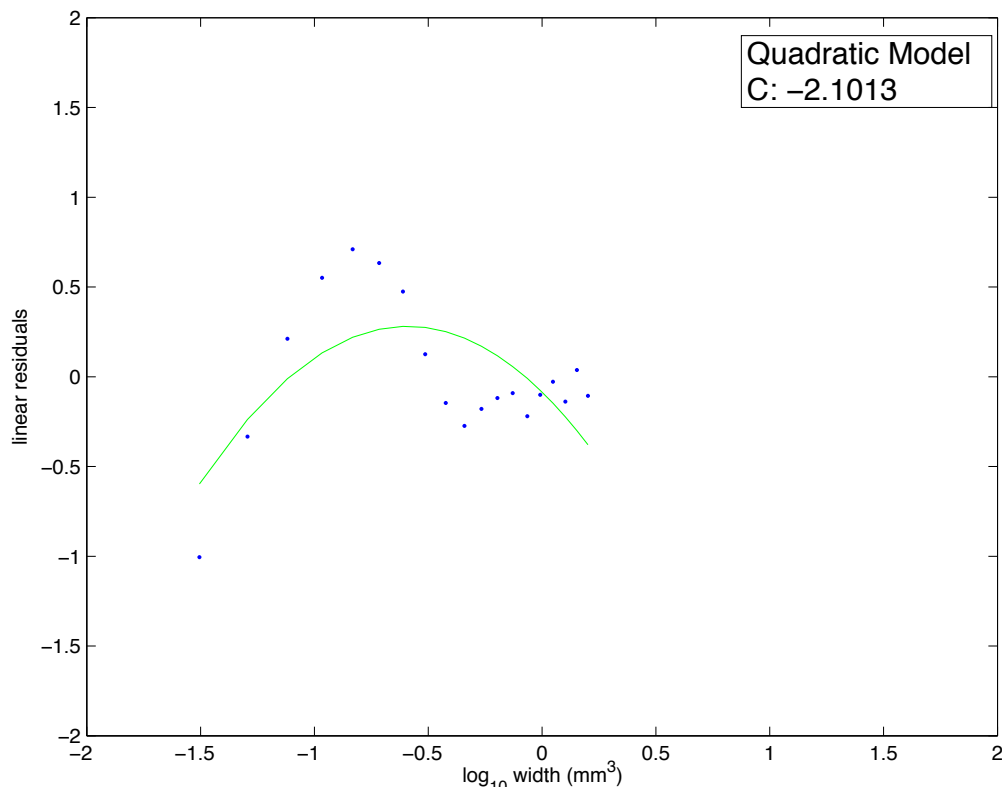


Figure 28. Example of residuals from linear function fitted to the \log_{10} normalized biomass size spectra (NBSS) as a function of size-class at station 22 in the Northumberland Strait during late spring of 2009 illustrating the a second peak at larger size classes.

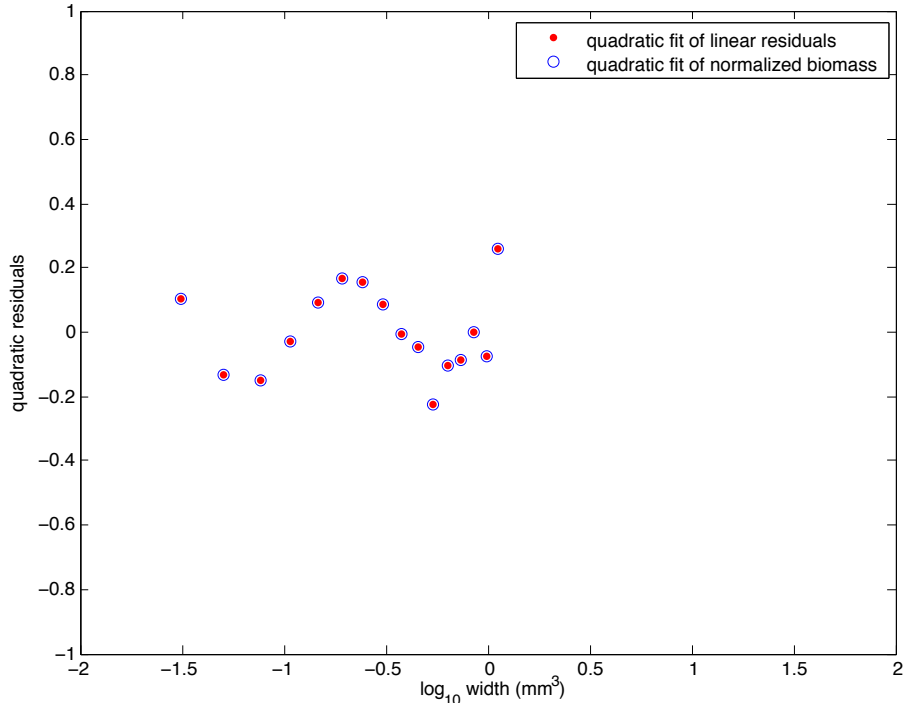


Figure 29. Example of residuals from quadratic function fitted to the \log_{10} normalized biomass size spectra (NBSS) (blue) and residuals from quadratic function fitted to the residuals from the linear function fitted to the \log_{10} NBSS (red) as a function of size-class at station 4 in the Northumberland Strait during autumn of 2009 illustrating the distribution of residuals over a single dome.

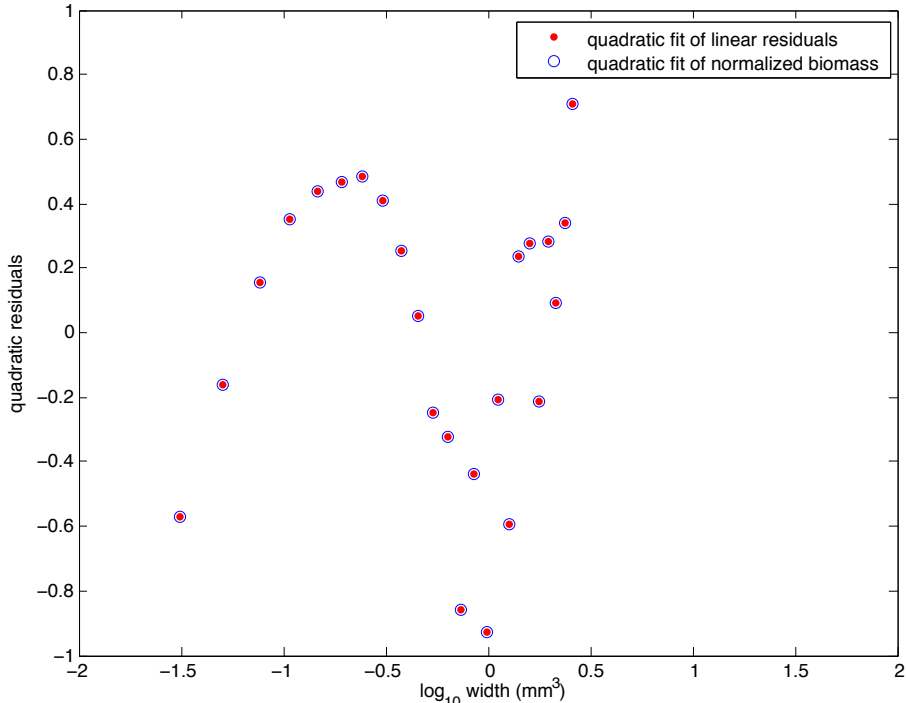


Figure 30. Example of residuals from quadratic function fitted to the \log_{10} normalized biomass size spectra (NBSS) (blue) and residuals from quadratic function fitted to the residuals from the linear function fitted to the \log_{10} NBSS (red) as a function of size-class at station 22 in the Northumberland Strait during late spring of 2009 illustrating a second peak at larger size classes.

3.4 Relationships amongst the NBSS parameters and environmental variables

Many of the NBSS parameters were correlated ($P < 0.05$) amongst themselves.

In late spring, the slope was correlated with the intercept ($r = 0.692$; Fig. 31a), i.e., a steeper slope was associated with less normalized biomass. Steeper slopes were also associated with a smaller x-coordinate of the vertex ($r = 0.606$; Fig. 31b). The x-coordinate of the vertex was also small when the intercept was small ($r = 0.573$; Fig. 32b), but larger when the curvature was more negative ($r = -0.439$; Fig. 33a). The y-coordinate was also large when the curvature was more negative ($r = -0.640$; Fig. 33b).

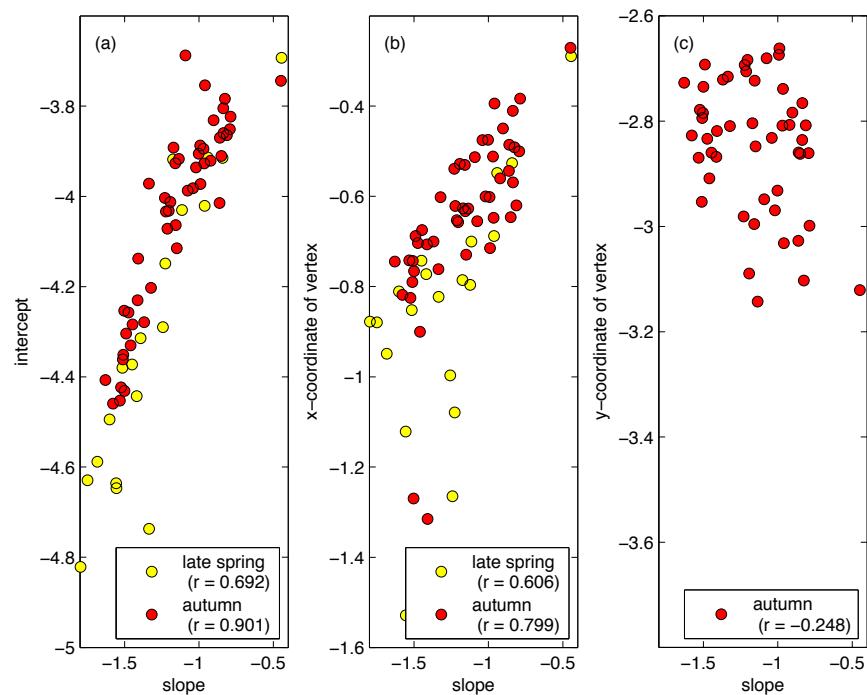


Figure 31. Scatterplot of (a) the intercept (late spring, yellow: $r = 0.692$, $n = 21$; autumn, red: $r = 0.901$, $n = 49$), (b) the x-coordinate of the vertex (late spring, yellow: $r = 0.606$, $n = 21$; autumn, red: $r = 0.799$, $n = 49$), and (c) the y-coordinate of the vertex (autumn $r = -0.248$, $n = 49$) of the normalized zooplankton size spectra (NBSS) in relation to the slope of the NBSS. All correlation coefficients (r) are significant.

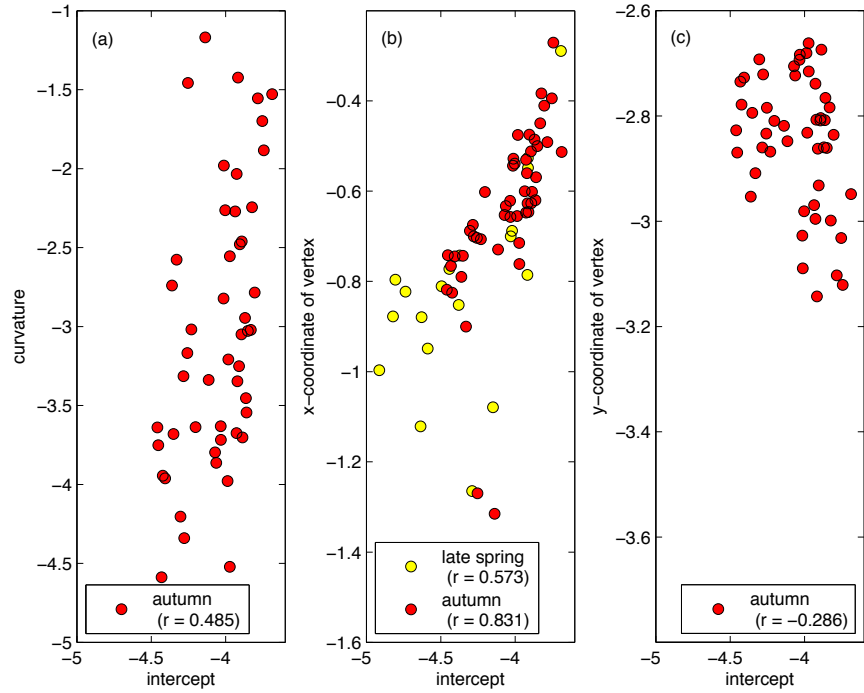


Figure 32. Scatterplot of (a) the curvature (autumn: $r = 0.85$, $n = 49$), (b) the x-coordinate of the vertex (late spring, yellow: $r = 0.573$, $n = 21$; autumn, red: $r = 0.831$, $n = 49$), and (c) the y-coordinate of the vertex (autumn: $r = -0.286$, $n = 49$) of the normalized zooplankton size spectra (NBSS) in relation to the intercept of the NBSS. All correlation coefficients (r) are significant.

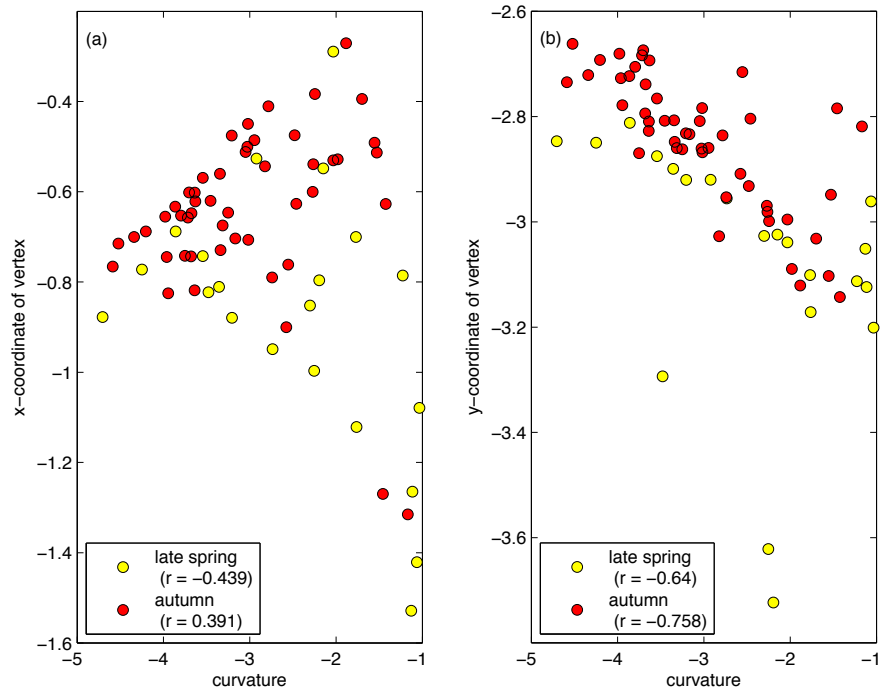


Figure 33. Scatterplot of (a) the x-coordinate of the vertex (late spring, yellow: $r = -0.439$, $n = 21$; autumn, red: $r = 0.391$, $n = 49$) and (b) the y-coordinate of the vertex (late spring, yellow: $r = -0.640$, $n = 21$; autumn, red: $r = -0.758$, $n = 49$) in relation to the curvature of the normalized zooplankton size spectra (NBSS). All correlation coefficients (r) are significant.

In autumn, the slope was also correlated with the intercept ($r = 0.901$), the x-coordinate of the vertex ($r = 0.799$) and the y-coordinate of the vertex ($r = -0.248$; Fig. 31). When the intercept was small, both the curvature ($r = 0.485$) and the x-coordinate of the vertex ($r = 0.831$) were small, but the y-coordinate of vertex was large ($r = -0.286$; Fig. 32). Additionally, when the curvature was small, the x-coordinate of the vertex was small ($r = 0.391$), but the y-coordinate of vertex was large ($r = -0.758$; Fig. 33). However, when the x-coordinate was small, the y-coordinate was large ($r = -0.420$; Fig. 34).

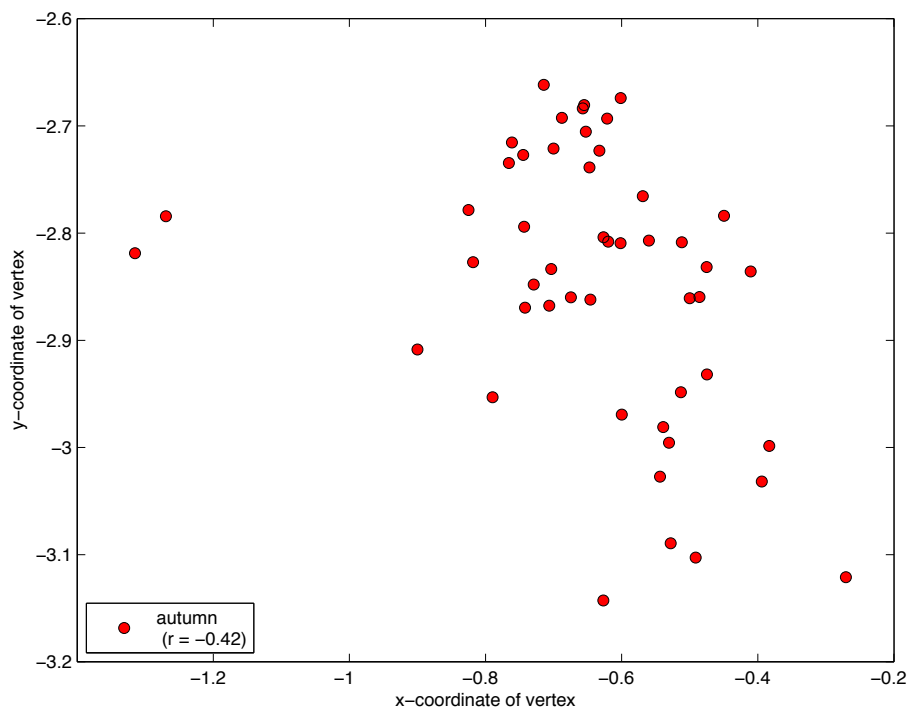


Figure 34. Scatterplot of the y-coordinate of the vertex in relation to the x-coordinate of the vertex of the normalized zooplankton size spectra during autumn ($r = -0.420$, $n = 49$). The correlation coefficient is significant.

All of the NBSS parameters were correlated ($P < 0.05$) with at least one environmental variable. In late spring, steeper slopes were associated with less total biomass ($r = 0.630$), and lower surface ($r = 0.443$) and average ($r = 0.442$) salinity (Fig. 35a & e). When the intercept was small, there was less total biomass ($r = 0.973$) and fresher water, i.e., average salinity ($r = 0.475$; Fig. 36a & d). Low curvature was associated with lower surface salinity ($r = 0.479$; Fig. 37c). When the x-coordinate of the vertex was small, there was less biomass ($r = 0.531$), and lower bottom ($r = 0.523$) and average light attenuation ($r = 0.538$; Fig. 38a & d). When the y-coordinate of the vertex was small, there was less bottom light attenuation ($r = 0.579$; Fig. 39c).

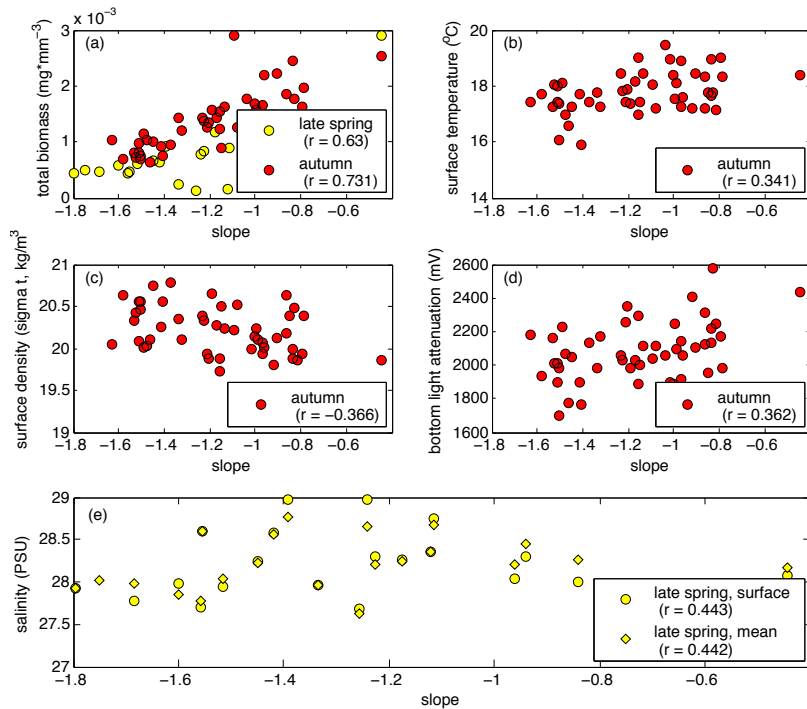


Figure 35. Scatterplot of (a) total biomass ($\text{mg} \cdot \text{mm}^{-3}$) (late spring, yellow: $r = 0.630$, $n = 21$; autumn, red: $r = 0.731$, $n = 49$), (b) surface temperature ($^{\circ}\text{C}$) (autumn: $r = 0.341$, $n = 49$), (c) surface density (σ_t , kg/m^3) (autumn: $r = -0.366$, $n = 49$), (d) bottom light attenuation (mV) (autumn: $r = 0.362$, $n = 49$), and (e) surface (late spring, circle: $r = 0.443$, $n = 21$) and average salinity (PSU) (late spring, diamond: $r = 0.442$, $n = 21$) in relation to the slope of the normalized zooplankton biomass spectra (NBSS). All correlation coefficients (r) are significant.

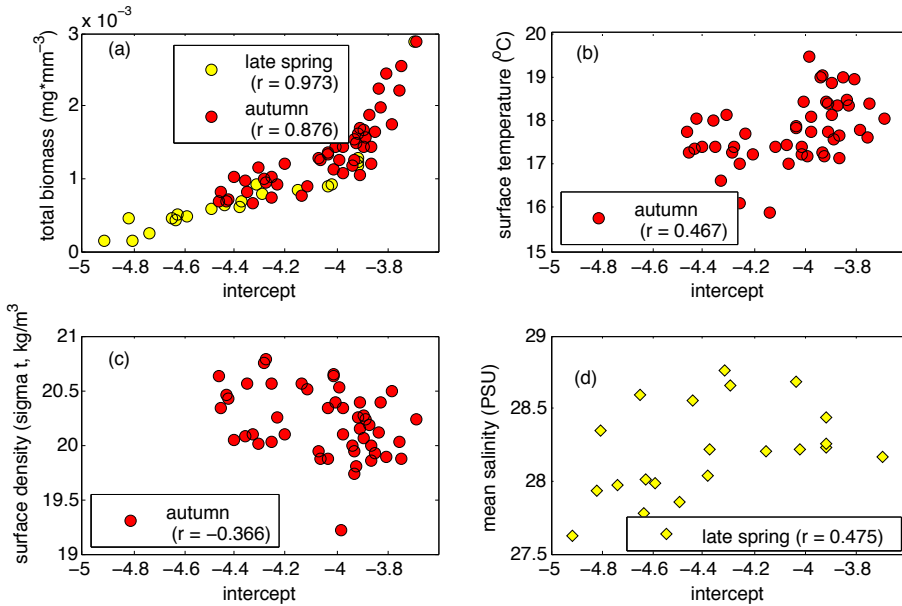


Figure 36. Scatterplot of (a) total biomass ($\text{mg} \cdot \text{mm}^{-3}$) (late spring, yellow: $r = 0.973$, $n = 21$; autumn, red: $r = 0.876$, $n = 49$), (b) surface temperature ($^{\circ}\text{C}$) (autumn: $r = 0.467$, $n = 49$), (c) surface density ($\sigma_t, \text{kg/m}^3$) (autumn: $r = -0.366$, $n = 49$), and (d) average salinity (PSU) (late spring: $r = 0.475$, $n = 21$) in relation to the intercept of the normalized zooplankton biomass spectra (NBSS). All correlation coefficients (r) are significant.

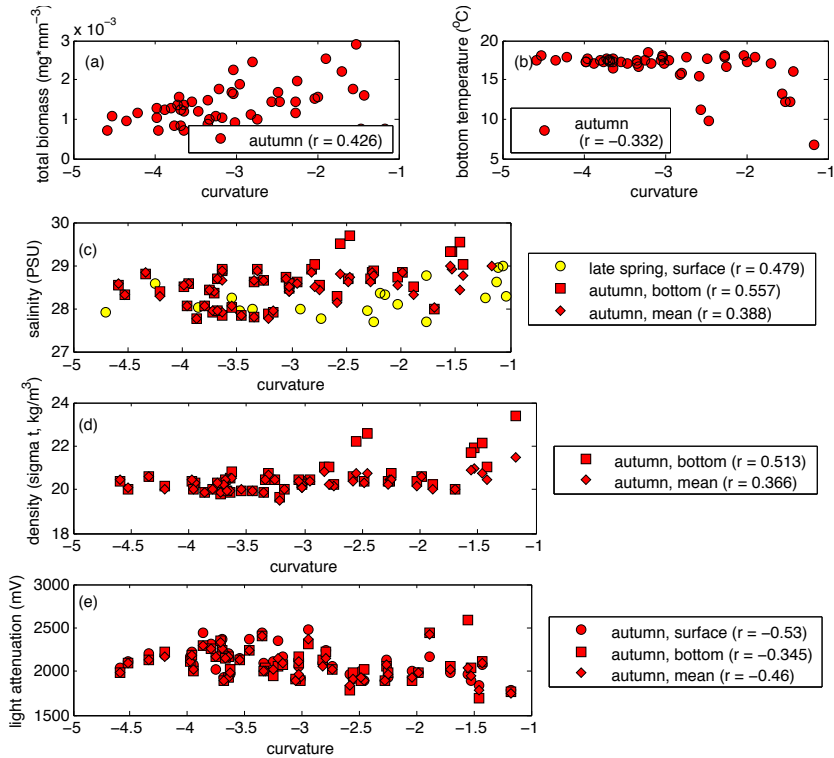


Figure 37. Scatterplot of (a) total biomass ($\text{mg} \cdot \text{mm}^{-3}$) (autumn: $r = 0.426$, $n = 49$), (b) bottom temperature ($^{\circ}\text{C}$) (autumn: $r = -0.332$, $n = 49$), (c) surface (late spring, yellow: $r = 0.479$, $n = 21$), bottom (autumn, red square: $r = 0.557$, $n = 49$) and average salinity (PSU) (autumn, red diamond: $r = 0.388$, $n = 49$), (d) bottom (square: $r = 0.513$, $n = 49$) and average density ($\sigma_t, \text{kg/m}^3$) (diamond: $r = 0.366$, $n = 49$) during autumn and (e) surface (circle: $r = -0.530$, $n = 49$), bottom (square: $r = -0.345$) and average light attenuation (mV) (diamond: $r = -0.460$, $n = 49$) during autumn in relation to the curvature of the normalized zooplankton biomass spectra (NBSS). All correlation coefficients (r) are significant.

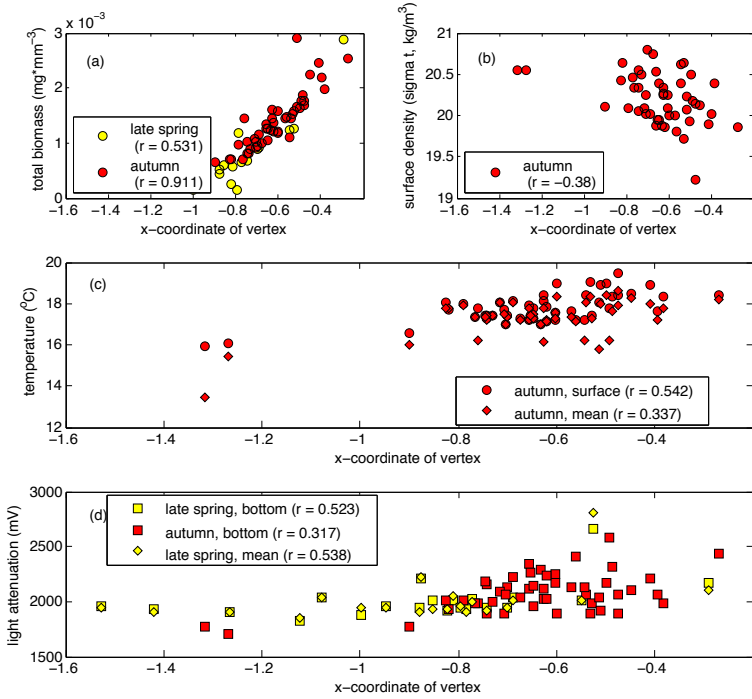


Figure 38. Scatterplot of (a) total biomass ($\text{mg} \cdot \text{mm}^{-3}$) (late spring, yellow: $r = 0.531$, $n = 21$; autumn, red: $r = 0.911$, $n = 49$), (b) surface density ($\sigma_t, \text{kg/m}^3$) (autumn: $r = -0.380$, $n = 49$), (c) surface (circle: $r = 0.542$, $n = 49$) and average temperature ($^{\circ}\text{C}$) (diamond: $r = 0.377$, $n = 49$) during autumn, and (d) bottom (late spring, yellow square: $r = 0.523$, $n = 21$; autumn, red: $r = 0.317$, $n = 49$) and average light attenuation (mV) (late spring, yellow diamond: $r = 0.538$, $n = 21$) in relation to the x-coordinate of the vertex of the normalized zooplankton biomass spectra (NBSS). All correlation coefficients (r) are significant.

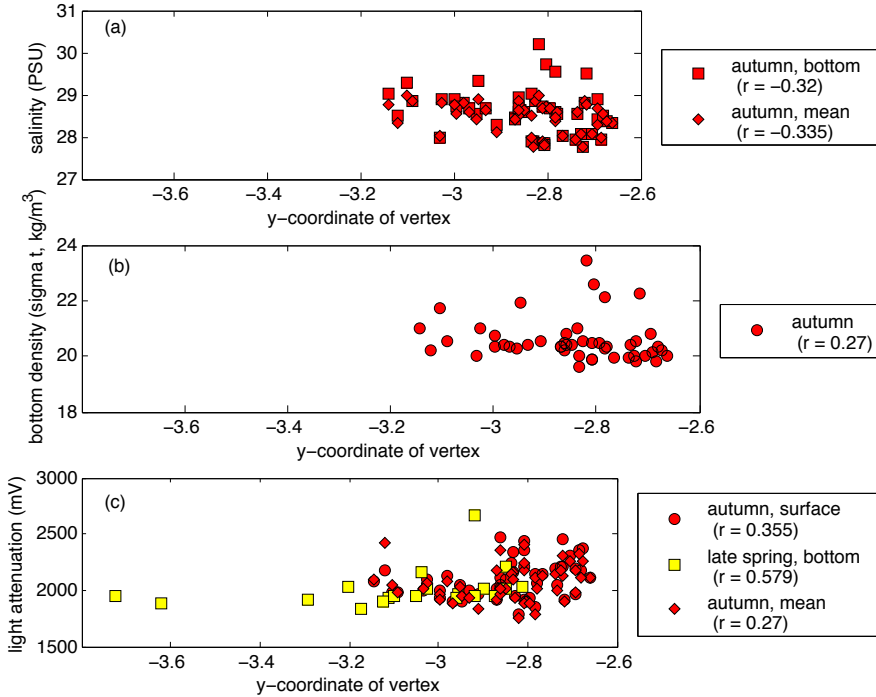


Figure 39. Scatterplot of (a) bottom (square: $r = -0.320$, $n = 49$) and average salinity (PSU) (diamond: $r = -0.335$, $n = 49$) during autumn, (b) bottom density ($\sigma_t, \text{kg/m}^3$) (autumn: $r = 0.270$, $n = 49$), and (c) surface (autumn, red circle: $r = 0.355$, $n = 49$), bottom (late spring, yellow: $r = 0.579$, $n = 21$) and average light attenuation (mV) (autumn, red diamond: $r = 0.270$, $n = 49$) in relation to the y-coordinate of the vertex of the normalized zooplankton biomass spectra (NBSS). The correlation coefficient (r) is significant.

In autumn, a steeper slope was associated with less total biomass ($r = 0.731$), colder surface temperatures ($r = 0.341$), higher density surface water ($r = -0.366$) and less bottom material < 250 μm ESD (i.e. light attenuation; ($r = 0.362$; Fig. 35a, b, c & d). When the intercept was small, there was less total biomass ($r = 0.876$), colder surface temperatures ($r = 0.467$) and higher density surface water ($r = -0.366$; Fig. 36a, b & c). A small curvature was associated with less total biomass ($r = 0.426$), warmer bottom temperatures ($r = -0.332$), lower bottom ($r = 0.557$) and average ($r = 0.388$) salinity, lower bottom ($r = 0.513$) and average ($r = 0.366$) density, and more surface ($r = -0.530$), bottom ($r = -0.345$) and average ($r = -0.460$) light attenuation (Fig. 37). Less total biomass ($r = 0.911$), higher density surface water ($r = -0.380$), less bottom light attenuation ($r = 0.317$), and colder surface ($r = 0.542$) and average ($r = 0.377$) temperatures were associated with a small x-coordinate of the vertex (Fig. 38). When the y-coordinate of the vertex was small, there was higher bottom ($r = -0.320$) and average ($r = -0.335$) salinity, lower bottom density ($r = 0.270$), and less surface ($r = 0.355$) and average ($r = 0.270$) light attenuation (Fig. 39).

3.5 Zooplankton spatial and temporal patterns

Distributions of linear NBSS parameters did not clearly show any geographic spatial or temporal patterns (Fig. 40 & 41). However, distributions of quadratic NBSS parameters showed clear seasonal patterns with more negative curvatures, and more positive x- and y-coordinates of the vertex in autumn (Fig. 42-44). In late spring, stations upstream and downstream of Shédiac, NB were different in that curvatures were more negative, x-coordinates of the vertex were more positive and y-coordinates of the vertex

were more negative upstream of Shédiac, NB. In autumn, stations up- and down-stream of Pugwash, NS were different in that curvatures were more negative and x-coordinates of the vertex were more negative upstream of Pugwash, NS. Downstream, the x-coordinates were more positive until around Tatamagouche, NS where they were similar to the negative values upstream of Pugwash, NS. Distributions of y-coordinates for the vertex in autumn did not show clear geographic spatial pattern.

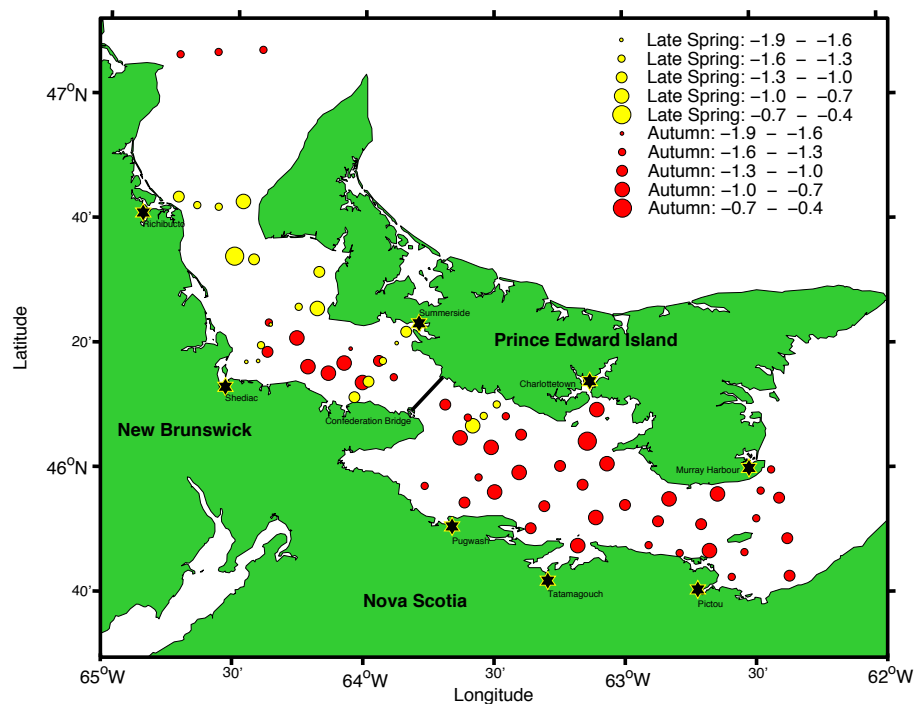


Figure 40. Distribution of the slope of normalized biomass size spectra (NBSS) within the Northumberland Strait in late spring (yellow, n = 21) and autumn of 2009.

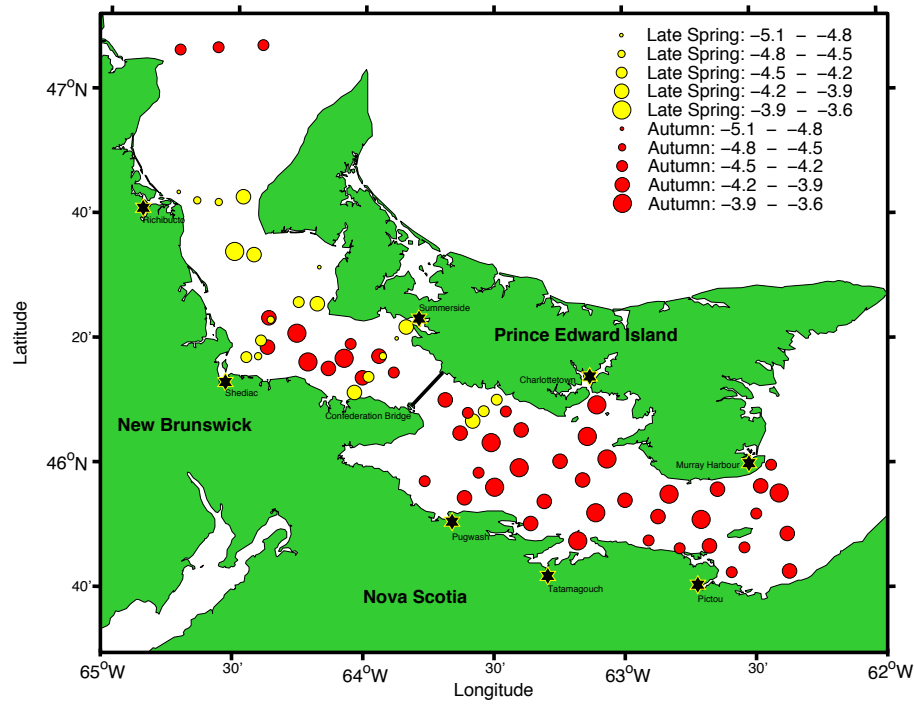


Figure 41. Distribution of the intercept of normalized biomass size spectra (NBSS) within the Northumberland Strait in late spring (yellow, n = 21) and autumn of 2009 (red, n = 49).

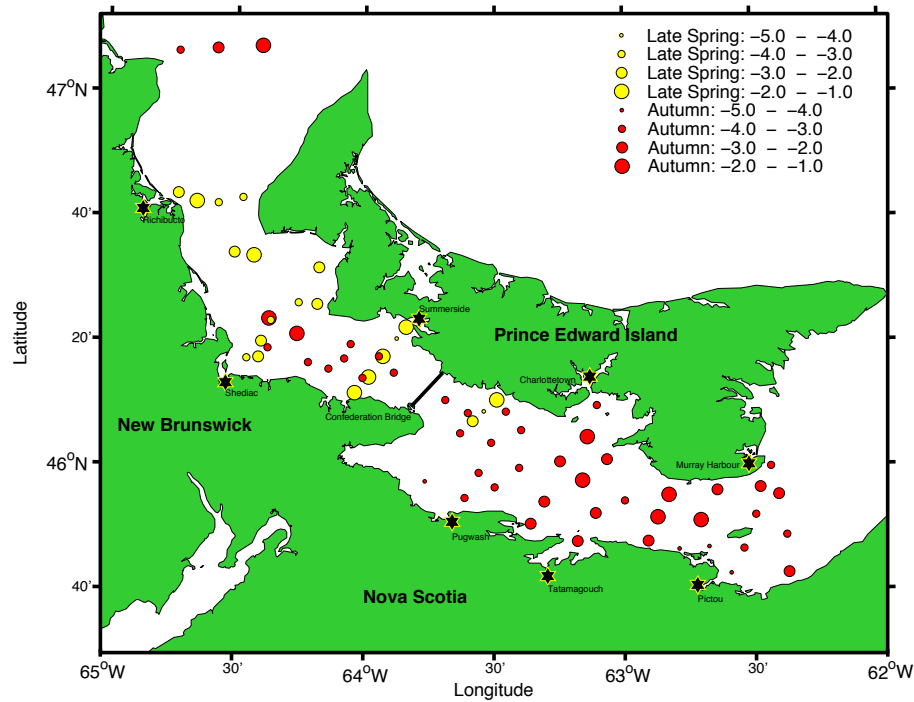


Figure 42. Distribution of the curvature of the normalized biomass size spectra (NBSS) within the Northumberland Strait in late spring (yellow, n = 21) and autumn of 2009 (red, n = 49).

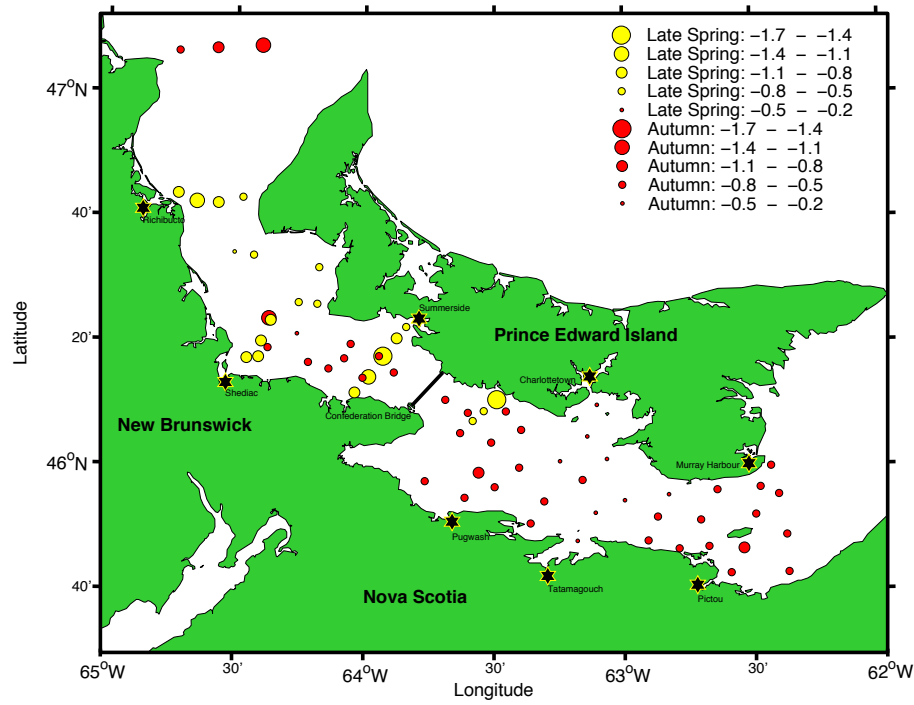


Figure 43. Distribution of the x-coordinate of the vertex of normalized biomass size spectra (NBSS) within the Northumberland Strait in late spring (yellow, $n = 21$) and autumn of 2009.

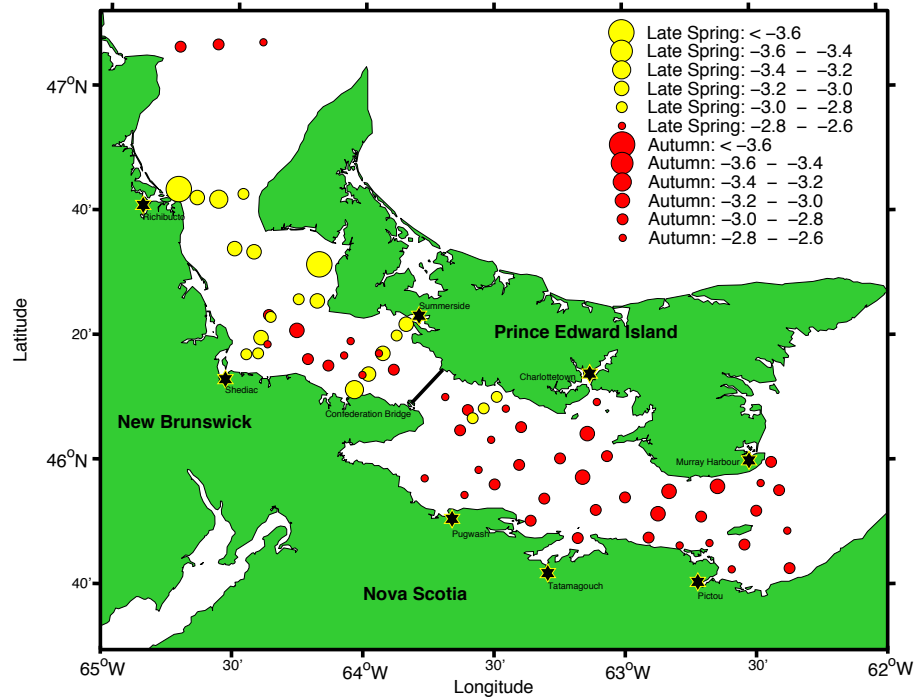


Figure 44. Distribution of the y-coordinate of the vertex of normalized biomass size spectra (NBSS) within the Northumberland Strait in late spring (yellow, $n = 21$) and autumn of 2009.

When NBSS parameters among the oceanographic zones defined using cluster analysis were compared, there were differences ($P < 0.05$) among all NBSS parameters, respectively, except for the slope between seasons (Table 6). As there was no difference (KW, $p > 0.05$) within clusters defined as core and coastal waters, respectively, for the slope, this NBSS parameter was compared between all core and all coastal stations during both late spring and autumn. Slopes in coastal waters were steeper than slopes in core waters (WRS, $p = 0.01$). However, when only autumn stations are included, there were no differences among all of the NBSS parameters, respectively, between core and coastal waters (WRS, $p > 0.05$). In autumn, there was no difference (KW, $p > 0.05$) within clusters defined as open ocean, upper Strait and lower Strait waters, respectively, for all NBSS parameters. Although there was no difference (WRS, $p > 0.05$) between NBSS parameters in upper and lower Strait waters, there were steeper slopes (WRS, $p = 0.03$), smaller intercepts (WRS, $p < 0.05$), less negative curvatures (WRS, $p = 0.01$) and smaller x-coordinates of the vertex (WRS, $p = 0.007$) in open ocean waters compared to upper Strait waters. Additionally, similar significant differences were observed for both the curvature and x-coordinate of the vertex in open ocean and lower Strait waters (WRS, $p = 0.01$; $p < 0.001$).

Table 6. P-values from the Wilcoxon rank-sum test for the slope, intercept, curvature, x-coordinate of the vertex and y-coordinate of the vertex comparisons between late spring vs. autumn, core vs. coastal water, open ocean vs. upper Strait water in autumn and open ocean vs. lower Strait in autumn. (-) indicates that the comparison was not done as a Kruskal-Wallis ANOVA revealed that there were significant differences within the clusters. Factors in bold are significant at $p < 0.05$.

Groups	slope	intercept	curvature	x-coordinate of vertex	y-coordinate of vertex
late spring vs. autumn	0.06	< 0.001	0.002	< 0.001	< 0.001
core vs. coastal (both seasons)	0.01	-	-	-	-
open ocean vs. upper Strait (autumn)	0.03	0.05	0.02	0.007	0.3
open ocean vs. lower Strait (autumn)	0.2	0.3	0.02	< 0.001	0.9

4.0 Discussion

4.1 Spatial and temporal patterns of water masses

This study demonstrated that the Northumberland Strait is, in general, well-defined as a well-mixed water body in both late spring and autumn. Some vertical stratification of the water column occurred near the coasts, especially where there is freshwater input such as that from the Richibucto River (near Richibucto, NB) and the Hillsborough River (near Charlottetown, PEI). However, distinct cline structure occurred only at deep stations near the inflow and outflow of the Strait. Thus, the cline structure likely resulted from the Strait waters at either extent of the Strait being impinged by Gulf of St. Lawrence water, which is colder, saltier and denser, that can enter the Strait at depth.

Water masses showed some unique spatial patterns during each season. Water from the Gulf of St Lawrence entering from the NW end of the Strait appeared to have created a high-density core of cold, salty water. As this water mass moved along the Strait, it was mixed with various freshwater inputs. In late spring, the water column was not completely mixed across the Strait, as the high-density core remained as seen in Figure 12. However, by autumn, waters in the upper Strait region were completely mixed and the lower Strait showed evidence of localized freshwater input as was apparent in Figure 15. Freshwater input from Hillsborough River near Charlottetown, PEI and the French River near Tatamagouche, NS likely created the 1st distinct water parcel observed as it did not vary across the Strait. The 2nd distinct water parcel likely resulted from a freshwater input near Pictou, NS as the water mass characteristics

across the Strait were consistent with a single warm, freshwater input from the NS coast and colder, salty, dense water near the PEI coast. Near the outflow of the Strait, mixing with Gulf of St. Lawrence water was evident, as waters were colder, saltier and denser than neighbouring regions.

The clustering analysis revealed that the water masses in the Northumberland Strait are clearly defined by the season, depth, and location along and across the Strait, and consistent with vertical, horizontal and temporal patterns observed in structure. However, clustering in this study was not consistent with the four oceanographic zones described by Debertin et al. (2012) wherein the zones were spatially distributed along the Strait, similarly to the open ocean, upper Strait and lower Strait regions described here. However, the four oceanographic zones defined by Debertin et al. (2012) were defined by nodes at a larger distance from the base of the dendrogram than the regions described in this study. Further, Debertin et al. (2012) did not observe similar patterns across the Strait (e.g., warmer and fresher near the coast); however, that may have been due to differences between the two studies in the cut-off thresholds used to define clusters. Discrepancies could have also resulted from using two different seasons and somewhat limited spatial coverage, in addition to fewer, though more physically traceable variables (e.g., salinity) to define the oceanographic zones in this study.

4.2 Biological and physical influences on the size structure of the zooplankton community

Biological processes governing the size structure of the zooplankton community were inherently related to the size structure itself. When slopes were steep (i.e., more

negative), there tended to be less biomass and fewer organisms > 1 mg (i.e., more negative intercept), less variability in size (i.e., more negative curvature), a smaller most frequently occurring size class (i.e., more negative x-coordinate of the vertex) and more normalized biomass in the most common size class (i.e., less negative y-coordinate of the vertex). These relationships among the NBSS parameters helped clarify whether bottom-up or top-down factors were influencing the size-structured biomass. In this case, it appeared that both types of factors were influencing the size structure as evidenced by the paucity of large zooplankton (i.e., negative residuals at larger size classes) and the abundance of small zooplankton (i.e., positive residuals at smaller size classes). Although not documented here, visual inspection of several BIONESS net-samples collected at the time of this study indicate that very small zooplankters clearly dominated.

The size structure of the zooplankton community appeared to have been influenced by different environmental variables in late spring and autumn. In late spring, NBSS parameters were only correlated to total biomass, light attenuation and salinity. Thus, biological factors may have a greater influence on the size structure of the zooplankton community in late spring. In autumn, NBSS parameters were correlated with equal strength with both biological and physical environmental variables. Similar relationships to those in late spring occurred between NBSS parameters and biological variables in autumn. However, size structure also varied with temperature, salinity and density in autumn. Thus, water mass characteristics played a larger role in shaping the size structure of the zooplankton community in autumn.

4.3 Temporal patterns in the zooplankton community structure

Temporal patterns in the zooplankton community conformed to the temporal patterns described for the water masses in the Strait. Similarly to the water masses, the size structure of the zooplankton community differed between the seasons, although the NBSS slopes were not different between seasons. However, bottom-up processes such as increased nutrients (e.g., spring phytoplankton bloom and/or riverine input) likely resulted in some of the steeper slopes in the NBSS observed in late spring.

Phytoplankton blooms typically occur in spring and the increase in primary productivity was reflected in an increase in small zooplankton abundance in late spring. The most common size class of the zooplankton community was, on average, 632 µm and associated with an 8.8×10^{-4} mg*mm⁻³/Δ volume of normalized biomass. Few organisms were > 1 mg. In autumn, the most common size class was, on average, larger (759 µm) and associated with an order of magnitude more normalized biomass (1.4×10^{-3} mg*mm⁻³/Δ volume) in addition to more organisms > 1 mg (less negative intercept), indicating that relative to spring, energy from smaller zooplankton had been transferred to larger zooplankton. Top-down processes such as predation by various zooplanktivores can selectively remove zooplankton in larger size classes and thus, can also act to steepen slopes of the NBSS (e.g., as illustrated in Figure 1c). However, as negative residuals were present for larger size classes in both seasons, predation by zooplanktivores likely occurred continuously during both seasons. This may explain why, although less steep than the slopes in late spring, the slopes in autumn were steeper than the hypothetical steady state of -1.00; i.e., feeding down the food chain.

4.4 Spatial patterns in the zooplankton community structure

Some spatial patterns in the zooplankton community conformed to the spatial patterns described for the water masses in the Strait. Similarly to water masses, the processes influencing the structure of the zooplankton community differed between core and coastal waters. Constant predation of larger zooplankton by zooplanktivours illustrated by the negative residuals for these larger size classes explains why the NBSS slopes were steeper than the theoretical steady state. Yet, nutrient-rich estuarine input likely resulted in the steeper slopes of the NBSS observed in the coastal waters. Such bottom-up processes are typically related to increases in small zooplankton biomass; however, difference within clusters prevented comparisons of other NBSS parameters between core and coastal waters. As highlighted above, differences within clusters were due to the presence of NBSS parameters from both late spring and autumn, which were significantly different between seasons.

When the core and coastal waters in autumn were compared, there were no differences between all NBSS parameters, including the slopes. Thus, differences between the slopes in core and coastal waters must had occurred in late spring. During this season, less predation of larger zooplankton occurred in core waters, i.e., deviations from the parabolic shape and positive residuals occurred at larger size classes. However, the coastal waters were well-mixed and had a typical parabolic dome shape. Patterns of steeper slopes in coastal regions have also been observed in open ocean systems (Zhou 2006; Manríquez et al. 2012; Schultes et al. 2013; García-Comas et al. 2014).

Although oceanographic conditions in the upper and lower Strait regions are different during autumn, the biological structure and processes governing the structure of the zooplankton community appeared homogeneous as all spectra showed the parabolic dome with no large deviations at larger size classes. Thus, differences between the open ocean region and the upper Strait region should reflect differences between the open ocean region and the lower Strait region as well. However, this was not the case. Although both the upper and lower Strait regions had less variability in size and a larger most frequent size class relative to the open ocean region, only the upper Strait region had significantly more organisms > 1 mg and shallower slopes relative to the open ocean region. Linear NBSS parameters for the lower Strait region were intermediate in relation to both the upper Strait and open ocean region, and thus, did not differ from either region. Steeper slopes in the open ocean region, relative to the upper Strait region were, again, likely due to a combination of bottom-up and top-down processes as there was a higher abundance of zooplankton in smaller size classes and a lower abundance of zooplankton in larger size classes.

4.5 Comparing the linear and quadratic NBSS models

In this study, both the linear model and quadratic model of the NBSS were used to quantify the size structure of the zooplankton community. As all linear NBSS parameters had sufficient statistical significance, the size structure of the zooplankton community in the Northumberland Strait can be well represented by the linear model. In comparison, not all quadratic NBSS parameters were statistically significant and although the quadratic offered a superior fit in every case when significant, it failed to

represent the zooplankton community when the parabolic dome flattened and/or when more deviations from the hypothetical steady state occurred in larger size classes. In these cases, the quadratic model predicted a most frequent size class that was smaller than the sampling range of the OPC and that this size class had more normalized biomass than the total biomass; i.e., not possible. Further, if the coefficient of determination is considered as a measure of the stability of the community structure, as proposed by Quintana et al. (2002), instead of a goodness-of-fit index, the linear model can reveal the presence of deviations from expectation as well as relative magnitude.

As highlighted by Krupica et al. (2012), residuals around the linear fit are often non-random and show strong secondary patterns of curvature. This was clearly apparent in this study, as the curvature of the linear residuals were equal to the curvature of the normalized biomass. Though Krupica et al. (2012) argue that, because of this secondary curvature, applying the linear model to a single trophic group is less rigorous, it can be equally argued that because of this secondary curvature, the linear model provides the same information as the quadratic and more. There also appears to be some confusion regarding the interpretation of the parabolic dome structure in the literature as it is often described as an artefact of the residuals and elsewhere argued to be an artefact of the normalized biomass itself (e.g., Quintana et al. 2002 and Thompson et al. 2013 for interpretation as residuals; e.g., Sprules and Goyke 1994 and Krupica et al. 2012 for interpretation as normalized biomass). Thus, considering that both models are strongly based on ecological theory, the simplicity of the linear model favours its use in describing the size structure of presumably single functional groups

over the quadratic model simply because the deviations from expected linearity are as equally informative within a presumed single functional group as across; i.e., it has a diagnostic capability not offered by the quadratic, if the latter is used in isolation.

4.6 Methodological considerations and limitations

The interpretation of observed spatial and temporal patterns addressed above must be considered with a modicum of caution as sampling a moving fluid from a moving platform, over time, as well as logistical constraints, give rise to some methodological shortfalls. First, both the spatial and temporal distribution of sampling in the Northumberland Strait was not balanced. Sampling in late spring was limited to the upper Strait region. Additionally, sampling in the open ocean region was limited to three stations in autumn. Thus, any spatial or temporal patterns observed (or lack thereof) should be considered in terms of the data, and their interpretations being compromised by temporal and spatial aliasing; i.e., a distortion or artefact that results when the signal reconstructed from the data/samples is different from the actual signal occurring in nature. Second, the Northumberland Strait is a dynamic ecosystem. As the net flow through the system is on average 5.5 km/day from NW to SE (Lauzier 1965), water masses and organisms sampled in the upper Strait region may be located 55 km further SE within a period of 10 days. Further, a point-source particle dispersion field in the lower Strait region can cover as much as 3×10^3 km² over four tidal cycles (Hrycik et al. 2013). The impact of a constrained sampling protocol on measuring spatial and temporal patterns can be amplified when, as in this study, sampling occurred over a period of 7 days in late spring and 14 days in autumn, though into the flow in autumn to

avoid the probability of repeatedly sampling the same water mass (though such a study would have its own merits). However, to minimize confounding these analyses as above, and their interpretation based on sampling a moving, fluid system, the patterns were described more so in water mass space than in geographic space. Thus, any geographic patterns observed, particularly at smaller scales are likely ephemeral. Finally, few stations were sampled within each oceanographic zone defined by the water mass characteristics. The paucity of replicates (though in a moving system more correctly pseudo-replicates) not only within, but also between seasons, makes robust statistical analyses difficult. As such, additional fine-scale sampling is likely required to confirm the generality of the environmental and biological gradients observed. Future studies should strive to capture a more synoptic view of the Strait ecosystem, though the logistics and costs may prove insurmountable to achieve something truly synoptic, though a modelling approach may prove informative (Hrycik et al. 2013).

The methodological framework used here to describe the zooplankton community in water mass space was inspired by the methods used by Debertin et al. (2012) to describe four distinct oceanographic zones in the Northumberland Strait. Although the zones identified in their study were different than those identified above in this study of the Strait, there are clear advantages of such an approach, namely a statistical quantification of spatial pattern in oceanographic biological and physical states in water mass space. Spatial patterns, in water mass space, among the NBSS parameters could

also be quantified using a similar PCA and clustering approach used to characterise the physical states in the Strait. Further, identifying the dominant species among size classes may help inform the spatial and temporal patterns of the zooplankton community. Thus, the application of this approach in concert with taxonomic information to other coastal systems or even to open ocean systems may provide a relatively simple, but robust method to describe the ecological zonation of the Strait environment.

4.7 Implications of the zooplankton community size structure for fishery resources in the Northumberland Strait

Zooplanktonic organisms are the link between phytoplankton and fish production. Thus, fishery yield is directly associated with the size structure and biomass available within the zooplankton community. Recently observed declines in the commercial fisheries of the Northumberland Strait (AMEC Earth and Environmental LTD 2007) may be related to lower-than-normal zooplankton biomass. However, because historical records of zooplankton community structure and abundance within the Strait simply do not exist, it is impossible to determine if the zooplankton biomass characterised here is the normal characteristic for the Strait, even in the face of hypothetical changes induced through climate change or increased eutrophication of coastal waters. However, the one major contribution of this study is that it provides a quantitative baseline to diagnose future change. Future studies should determine if there is close spatial association between zooplankton and fishery-dependent ecological communities; benthic and pelagic. If such associations exist, then the observed zonation in the Strait may provide a means for fisheries managers to determine how acute or chronic disturbances may influence such communities.

References

- AMEC Earth and Environmental LTD for Fisheries and Oceans Canada (2007) Northumberland Strait Ecosystem Overview Report. Moncton, New Brunswick
- Chassé J, Miller RJ (2010) Lobster larval transport in the southern Gulf of St. Lawrence. *Fish Oceanogr* 19:319–338.
- Debertin AJ, Hanson JM, Courtenay SC (2012) Fine-scale sampling reveals distinct oceanographic zones in a North Temperate, marine, coastal ecosystem. pp 1–39
- Dickie LM, Keer SR, Boudreau PR (1987) Size-dependent processes underlying regularities in ecosystem structure. *Ecol. Monogr.* 57:233–250.
- Dutil J, Proulx S, Galbraith PS, et al (2012) Coastal and epipelagic habitats of the estuary and Gulf of St . Lawrence.
- García-Comas C, Chang C-Y, Ye L, et al (2014) Mesozooplankton size structure in response to environmental conditions in the East China Sea: How much does size spectra theory fit empirical data of a dynamic coastal area? *Prog Oceanogr* 121:141–157.
- Heath MR (1995) Size spectrum dynamics and the planktonic ecosystem of Loch Linnhe. *ICES J Mar Sci* 52:627–642.
- Herman AW (1988) Simultaneous measurement of zooplankton and light attenuation with a new optical plankton counter. *Cont. Shelf Res.* 8:205–221.
- Herman AW (1992) Design and calibration of a new optical plankton counter capable of sizing small zooplankton. *Deep Sea Res. Part A. Oceanogr. Res. Pap.* 39:395–415.
- Herman AW, Beanlands B, Phillips EF (2004) The next generation of Optical Plankton Counter: the Laser-OPC. *J Plankton Res* 26:1135–1145.
- Hrycik JM, Chassé J, Ruddick BR, Taggart CT (2013) Dispersal kernel estimation: A comparison of empirical and modelled particle dispersion in a coastal marine system. *Estuar Coast Shelf Sci* 133:11–22.
- Kerr SR, Dickie LM (2001) The biomass spectrum: a predator-prey theory of aquatic production. Columbia University Press
- Krupica KL, Sprules WG, Herman AW (2012) The utility of body size indices derived from optical plankton counter data for the characterization of marine zooplankton assemblages. *Cont Shelf Res* 36:29–40.

- Lauzier L (1965) Drift Bottle Observations in Northurnberland Gulf of St. Lawrence. *J Fish Res Board Canada* 22:353–368.
- Macpherson E, Gordoa A (1996) Biomass spectra in benthic fish assemblages in the Benguela system. *Mar Ecol Prog Ser* 138:27–32.
- Manríquez K, Escribano R, Hidalgo P (2009) The influence of coastal upwelling on the mesozooplankton community structure in the coastal zone off Central/Southern Chile as assessed by automated image analysis. *J Plankton Res* 31:1075–1088.
- Manríquez K, Escribano R, Riquelme-Bugueño R (2012) Spatial structure of the zooplankton community in the coastal upwelling system off central-southern Chile in spring 2004 as assessed by automated image analysis. *Prog Oceanogr* 92–95:121–133.
- Marcolin C da R, Schultes S, Jackson GA, Lopes RM (2013) Plankton and seston size spectra estimated by the LOPC and ZooScan in the Abrolhos Bank ecosystem (SE Atlantic). *Cont Shelf Res* 70:74–87.
- Moore SK, Suthers IM (2006) Evaluation and correction of subresolved particles by the optical plankton counter in three Australian estuaries with pristine to highly modified catchments. *J Geophys Res* 111:1–14.
- Platt T, Denman K (1977) Organisation in the pelagic ecosystem. *Helgoländer Wissenschaftliche Meeresunters* 581:575–581.
- Quintana X, Comin F, Moreno-Amich R (2002) Biomass-size spectra in aquatic communities in shallow fluctuating Mediterranean salt marshes (Empordà wetlands, NE Spain). *J Plankton Res* 24:1149–1161.
- Rodriguez J, Mullin MM (1986) Relation between biomass and body weight of plankton in a steady state oceanic ecosystem. *Limnol Oceanogr* 31:361–370.
- Sameoto D, Jaroszynski L, Fraser W (1980) BIONESS, a new design in multiple net zooplankton samplers. *Can J Fish Aquat Sci* 37:722–724.
- Schultes S, Sourisseau M, Le Masson E, et al (2013) Influence of physical forcing on mesozooplankton communities at the Ushant tidal front. *J Mar Syst* 109–110:S191–S202.
- Sheldon RW, Prakash A, Sutcliffe Jr. WH (1972) The size distribution of particles in the ocean. *Limnol Oceanogr* XVII:327–340.
- Silvert W, Platt T (1978) Energy flux in the pelagic ecosystem: a time-dependent equation. *Limnol Oceanogr* 23:813–816.

- Sprules W, Munawar M (1986) Plankton Size Spectra in Relation to Ecosystem Productivity, Size, and Perturbation. *Can J Fish Aquat Sci* 43:1789–1794.
- Sprules WG, Goyke AP (1994) Size-Based Structure and Production in the Pelagia of Lakes Ontario and Michigan. *Can. J. Fish. Aquat. Sci.* 51:2603–2611.
- Suthers IM, Taggart CT, Rissik D, Baird ME (2006) Day and night ichthyoplankton assemblages and zooplankton biomass size spectrum in a deep ocean island wake. *Mar Ecol Prog Ser* 322:225–238.
- Thiebaux M, Dickie L (1993) Structure of the Body-Size Spectrum of the Biomass in Aquatic Ecosystems: A Consequence of Allometry in Predator-Prey Interactions. *Can J Fish Aquat Sci* 50:1308–1317.
- Thiebaux ML, Dickie LM (1992) Models of aquatic biomass size spectra and the common structure of their solutions. *J Theor Biol* 159:147–161.
- Thompson GA, Dinofrio EO, Alder VA (2013) Structure, abundance and biomass size spectra of copepods and other zooplankton communities in upper waters of the Southwestern Atlantic Ocean during summer. *J Plankton Res* 35:610–629.
- Zhou L, Huang L, Tan Y, et al (2014) Size-based analysis of a zooplankton community under the influence of the Pearl River plume and coastal upwelling in the northeastern South China Sea. *Mar Biol Res* 1–12.
- Zhou M (2006) What determines the slope of a plankton biomass spectrum? *J Plankton Res* 28:437–448.
- Zhou M, Huntley ME (1997) Population dynamics theory of plankton based on biomass spectra. *Mar Ecol Prog Ser* 159:61–73.

Appendix A: Normalized zooplankton biomass size spectra

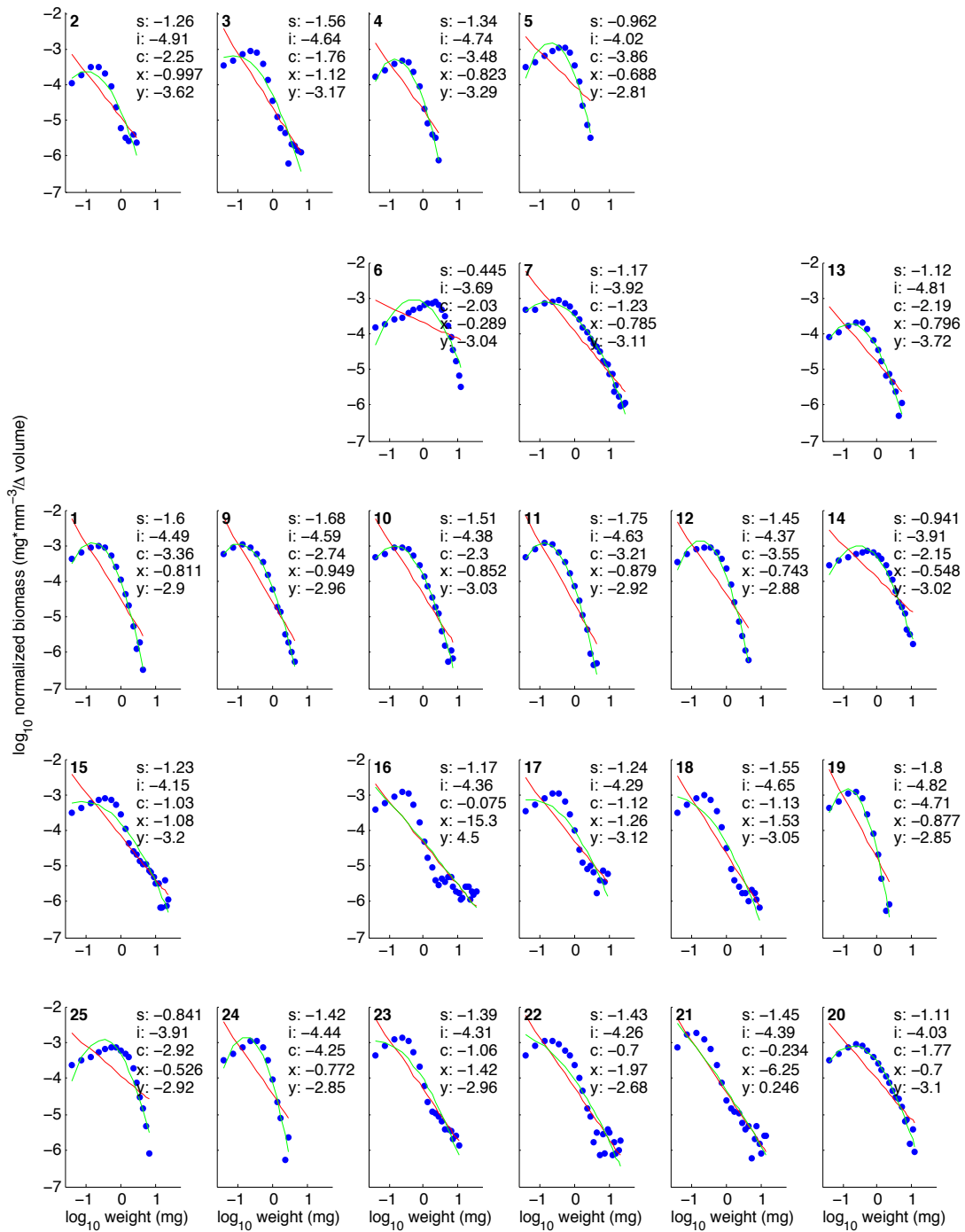


Figure A1. \log_{10} normalized biomass size spectra (NBSS) showing the normalized biomass ($\text{mg} \cdot \text{mm}^{-3}/\Delta \text{volume}$) as a function of size-classes from all stations in the Northumberland Strait during late spring of 2009. The linear slope (s), linear intercept (i), curvature of the quadratic function (c), x-coordinate of the vertex of the quadratic function (x) and y-coordinate of the vertex of the quadratic function (y) are provided for each station. Panels progress among stations in an along-Strait, NW → SE (top to bottom) and across-Strait, SW → NE (left to right).

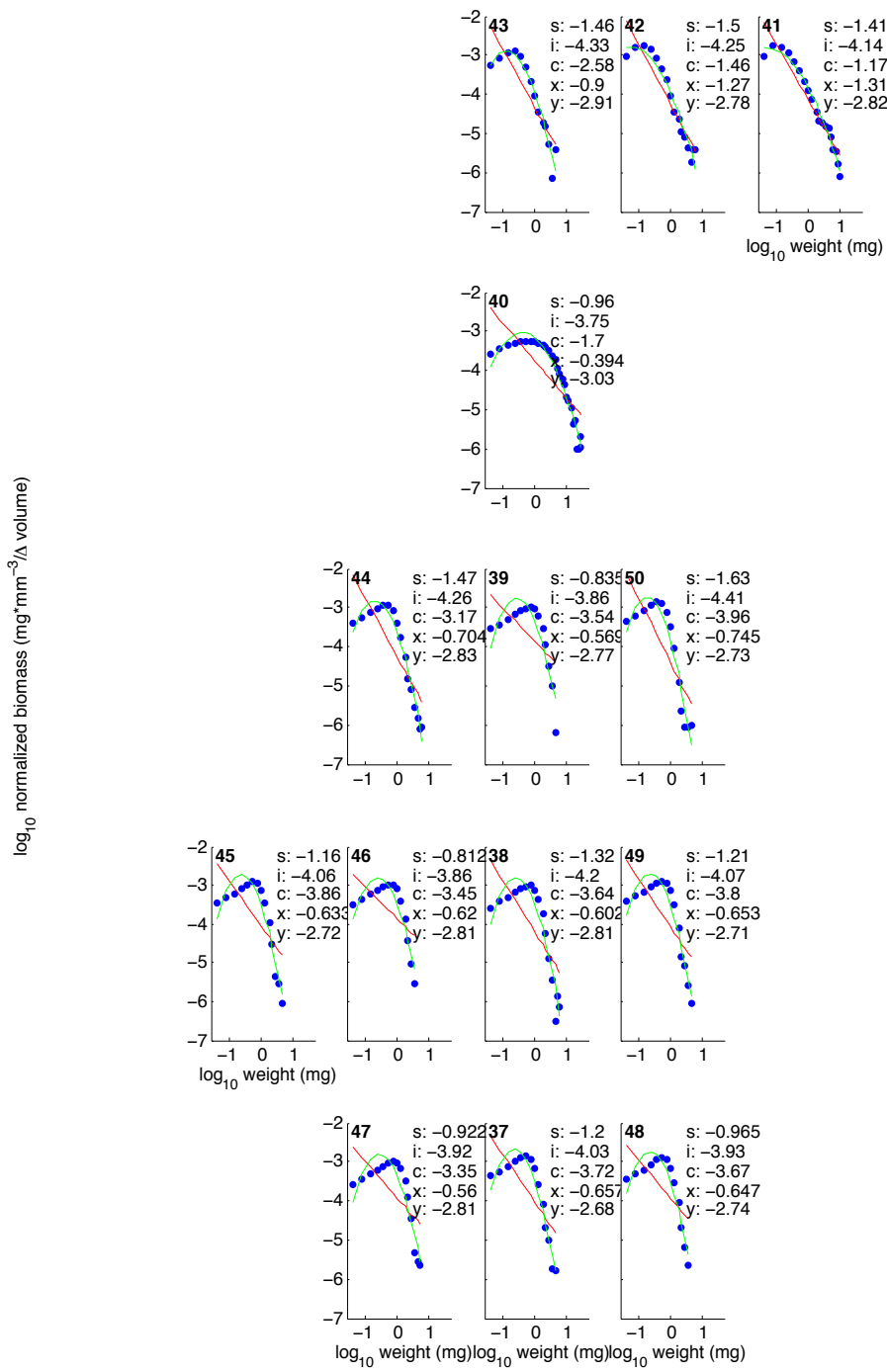


Figure A2. Log₁₀ normalized biomass size spectra (NBSS) showing the normalized biomass (mg mm⁻³/Δ volume) as a function of size categories from stations 37 to 50 in the Northumberland Strait during autumn of 2009 upstream of Confederation Bridge. The linear slope (s), linear intercept (i), curvature of the quadratic function (c), x-coordinate of the vertex of the quadratic function (x) and y-coordinate of the vertex of the quadratic function (y) are given for each station. Panels progress among stations in an along-Strait, NW→SE (top to bottom) and across-Strait, SW→NE (left to right).

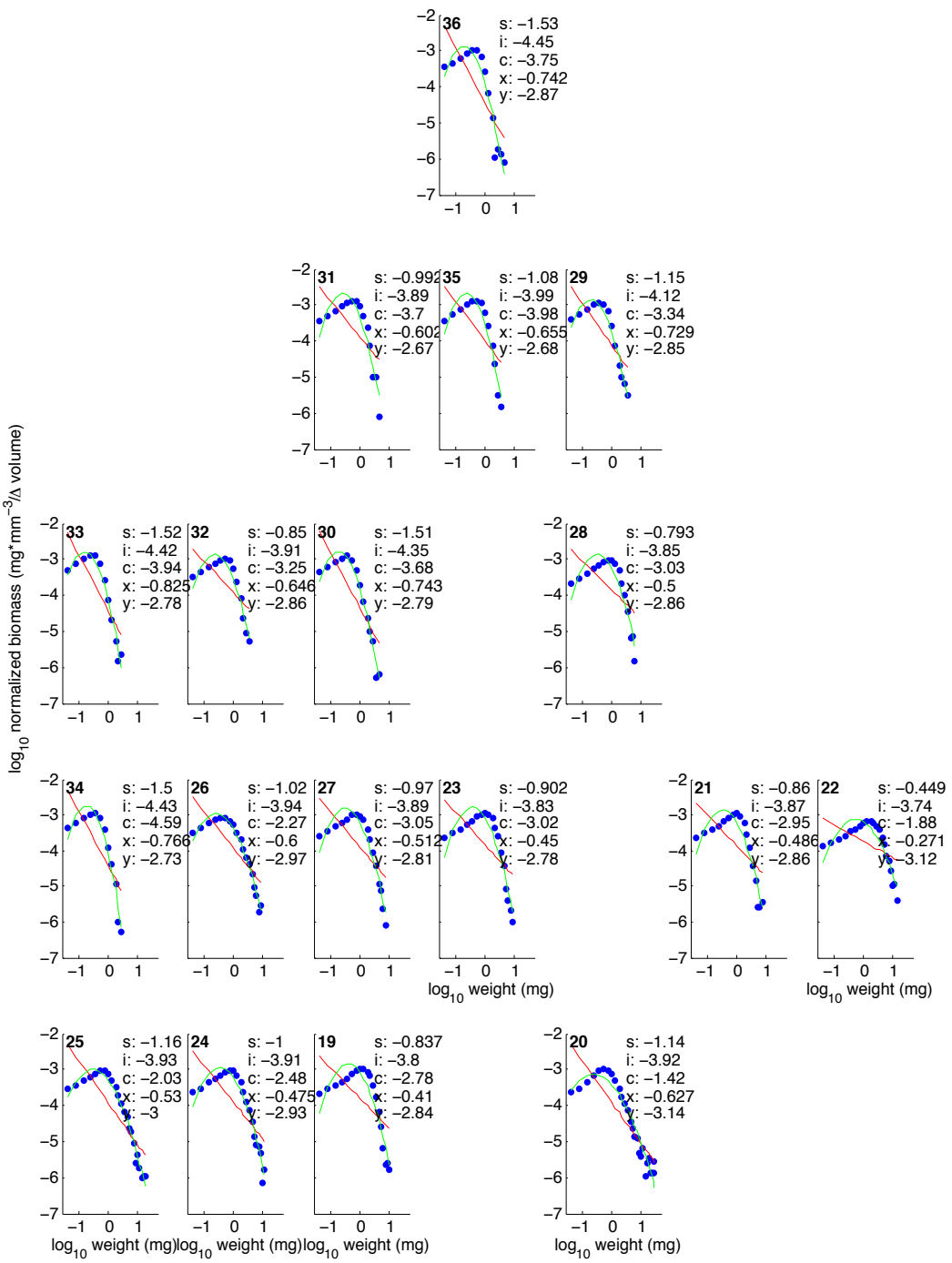


Figure A3. \log_{10} normalized biomass size spectra (NBSS) showing the normalized biomass ($\text{mg} \cdot \text{mm}^{-3}/\Delta \text{volume}$) as a function of size categories from stations 19 to 36 in the Northumberland Strait during autumn of 2009 located downstream of Confederation Bridge, but upstream of Tatamagouche, New Brunswick. The linear slope (s), linear intercept (i), curvature of the quadratic function (c), x-coordinate of the vertex of the quadratic function (x) and y-coordinate of the vertex of the quadratic function (y) are given for each station. Panels progress among stations in an along-Strait, NW→SE (top to bottom) and across-Strait, SW→NE (left to right).

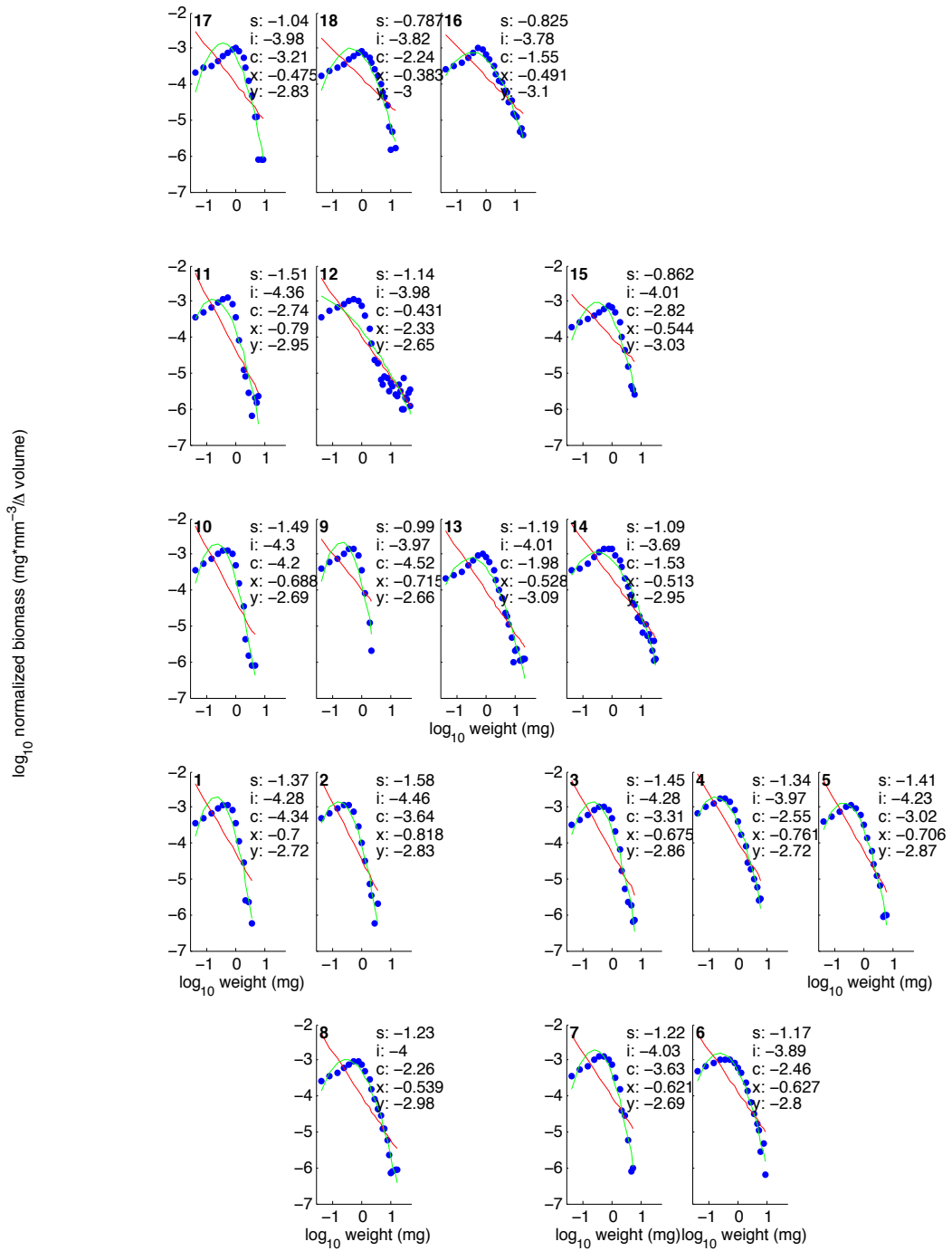


Figure A4. Log₁₀ normalized biomass size spectra (NBSS) showing the normalized biomass (mg mm⁻³/Δ volume) as a function of size categories from stations 1 to 18 in the Northumberland Strait during autumn of 2009 located downstream of Tatamagouche, New Brunswick. The linear slope (s), linear intercept (i), curvature of the quadratic function (c), x-coordinate of the vertex of the quadratic function (x) and y-coordinate of the vertex of the quadratic function (y) are given for each station. Panels progress among stations in an along-Strait NW→SE (top to bottom) and across-Strait SW→NE (left to right).

Appendix B: Residuals from the linear function

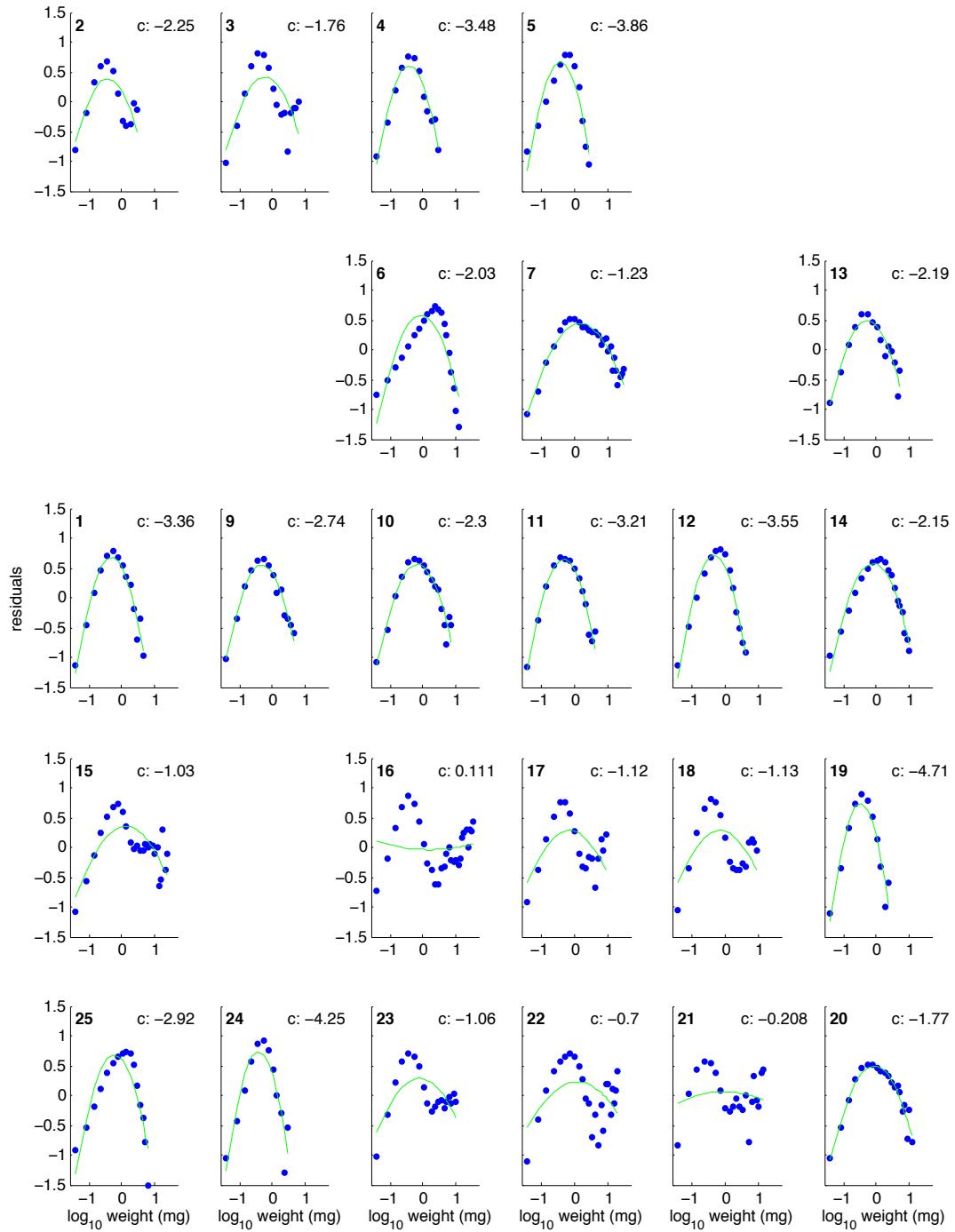


Figure B1. Residuals from linear function fitted to the \log_{10} normalized biomass size spectra (NBSS) as a function of size-class from all stations in the Northumberland Strait during late spring of 2009. The curvature value of the quadratic function (c) fitted to the linear residuals is given for each station. Panels progress among stations in an along-Strait, NW→SE (top to bottom) and across-Strait, SW→NE (left to right).

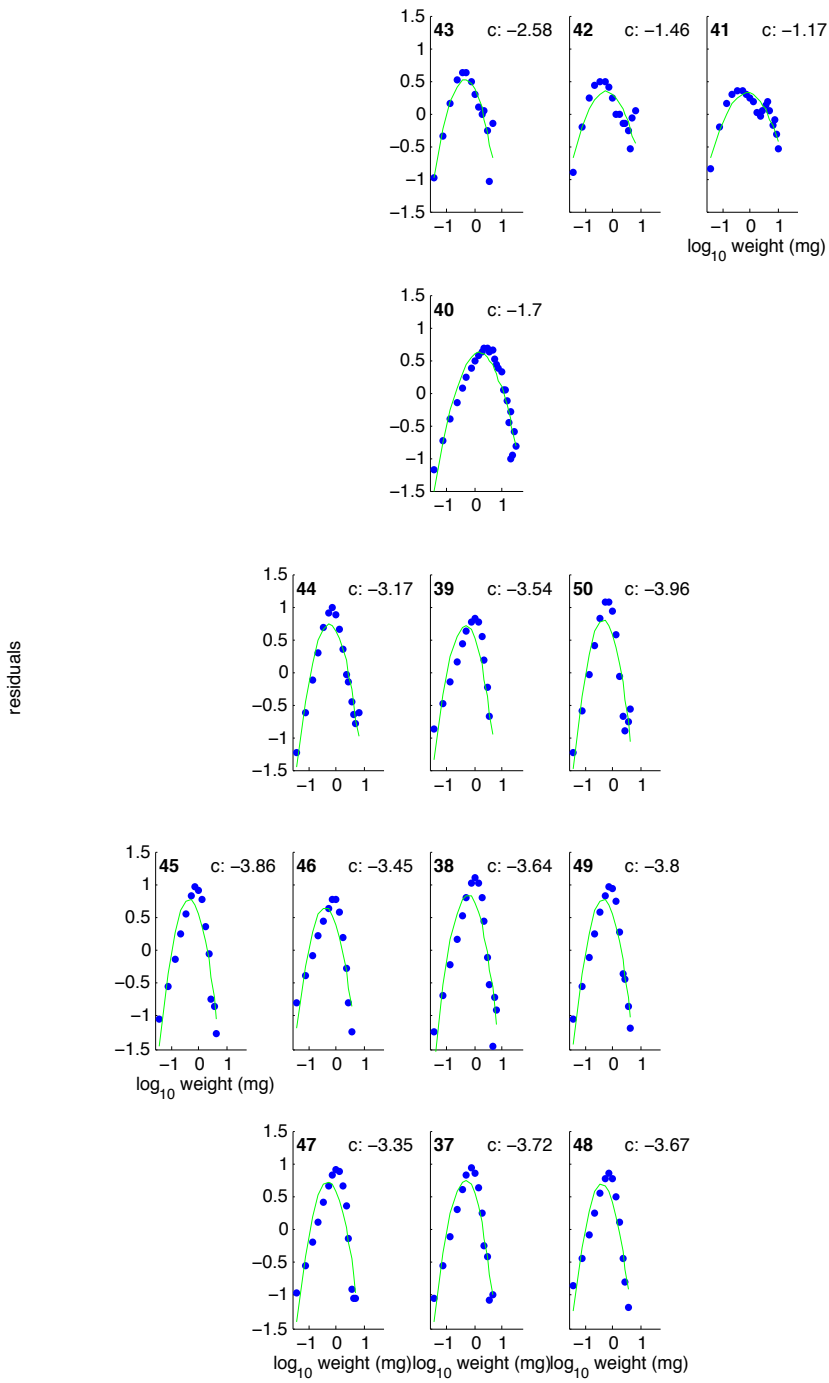


Figure B2. Residuals from linear function fitted to the \log_{10} normalized biomass size spectra (NBSS) as a function of size-class from stations 37 to 50 in the Northumberland Strait during autumn 2009 located upstream of Confederation Bridge. The curvature value of the quadratic function (c) fitted to the linear residuals (c) is given for each station. Panels progress among stations in an along-Strait, NW→SE (top to bottom) and across-Strait, SW→NE (left to right).

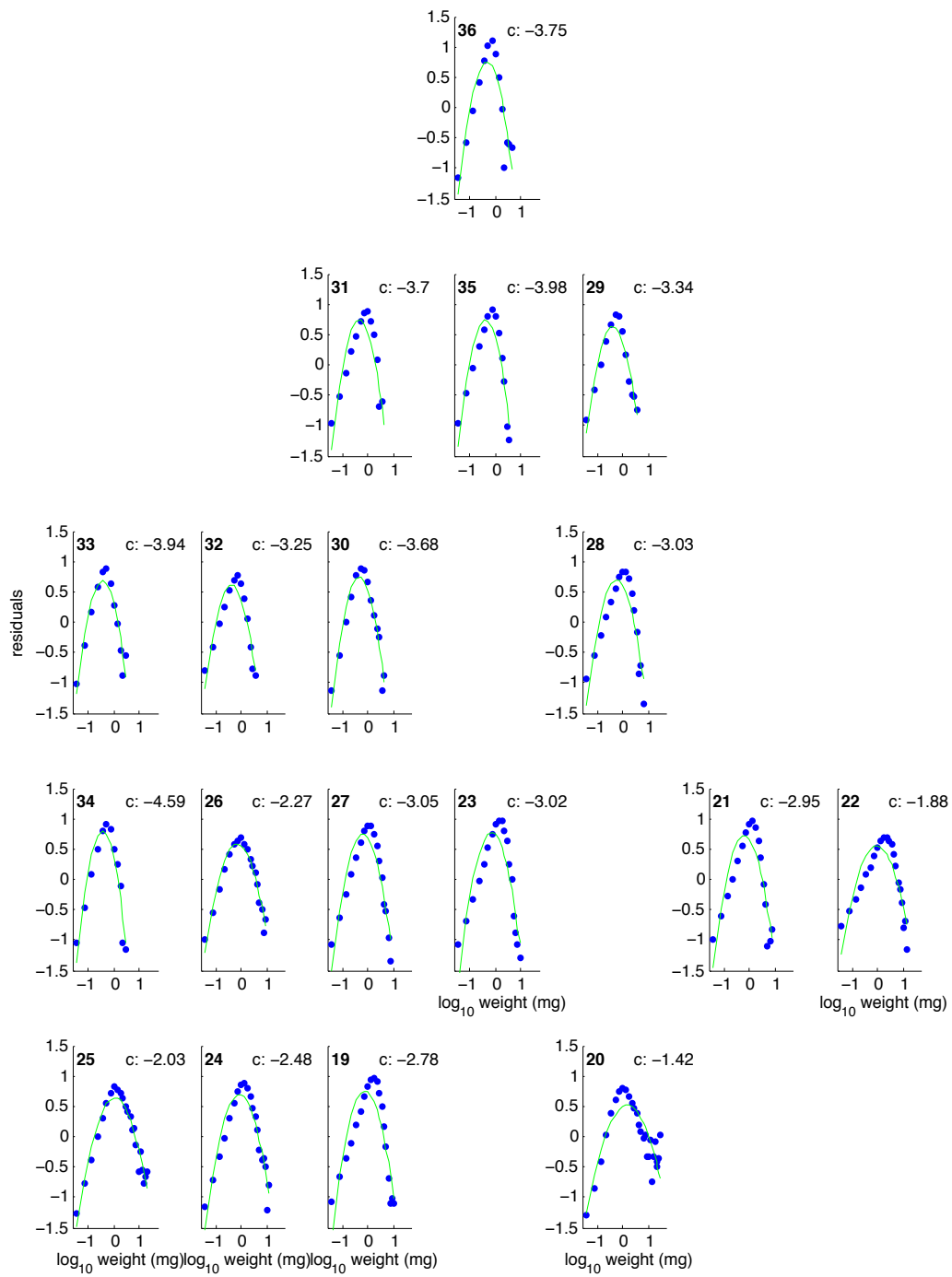


Figure B3. Residuals from linear function fitted to the \log_{10} normalized biomass size spectra (NBSS) as a function of size-class from stations 19 to 36 in the Northumberland Strait during autumn of 2009 located downstream of Confederation Bridge, but upstream of Tatamagouche, New Brunswick. The curvature value of the quadratic function (c) fitted to the linear residuals is given for each station. Panels progress among stations in an along-Strait, NW→SE (top to bottom) and across-Strait, SW→NE (left to right).

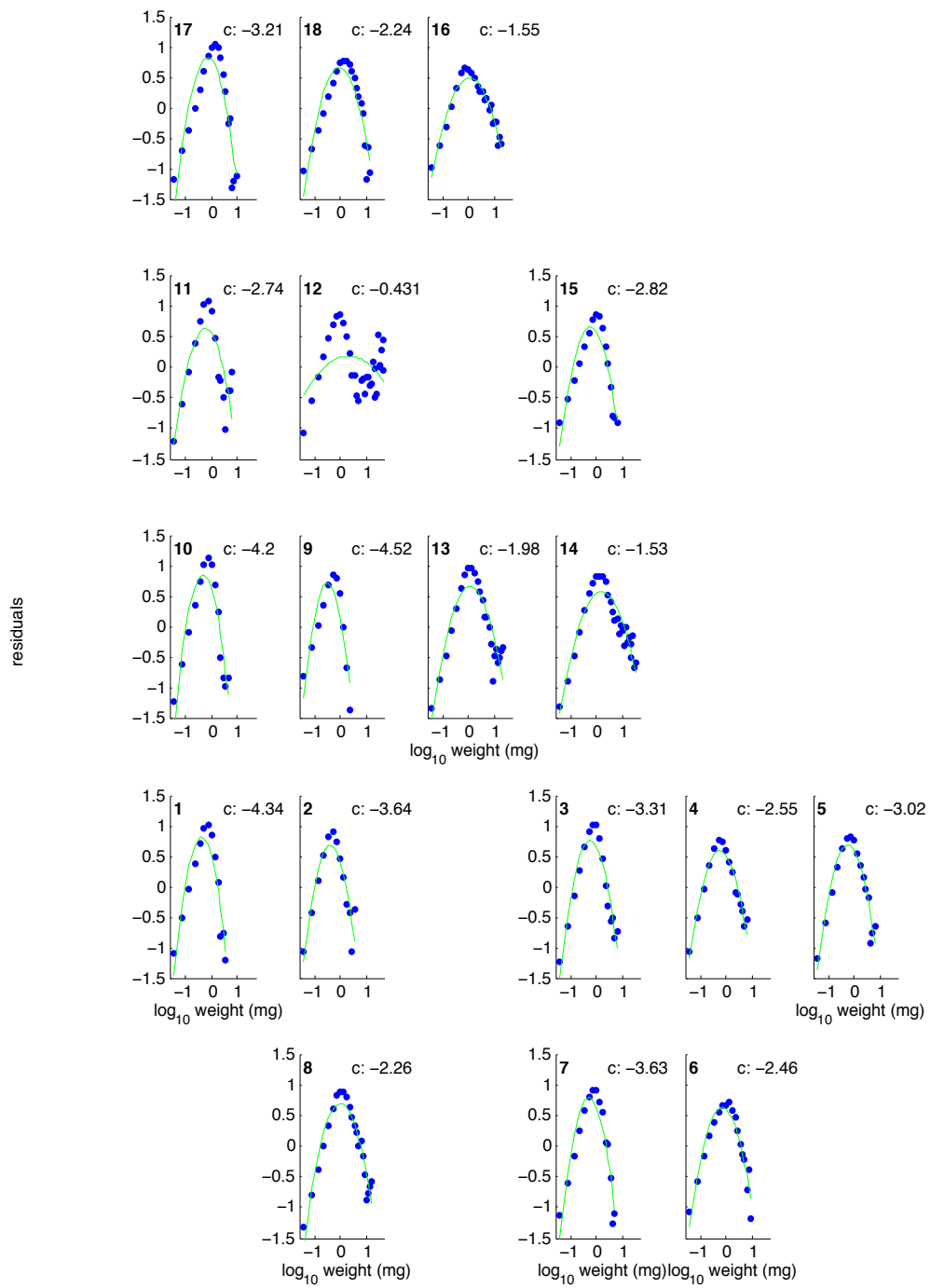


Figure B4. Residuals from linear function fitted to the \log_{10} normalized biomass size spectra (NBSS) as a function of size-class from stations 1 to 18 in the Northumberland Strait during autumn 2009 located downstream of Tatamagouche, New Brunswick. The curvature value of the quadratic function (c) fitted to the linear residuals is given for each station. Panels progress among stations in an along-Strait, NW→SE (top to bottom) and across-Strait, SW→NE (left to right).

Appendix C: Residuals from the quadratic function

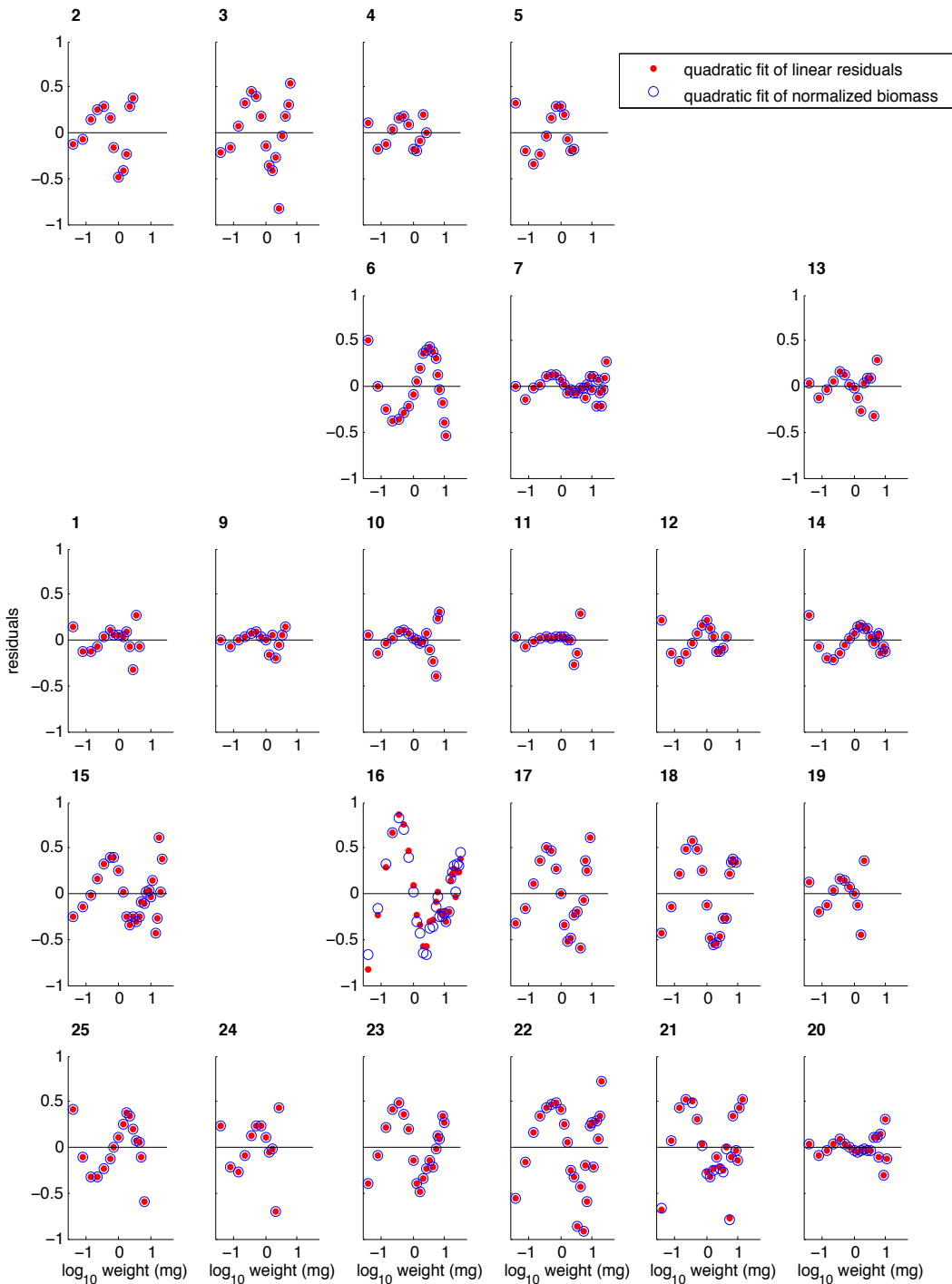


Figure C1. Residuals from quadratic function fitted to the \log_{10} normalized biomass size spectra (NBSS) (blue) and residuals from quadratic function fitted to the residuals from the linear function fitted to the \log_{10} NBSS (red) as a function of size-class from all stations in the Northumberland Strait during late spring of 2009. Panels progress among stations in an along-Strait, NW→SE (top to bottom) and across-Strait, SW→NE (left to right).

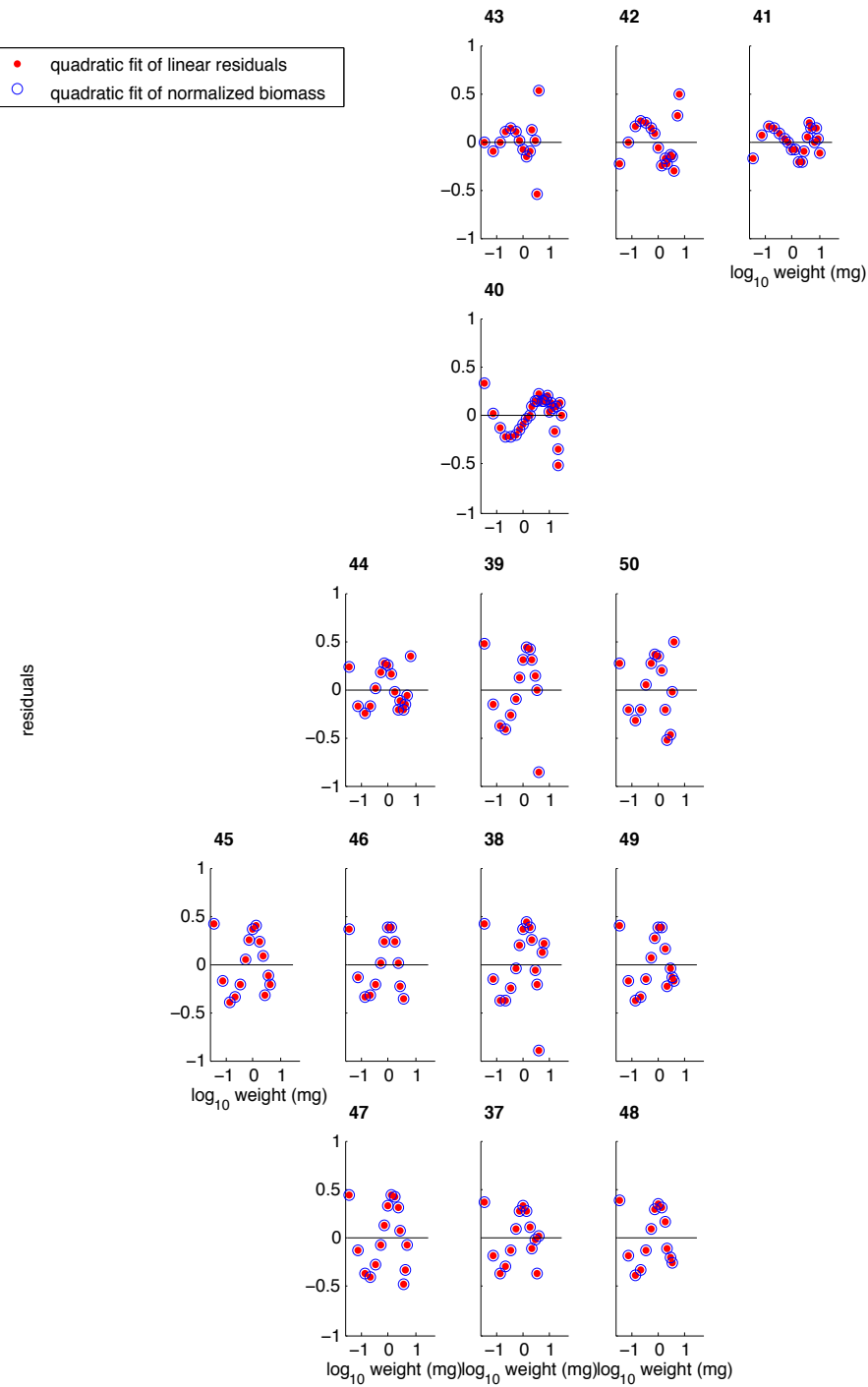


Figure C2. Residuals from quadratic function fitted to the \log_{10} normalized biomass size spectra (NBSS) (blue) and residuals from quadratic function fitted to the residuals from the linear function fitted to the \log_{10} NBSS (red) as a function of size-class from stations 37 to 50 in the Northumberland Strait during autumn 2009 located upstream of Confederation Bridge. Panels progress among stations in an along-Strait, NW→SE (top to bottom) and across-Strait, SW→NE (left to right).

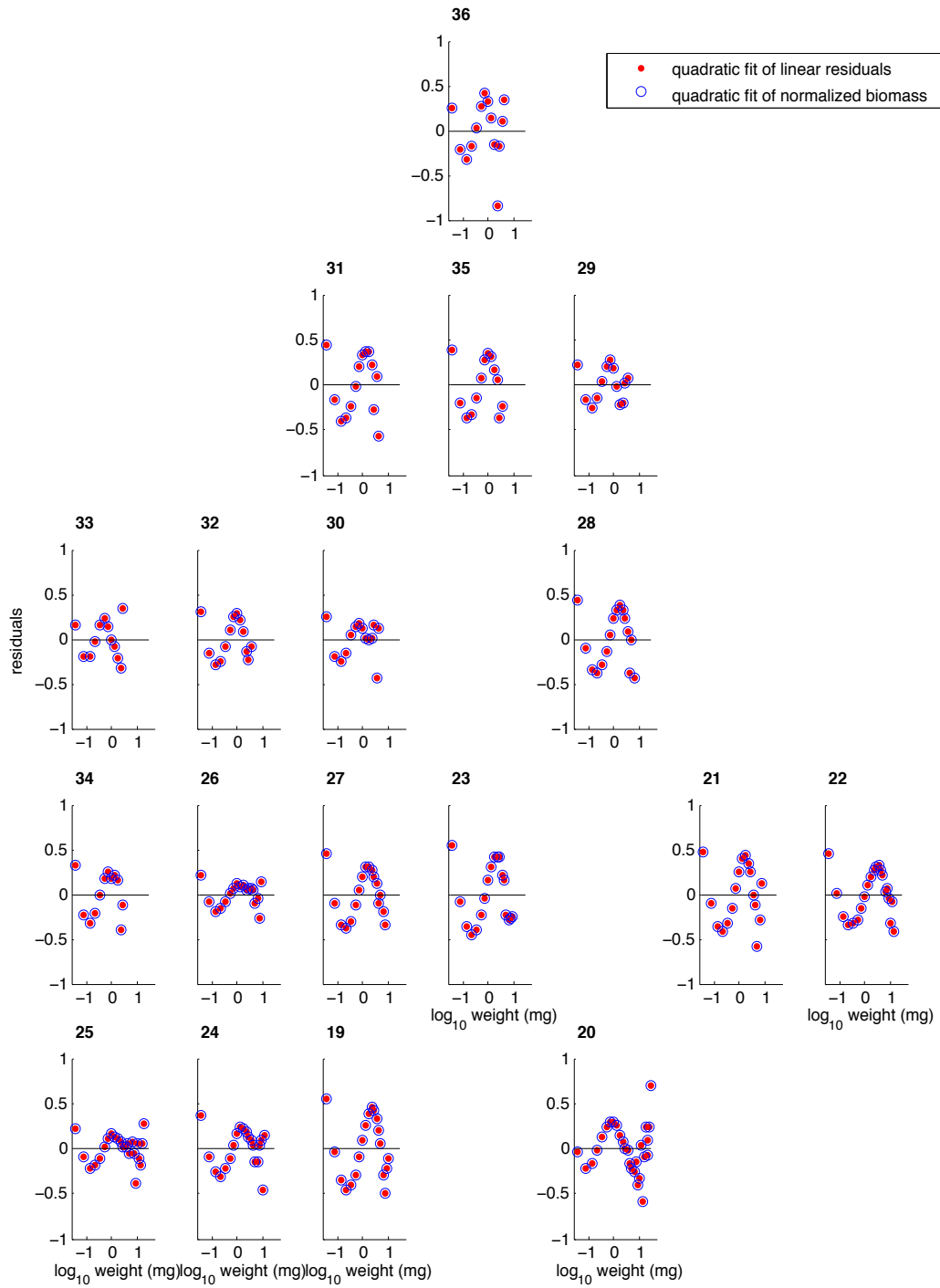


Figure C3. Residuals from quadratic function fitted to the \log_{10} normalized biomass size spectra (NBSS) (blue) and residuals from quadratic function fitted to the residuals from the linear function fitted to the \log_{10} NBSS (red) as a function of size-class from stations 19 to 36 in the Northumberland Strait during autumn of 2009 located downstream of Confederation Bridge, but upstream of Tatamagouche, New Brunswick. Panels progress among stations in an along-Strait, NW→SE (top to bottom) and across-Strait, SW→NE (left to right).

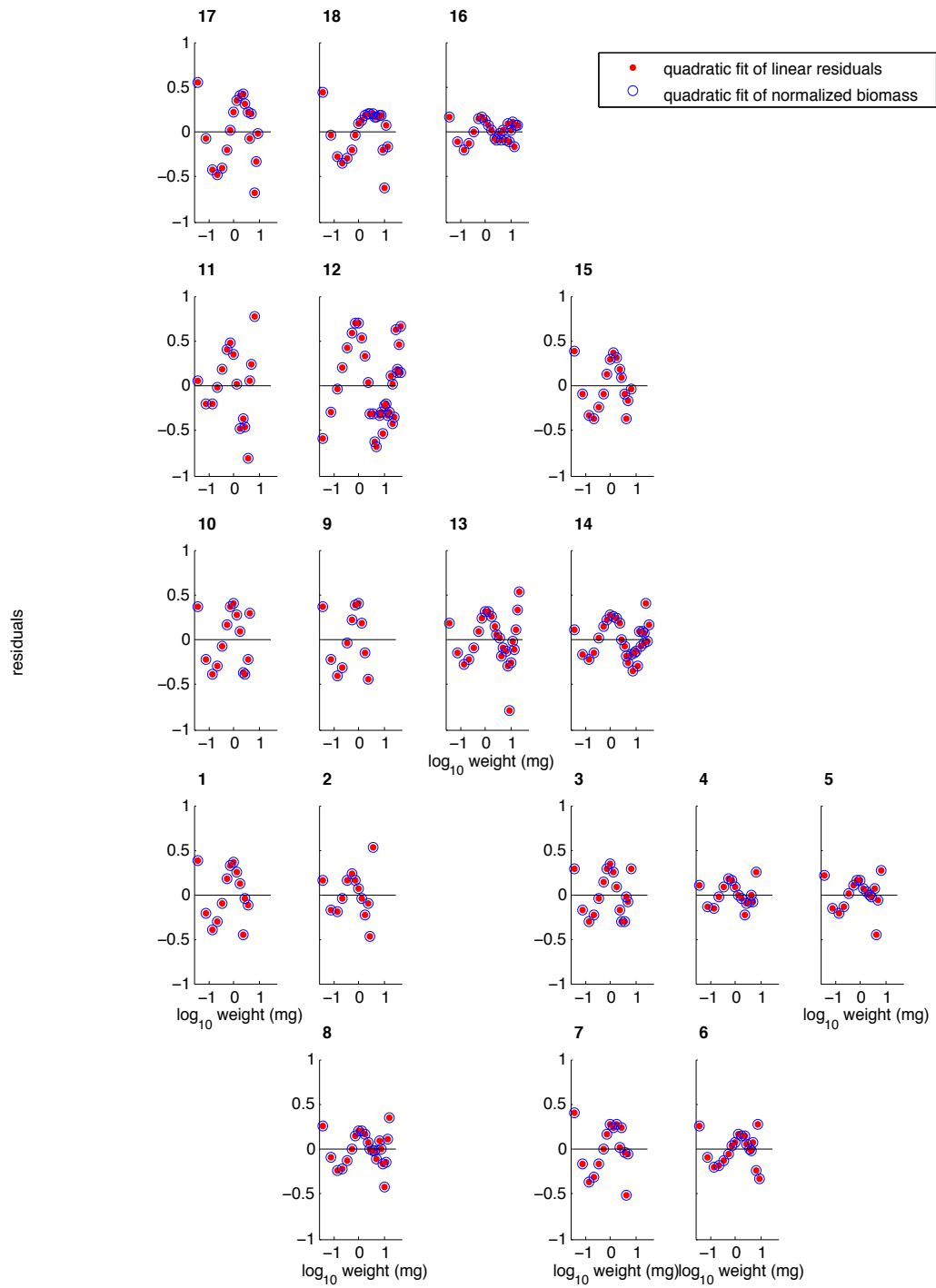


Figure C4. Residuals from quadratic function fitted to the \log_{10} normalized biomass size spectra (NBSS) (blue) and residuals from quadratic function fitted to the residuals from the linear function fitted to the \log_{10} NBSS (red) as a function of size-class from stations 1 to 18 in the Northumberland Strait during autumn 2009 located downstream of Tatamagouche, New Brunswick. Panels progress among stations in an along-Strait, NW→SE (top to bottom) and across-Strait, SW→NE (left to right).